# Silicon and Oxygen's Bond of Affection: An Acyclic Three-Coordinate Silanone and Its Transformation to an Iminosiloxysilylene

Daniel Wendel,[†,‡] Dominik Reiter,[†,§] Amelie Porzelt,[§] Philipp J. Altmann,[⊥] Shigeyoshi Inoue[*,§] and Bernhard Rieger[*,‡]

[‡]WACKER-Chair of Macromolecular Chemistry, [§]WACKER-Institute of Silicon Chemistry, [⊥]Catalysis Research Center, Technische Universität München, Lichtenbergstraße 4, 85748 Garching bei München, Germany

*s.inoue@tum.de; rieger@tum.de

# Supporting Information



Total: S65 pages

# 1. Experimental Procedures

## A) General Methods and Instrumentation

All manipulations were carried out under argon atmosphere using standard Schlenk or glovebox techniques. Glassware was heat-dried under vacuum prior to use. Unless otherwise stated, all chemicals were purchased from Sigma-Aldrich or ABCR and used as received. Benzene, $Et_2O$, *n*-hexane, THF and toluene were refluxed over sodium/benzophenone, acetonitrile over $CaH_2$ and methanol over magnesium, distilled and deoxygenated prior to use. Deuterated benzene ($C_6D_6$), THF (THF-$d_8$) and acetonitrile ($CD_3CN$) were obtained from Deutero Deutschland GmbH and were dried over 3 Å molecular sieves. All NMR samples were prepared under argon in J. Young PTFE tubes. Silepin **1a**, IPrNSiBr$_3$, IMe$_4$ and NaSi*t*-Bu$_3$(THF$_2$) were synthesized according to procedures described in literature.[S1-4] Dinitrogen monoxide (5.0), carbon dioxide (5.0), hydrogen (5.0) and ethylene (3.5) were purchased from Westfalen AG and used as received. NMR spectra were recorded on Bruker AV-500C, AV-500 or DRX-400 spectrometers at ambient temperature (300 K), unless otherwise stated. $^{1}$H, $^{13}$C and $^{29}$Si NMR spectroscopic chemical shifts δ are reported in ppm relative to tetramethylsilane. δ($^{1}$H) and δ($^{13}$C) were referenced internally to the relevant residual solvent resonances. δ($^{29}$Si) was referenced to the signal of tetramethylsilane (TMS) (δ = 0 ppm) as external standard. Elemental analyses (EA) were conducted with a EURO EA (HEKA tech) instrument equipped with a CHNS combustion analyzer. Mass spectra (MS-CI) were recorded on a double focusing Finnigan MAT 90 mass spectrometer (isobutene, 150 eV). UV-Vis spectra were taken on an Agilent Cary 60 spectrophotometer. ATR-FTIR spectra were recorded on a Perkin Elmer FTIR spectrometer (diamond ATR, Spectrum Two; located inside an argon-filled glovebox) in a range of 400 – 4000 cm$^{-1}$. Melting Points ($M_p$) were determined in sealed glass capillaries under inert gas by a Büchi M-565 melting point apparatus.

## B) Synthesis and Characterization of New Compounds

### Synthesis of Silepin (Si*t*-Bu$_3$ Substituted) (1b)

An analogue procedure as for the preparation of SiTMS$_3$ substituted silepin **1a** was applied.[S1] A solution of NaSi*t*-Bu$_3$(THF$_2$) (134 mg, 0.18 mmol, 2.00 eq) in toluene (2 mL) was added to IPrNSiBr$_3$ (123 mg, 0.36 mmol, 1.00 eq) in toluene (2 mL) at room temperature. The color rapidly changed to light green (approx. 1 sec) and then immediately to yellow with formation of a white precipitate. After stirring the solution for 20 min, the solvent was removed *in vacuo*. The obtained residue was extracted with *n*-hexane (3 × 5 mL) and filtered through a microfiber glass filter. For further studies, mixtures of **1b**/*t*-Bu$_3$SiBr were prepared in analogue fashion, since attempts to separate both products by fractional crystallization or sublimation were unsuccessful.

$^1$H NMR (500 MHz, C$_6$D$_6$, r.t.): δ = 7.19 – 7.00 (m, 3H, *p*-/*m*-C*H*-Ar), 6.70 (d, *J* = 2.9 Hz, 1H, C*H*-N), 6.63 (d, *J* = 6.5 Hz, 1H, C*H*-Ar), 6.49 (d, *J* = 12.9 Hz, 1H, C*H*-Ar), 6.37 (dd, *J* = 12.9, 6.5 Hz, 1H, C*H*-Ar), 5.88 (d, *J* = 2.9 Hz, 1H, C*H*-N), 3.39 (hept, *J* = 6.8 Hz, 1H, C*H*), 3.22 (hept, *J* = 6.8 Hz, 1H, C*H*), 3.12 (hept, *J* = 6.8 Hz, 1H, C*H*), 3.05 (hept, *J* = 6.8 Hz, 1H, C*H*) 1.35 (d, *J* = 6.8 Hz, 6H, C*H*$_3$), 1.31 (d, *J* = 6.8 Hz, 6H, C*H*$_3$), 1.25 (s, 27H, Si*t*-*Bu*$_3$), 1.21 (d, *J* = 6.8 Hz, 3H, C*H*$_3$), 1.20 (d, *J* = 6.8 Hz, 3H, C*H*$_3$), 1.09 (d, *J* = 6.8 Hz, 3H, C*H*$_3$), 0.93 (d, *J* = 6.8 Hz, 3H, C*H*$_3$).

$^{29}$Si NMR (99 MHz, C$_6$D$_6$, r.t.): δ = 11.6 (*central Si*), 7.8 (*Sit*-Bu$_3$).

The obtained NMR and UV-VIS data of **1b** are in accordance with the one of SiTMS$_3$ substituted silepin **1a**.[S1]

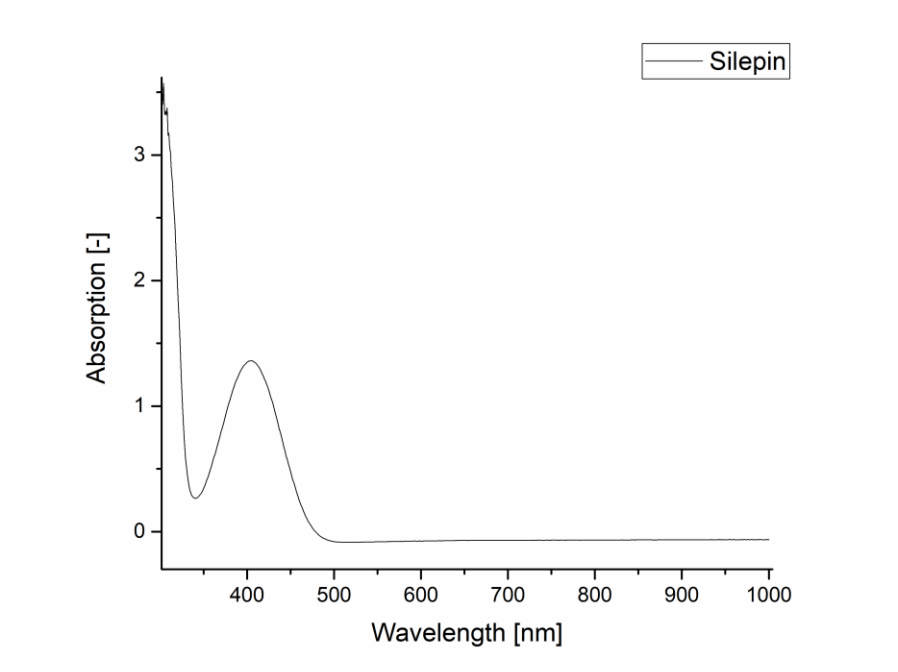


Figure S1. UV-Vis spectrum of silepin **1b**/*t*-Bu$_3$SiBr mixture $\lambda_{max}$ (r.t., hexane, 8.0×10$^{-4}$ M) = 405 nm.

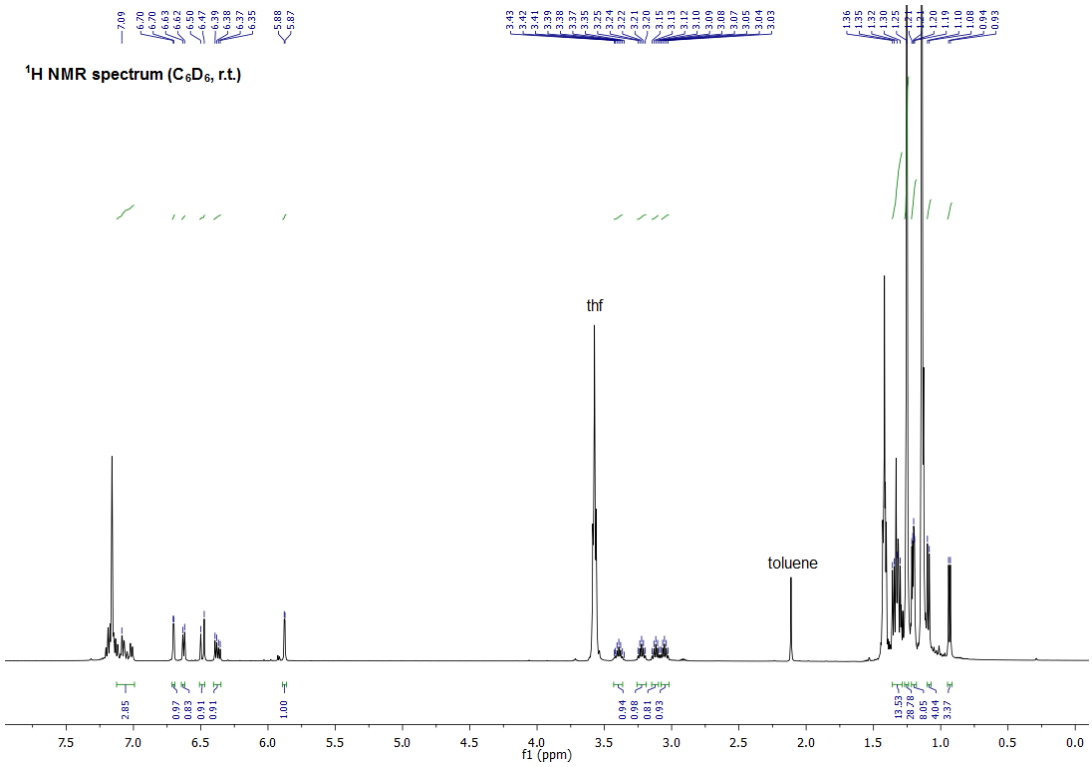


Figure S2: $^{1}$H NMR spectrum of silepin **1b**/*t*-Bu$_3$SiBr mixture ($C_6D_6$, r.t.).

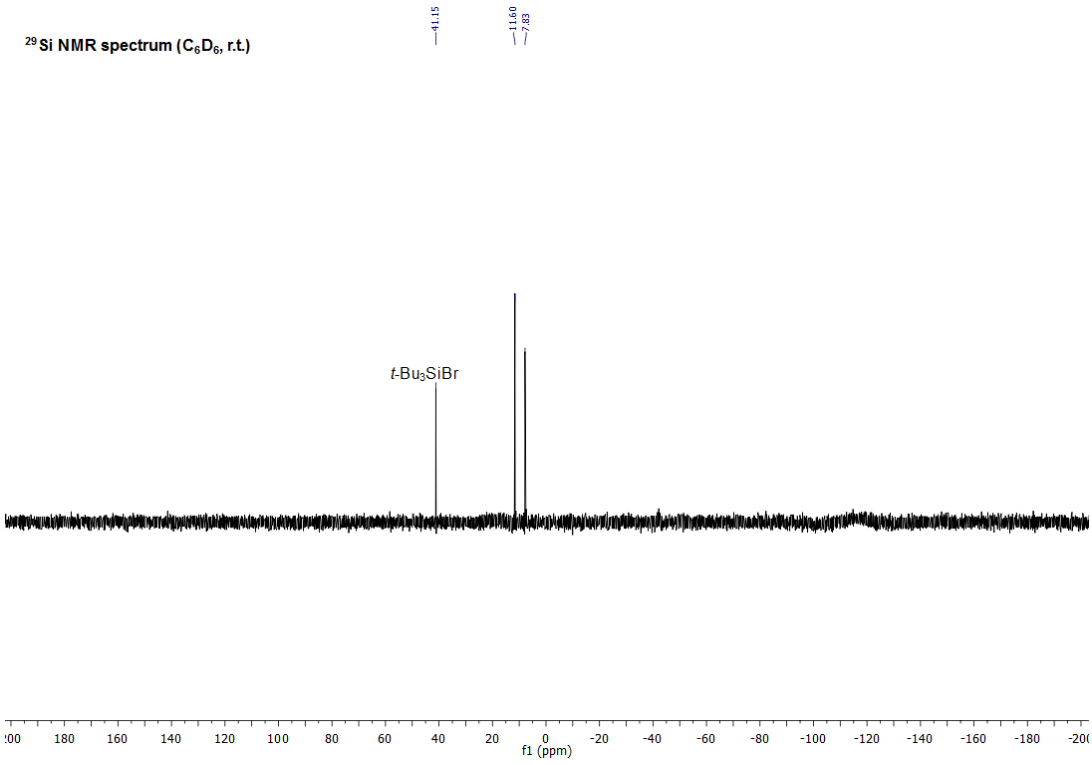


Figure S3: $^{29}$Si NMR spectrum of silepin **1b**/*t*-Bu$_3$SiBr mixture ($C_6D_6$, r.t.).

**Synthesis of Silanone ($SiTMS_3$ Substituted) (2a)**

A solution of $KSiTMS_3$ (726 mg, 2.53 mmol, 2.00 eq) in toluene (20 mL) was added to $IPrNSiBr_3$ (849 mg, 1.27 mmol, 1.00 eq) in toluene (20 mL) at room temperature. The color rapidly changed to light green (approx. 1 sec) and then immediately to yellow with formation of a white precipitate. After stirring the solution for 20 min, the solvent was removed *in vacuo*. The obtained residue was extracted with *n*-hexane (3 × 15 mL) and filtered through a microfiber glass filter. The yellow solution was concentrated, cooled to –78 °C and exposed to $N_2O$ (1 bar). While warming up the solution to room temperature, a fine white precipitate forms, which is immediately separated *via* filtration, washed with *n*-hexane and dried *in vacuo* to give pure silanone **2a** (484 mg, 0.51 mmol, 41%) as a white powder. Attempts to crystallize the donor-free silanone **2a** failed in several solvents (e.g. toluene, monofluorobenzene, difluorobenzene or diethylether), however crystallization in acetonitrile at –35 °C yielded single crystals of tetra-coordinate acetonitrile-stabilized silanone **2a** × $CD_3CN$. The coordination of one acetonitrile molecule to the silicon center of **2a** was additionally verified *via* NMR spectroscopy (see below). Silanone **2a** is indefinitely stable as a solid at –35 °C, but decomposes in $C_6D_6$ at room temperature within 14 h ($t_{1/2}$ = 7 h). Still, the half-life time of silanone **2a** can be extended considerably by using **2a** × $CD_3CN$ solutions ($t_{1/2}$ = 4 d).

**Compound 2a:**

$^1$H NMR (500 MHz, $C_6D_6$, r.t.): δ = 7.34 – 7.05 (m, 6H, C*H*-Ar), 6.08 (s, 2H, C*H*-N), 3.19 (hept, *J* = 6.8 Hz, 4H, C*H*), 1.51 (d, *J* = 6.8 Hz, 12H, C$H_3$), 1.12 (d, *J* = 6.8 Hz, 12H, C$H_3$), 0.22 (s, 27H, Si*TMS*$_3$).

$^{13}$C NMR (126 MHz, $C_6D_6$, r.t.): δ = 148.8 (N-*C*-N), 147.7 (*C*-Ar), 133.1 (*C*-Ar), 130.2 (*C*H-Ar), 124.3 (*C*H-Ar), 115.7 (*C*H-N), 29.1 (*C*H), 25.4 (*C*$H_3$), 23.8 (*C*$H_3$), 2.5 (Si*TMS*$_3$).

$^{29}$Si NMR (99 MHz, $C_6D_6$, r.t.): δ = 33.7 (*central Si*), -9.6 (*TMS*$_3$), -130.6 (*Si*$TMS_3$).

MS-CI (150 eV): $m/z$ (%) = 693 $[M]^+$ (8), 711 $[M+H_2O]^+$ (5).

Reproducible EA could not be obtained for compound **2a** due to its extreme air and moisture sensitivity.

$M_p$: 111.0 °C (decomposition, color change from colorless to yellow).

**Compound 2a × $CD_3CN$:**

$^1$H NMR (500 MHz, $CD_3CN$, r.t.): δ = 7.46 – 7.38 (m, 2H, *p*-C*H*-Ar), 7.38 – 7.23 (m, 4H, *m*-C*H*-Ar), 6.56 (s, 2H, C*H*-N), 3.01 (overlapping hept, *J* = 6.8 Hz, 4H, C*H*), 1.35 (d, *J* = 6.8 Hz, 6H, C$H_3$), 1.32 (d, *J* = 6.8 Hz, 6H, C$H_3$) 1.18 (d, *J* = 6.8 Hz, 6H, C$H_3$) 1.14 (d, *J* = 6.8 Hz, 6H, C$H_3$), -0.04 (s, 27H, Si*TMS*$_3$).

$^{29}$Si NMR (99 MHz, $CD_3CN$, r.t.): δ = -10.9 (*TMS*$_3$), -48.3 (*central Si*), -133.6 (*Si*$TMS_3$).

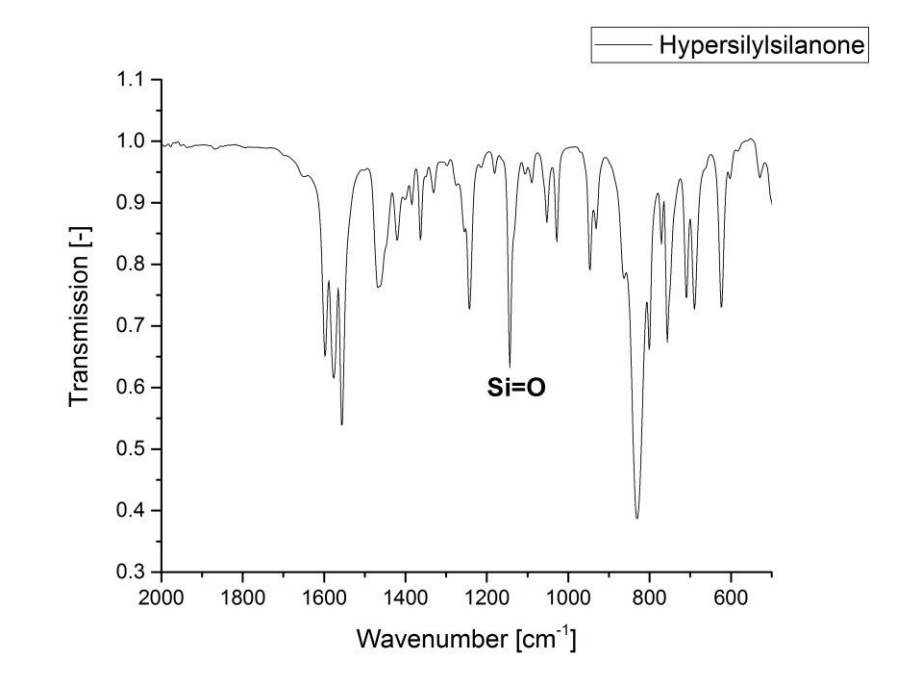


Figure S4: IR spectrum of silanone **2a** ($cm^{-1}$): 1598 (m), 1577 (m), 1552 (s), 1456 (m), 1420 (w), 1244 (m), 1144 (m, Si=O), 1053 (w), 1023 (w), 944 (w), 825 (s), 751 (m), 721 (m), 685 (m), 622 (m).

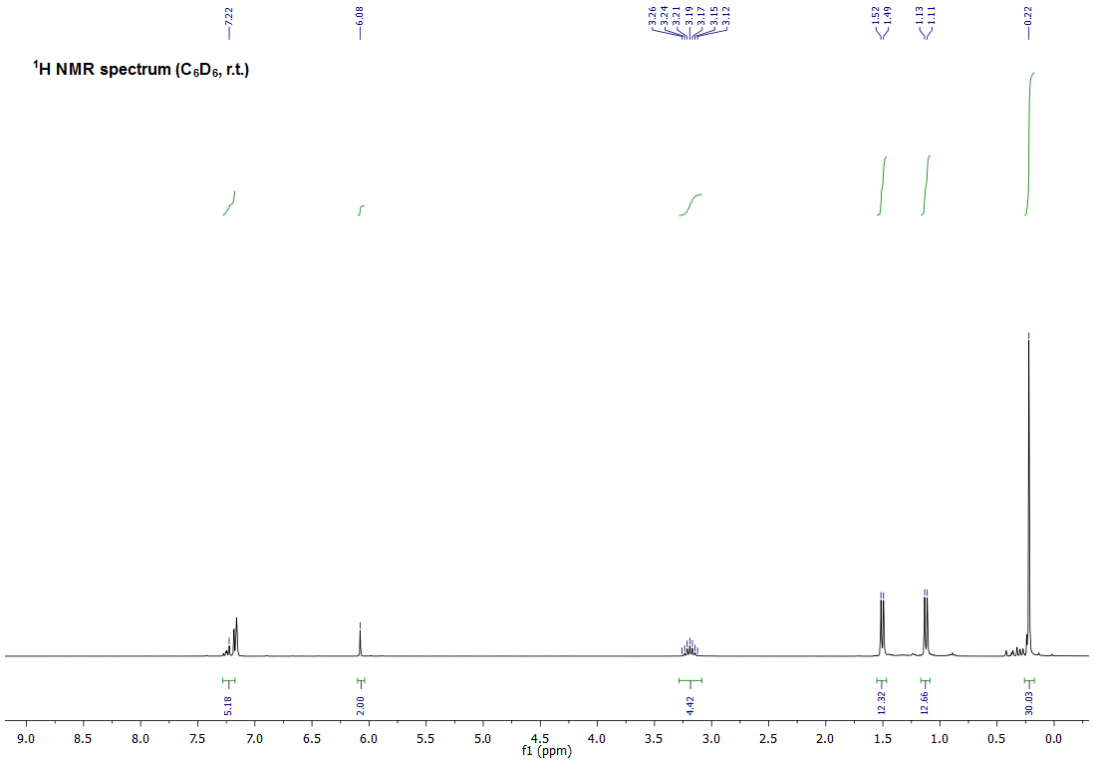


Figure S5: $^1$H NMR spectrum of silanone **2a** ($C_6D_6$, r.t.).

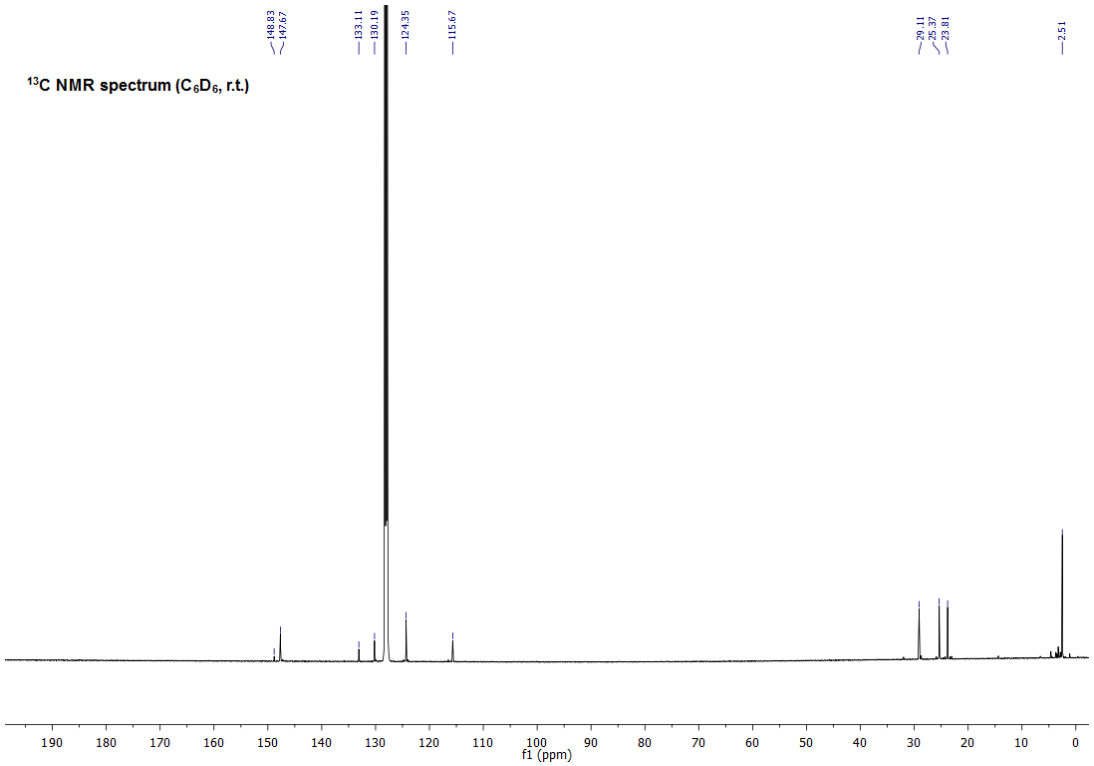


Figure S6: $^{13}C$ NMR spectrum of silanone **2a** ($C_6D_6$, r.t.).

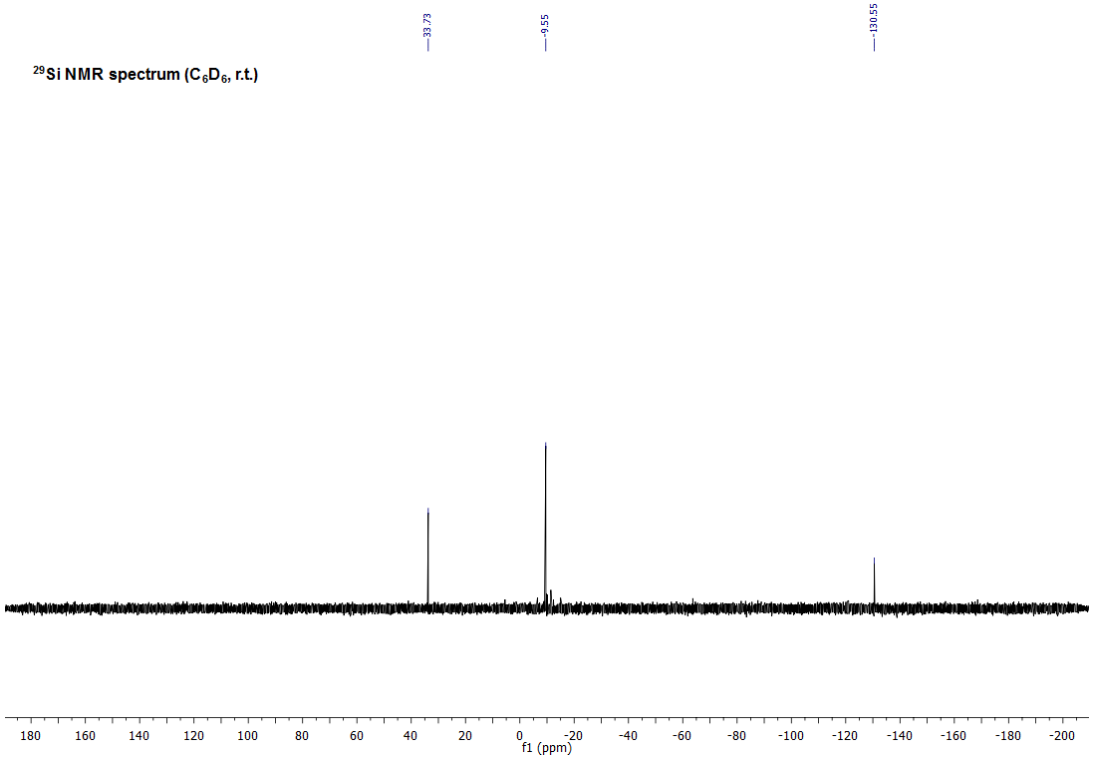


Figure S7: $^{29}Si$ NMR spectrum of silanone **2a** ($C_6D_6$, r.t.).

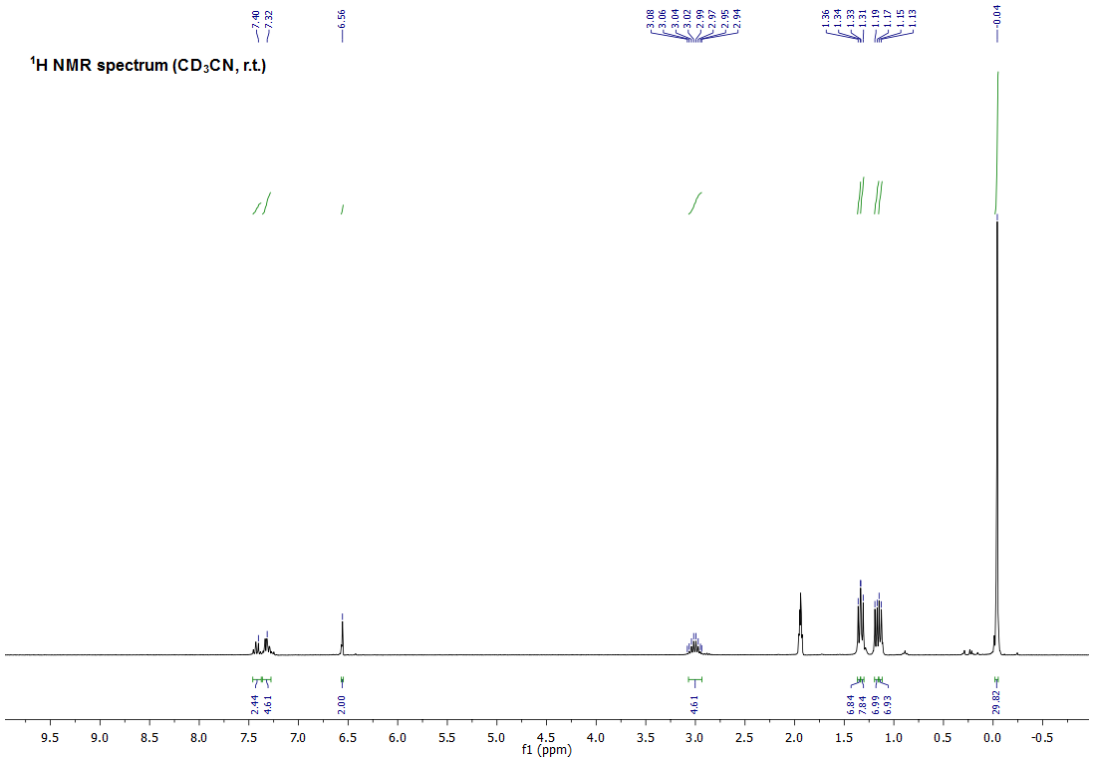


Figure S8: $^{1}$H NMR spectrum of tetra-coordinate silanone **2a** × $CD_3CN$ ($CD_3CN$, r.t.).

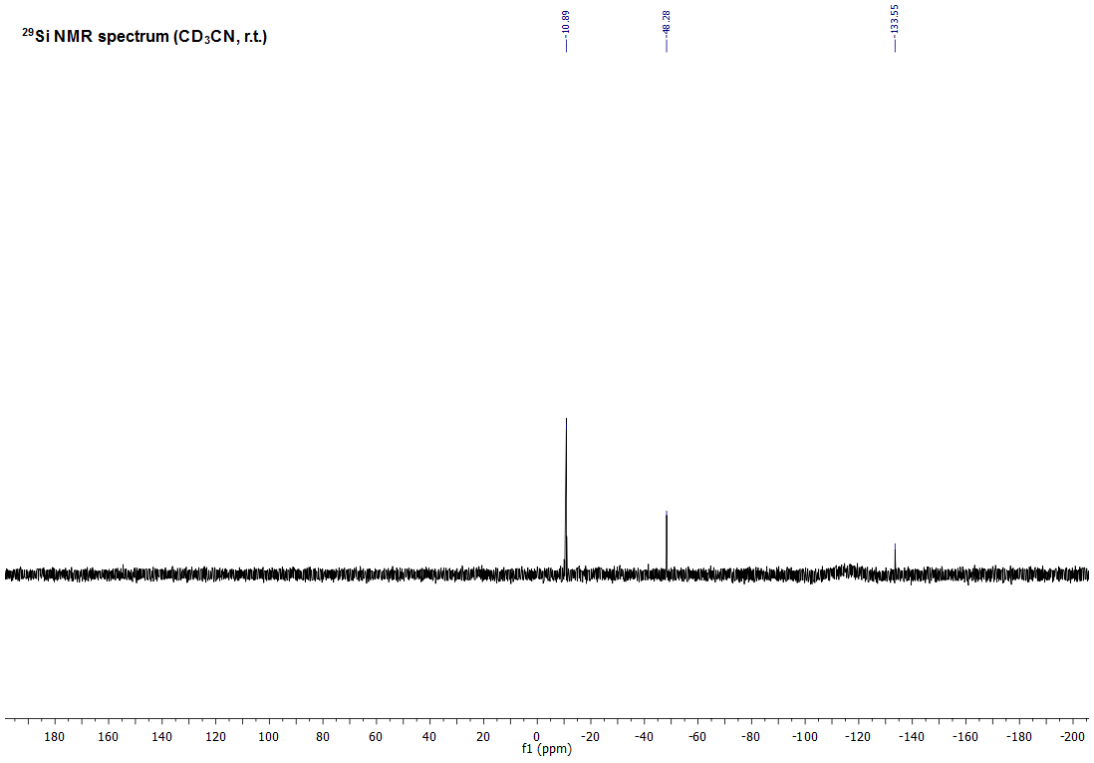


Figure S9: $^{29}$Si NMR spectrum of tetra-coordinate silanone **2a** × $CD_3CN$ ($CD_3CN$, r.t.).

**Decomposition of Silanone 2a**

In general, the decomposition process of **2a** in $C_6D_6$ is rather unspecific and led to several unidentified compounds within 14 h. However, according to the obtained $^{1}H$, $^{29}Si$ and $^{1}H/^{29}Si$ HMBC NMR data one major asymmetric product was identified, presumably formed by TMS migration from the hypersilyl group to the Si=O center and subsequent activation of the NHI ligand (see Figure S11 and Figure S12). A comparable 1,3-silyl migration has been reported for Kira's transient cyclic dialkylsilanone to form an intermediary silene.[S5] For silanone **2a** the identical decomposition pathway leads to transient disilene **INT** (see Figure S10), which probably due to the strong donation of NHI and OTMS group possesses a highly polarized Si=Si bond. Therefore also a zwitterionic resonance form **INT'** should be considered. We propose, that this highly reactive intermediate is capable to intra- or intermolecularly activate the NHI ligand. Although currently specific details are unclear, this reaction seems very likely, since a similar NHI activation has been observed in literature.[S2]

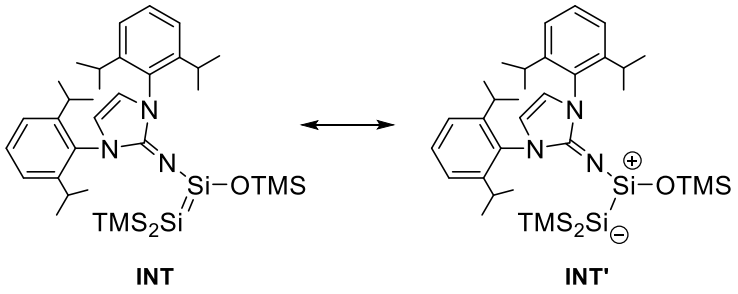


Figure S10: Proposed intermediate **INT** in the decomposition process of silanone **2a** formed by 1,3-silyl migration to the Si=O center.

Moreover, we figured out that the same 1,3-silyl migration can be instantly induced by addition of THF-$d_8$ to solid **2a**, resulting in a strongly yellow colored solution. Subsequent NMR analysis indicated the quantitative formation of the proposed transient disilene **INT** (NMR data see below). By comparing the NMR shifts of **INT** with the theoretical data (Table S13), exclusively the $^{29}Si$ NMR shift of the positively polarized $Si^{+}$ atom showed a strong deviation ($\Delta$67.5 ppm). We therefore believe that (very similar to compound **6**) a THF molecule can act as potential donor and coordinate to the silicon center, forming **INT** × THF. This species is highly reactive and decomposed in analogue fashion to **2a** in $C_6D_6$ within a few hours. All attempts to isolate and crystallize **INT** × THF failed, however trapping experiments with ethylene led to the corresponding [2+2]-cycloaddition product **5**. Further, by using a stronger external NHC donor the $IMe_4$ stabilized zwitterionic disilene **6** was isolated (for details see compound **5** and **6**).

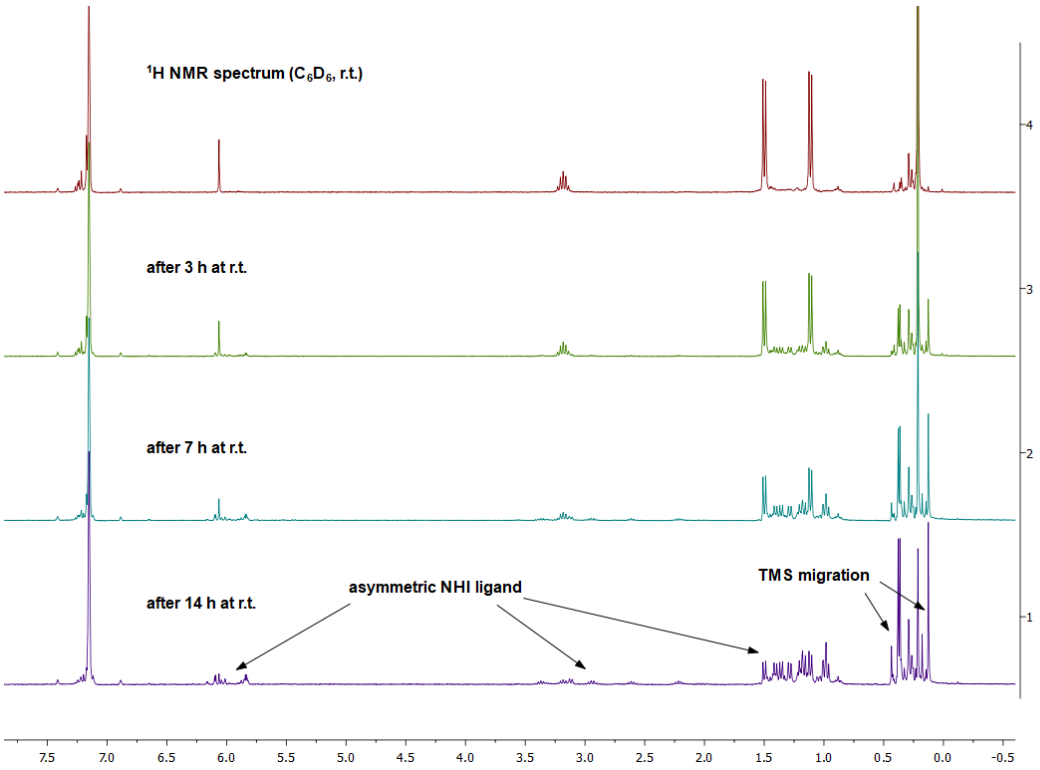


Figure S11: $^1$H NMR spectra of the decomposition process of silanone **2a** after 3, 7 and 14 h in solution ($C_6D_6$, r.t.).

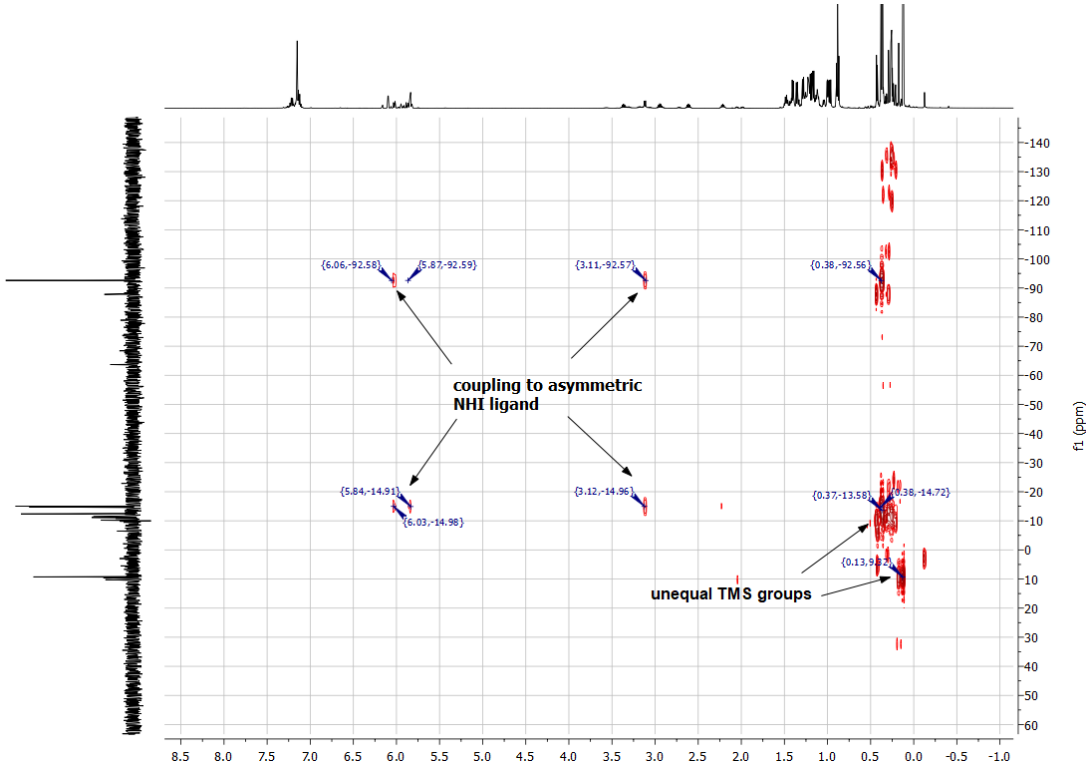


Figure S12: $^1$H/$^{29}$Si HMBC NMR spectrum of the decomposition mixture of silanone **2a** after 14 h in solution ($C_6D_6$, r.t.).

**NMR data of transient disilene INT (THF-$d_8$ induced TMS migration):**

$^{1}$H NMR (500 MHz, THF-$d_8$, r.t.): δ = 7.39 – 7.35 (m, 4H, *m*-C*H*-Ar), 7.30 – 7.27 (m, 2H, *o*-C*H*-Ar), 6.56 (s, 2H, C*H*-N), 3.16 (hept, *J* = 6.8 Hz, 4H, C*H*), 1.41 (d, *J* = 6.8 Hz, 12H, C$H_3$), 1.16 (d, *J* = 6.8 Hz, 12H, C$H_3$), 0.01 (s, 18H, Si*TMS*$_2$), -0.11 (s, 9H, O*TMS*).

$^{13}$C NMR (126 MHz, THF-$d_8$, r.t.): δ =, 148.7 (*C*-Ar), 143.0 (N-*C*-N), 136.1 (*C*-Ar), 130.3 (*C*H-Ar), 125.1 (*C*H-Ar), 117.0 (*C*H-N), 29.4 (*C*H), 25.9 (*C*H$_3$), 24.4 (*C*H$_3$), 7.4 (Si*TMS*$_2$), 3.4 (O*TMS*).

$^{29}$Si NMR (99 MHz, THF-$d_8$, r.t.): δ = 4.3 (O*TMS*), -7.2 (Si*TMS*$_2$), -8.0 (*Si*OTMS), -196.6 (*Si*TMS$_2$).

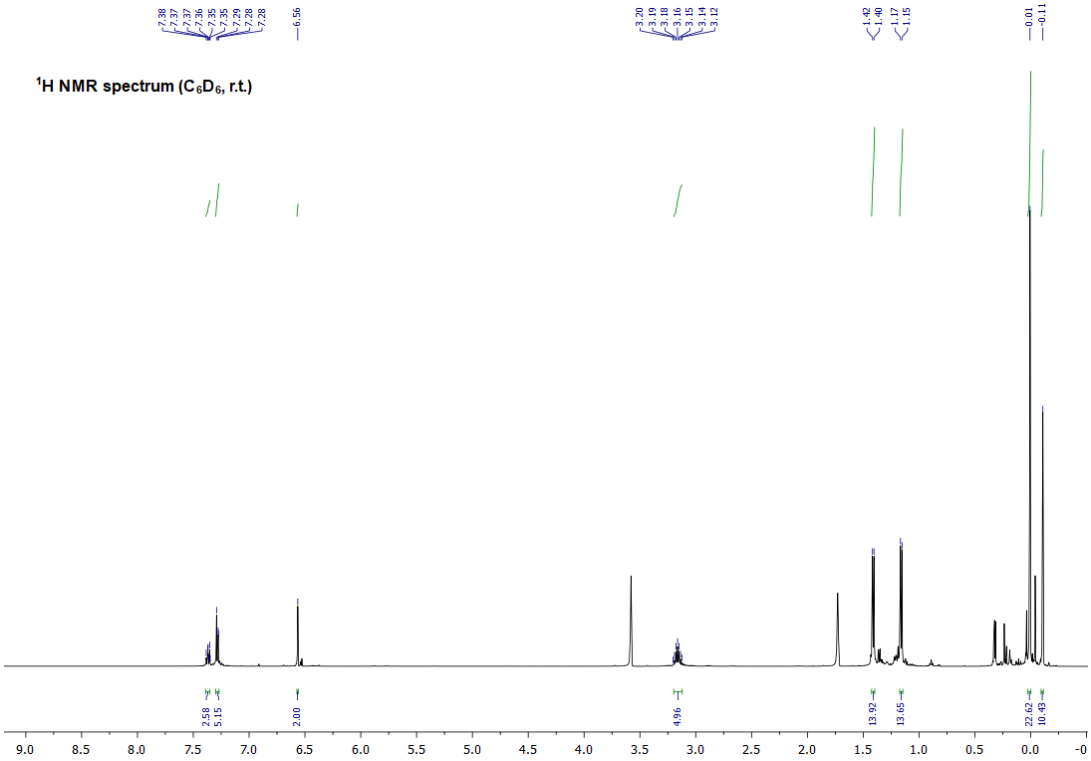


Figure S13: $^{1}$H NMR spectrum of transient disilene **INT** (THF-$d_8$, r.t.).

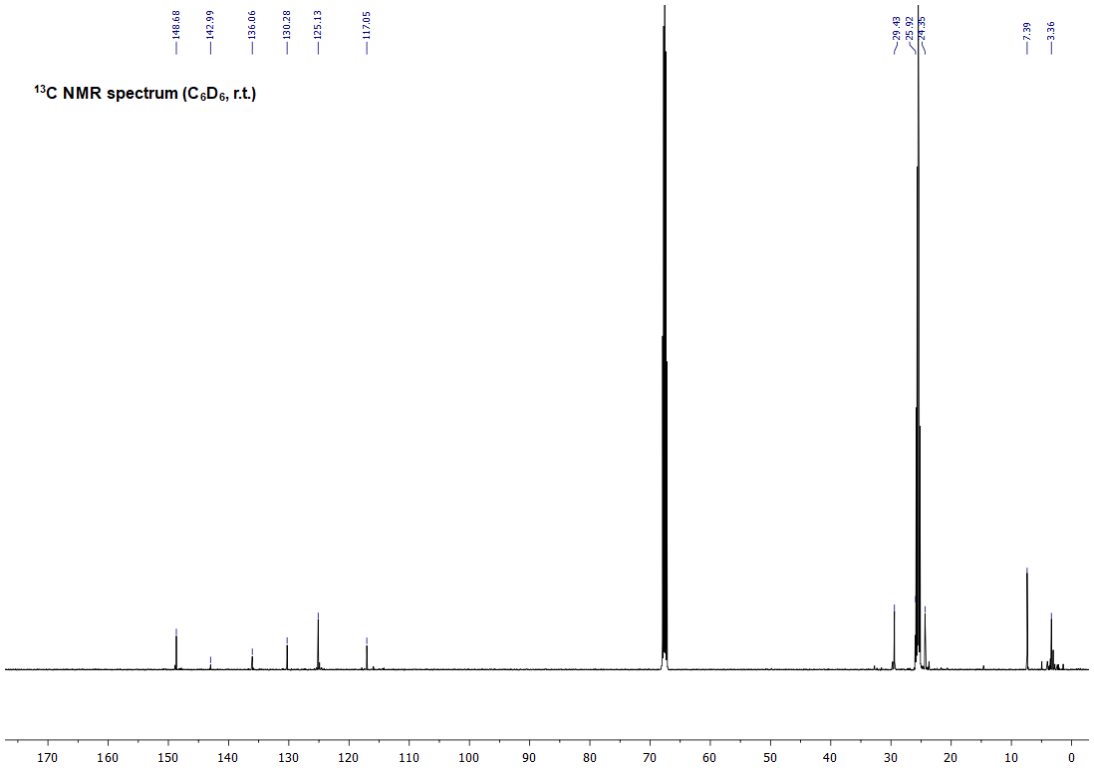


Figure S14: $^{13}$C NMR spectrum of transient disilene **INT** (THF-$d_8$, r.t.).

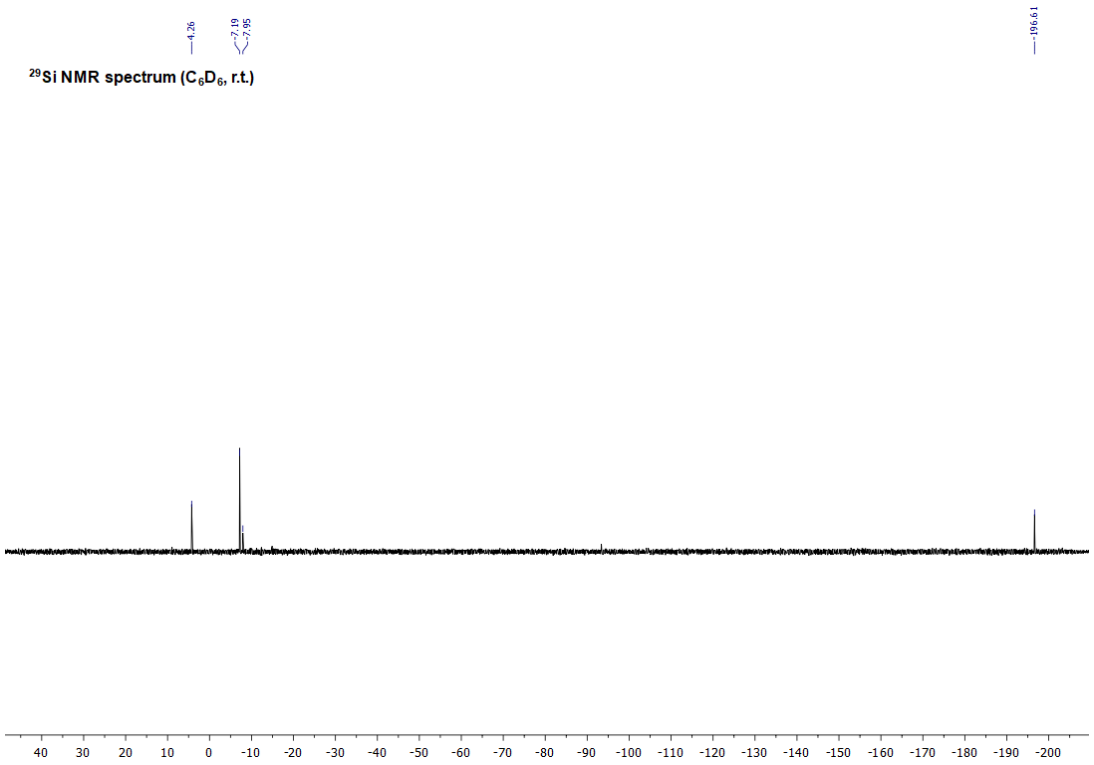


Figure S15: $^{29}$Si NMR spectrum of transient disilene **INT** (THF-$d_8$, r.t.).

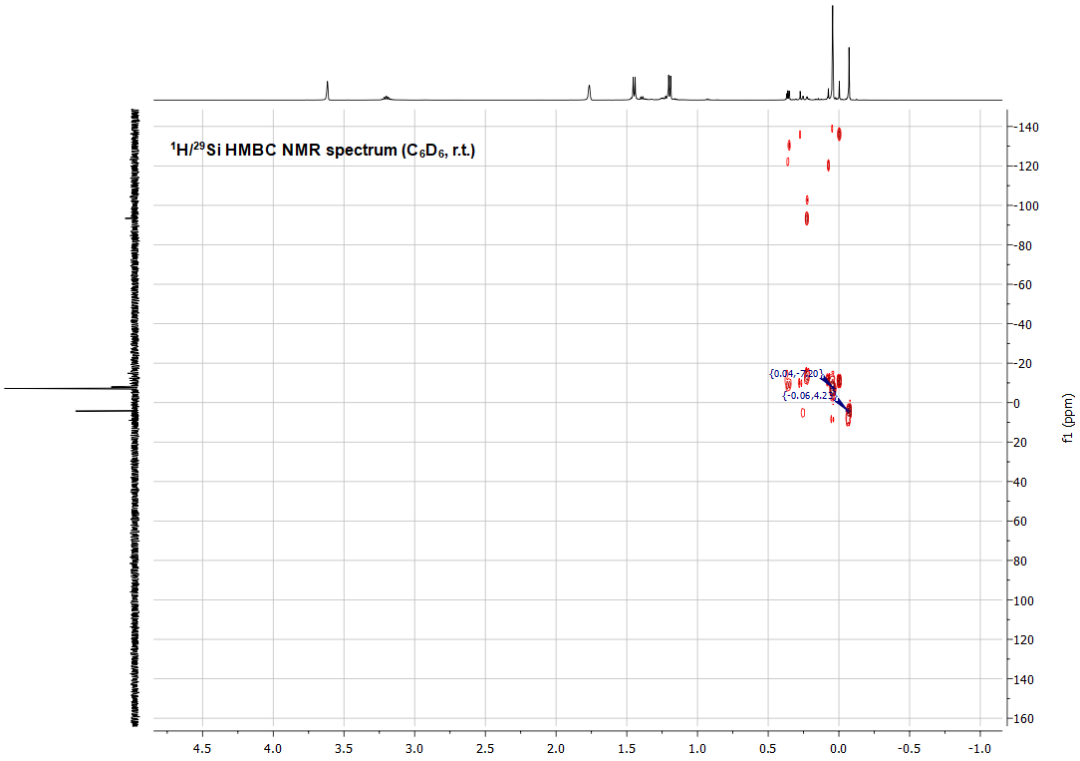


Figure S16: $^{1}$H/$^{29}$Si HMBC NMR spectrum of transient disilene **INT** (THF-$d_8$, r.t.).

**Synthesis of Silanone (Si*t*-Bu$_3$ Substituted) (2b)**

A solution of NaSi*t*-Bu$_3$(THF$_2$) (1.09 g, 2.98 mmol, 2.00 eq) in benzene (20 mL) was added to IPrNSiBr$_3$ (1.00 g, 1.49 mmol, 1.00 eq) in benzene (20 mL) at room temperature. The color rapidly changed to light green (approx. 1 sec) and then immediately to yellow with formation of a white precipitate. After stirring the solution for 20 min, the solvent was removed *in vacuo*. The obtained residue was extracted with *n*-hexane (3 × 20 mL) and filtered through a microfiber glass filter. The yellow solution was concentrated, cooled to –78 °C and exposed to $N_2O$ (1 bar). While warming up the solution to room temperature, a fine white precipitate forms, which is immediately separated *via* filtration, washed with *n*-hexane and dried *in vacuo* to give pure silanone **2b** (521 mg, 0.81 mmol, 54%) as a white powder. Colorless crystals of **2b** suitable for single crystal X-ray analysis were obtained by slow diffusion of $Et_2O$ into a saturated THF solution at –35 °C for several days. Compound **2b** is indefinitely stable as a solid at r.t. (no changes after 1 month), but quantitatively forms *N*,*O*-silylene **7** in $C_6D_6$ or THF-$d_8$ at room temperature within 48 h ($t_{1/2}$ = 24 h).

**Compound 2b:**

$^1$H NMR (500 MHz, $C_6D_6$, r.t.): δ = 7.25 – 7.19 (m, 2H, *p*-C*H*-Ar), 7.16 – 7.11 (m, 4H, *m*-C*H*-Ar), 6.11 (s, 2H, C*H*-N), 3.17 (hept, *J* = 6.8 Hz, 4H, C*H*), 1.49 (d, *J* = 6.8 Hz, 12H, C$H_3$), 1.13 (s, 27H, Si*t*-*Bu*$_3$), 1.12 (d, *J* = 6.8 Hz, 12H, C$H_3$).

$^{13}$C NMR (126 MHz, $C_6D_6$, r.t.): δ = 148.4 (N-*C*-N), 147.6 (*C*-Ar), 133.2 (*C*-Ar), 130.2 (*C*H-Ar), 124.3 (*C*H-Ar), 115.7 (*C*H-N), 31.8 (C(*C*H$_3$)$_3$), 29.1 (*C*H), 25.5 (*C*H$_3$), 23.4 (*C*H$_3$), 23.1 (*C*(CH$_3$)$_3$).

$^{29}$Si NMR (99 MHz, $C_6D_6$, r.t.): δ = 28.8 (*central Si*), 13.7 (Si*t*-Bu$_3$).

$^{29}$Si NMR (99 MHz, THF-$d_8$, r.t.): δ = 26.2 (*central Si*), 13.0 (Si*t*-Bu$_3$).

EA experimental (calculated): C 72.32 (72.50), H 9.97 (9.83), N 6.45 (6.50) %.

$M_p$: 126.5 °C (decomposition, color change from colorless to yellowish).

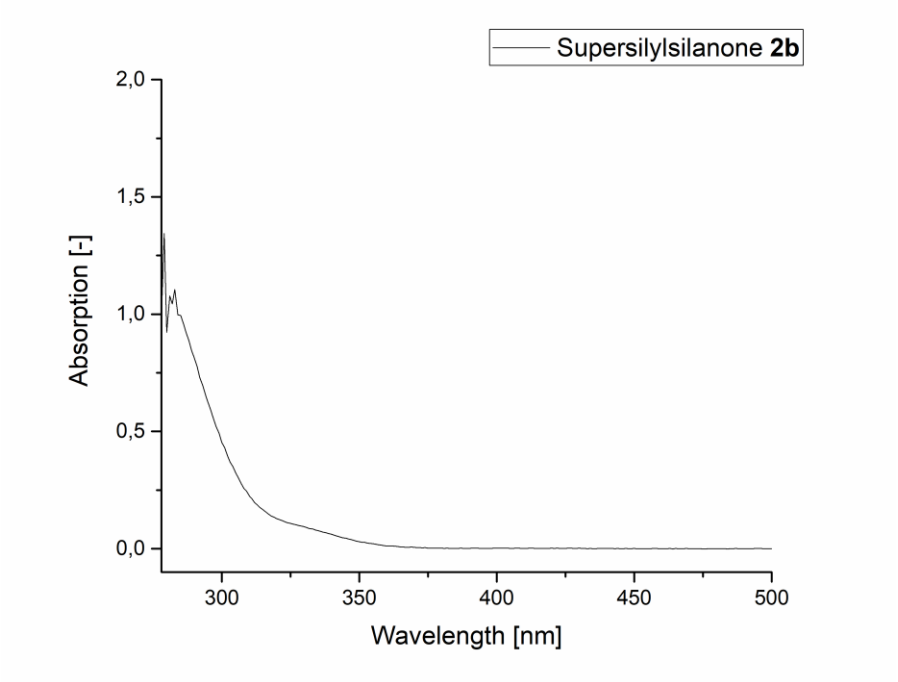


Figure S17. UV-Vis spectrum of silanone **2b** $\lambda_{max}$ (r.t., toluene, $4.0\times10^{-4}$ M) = 282 nm.

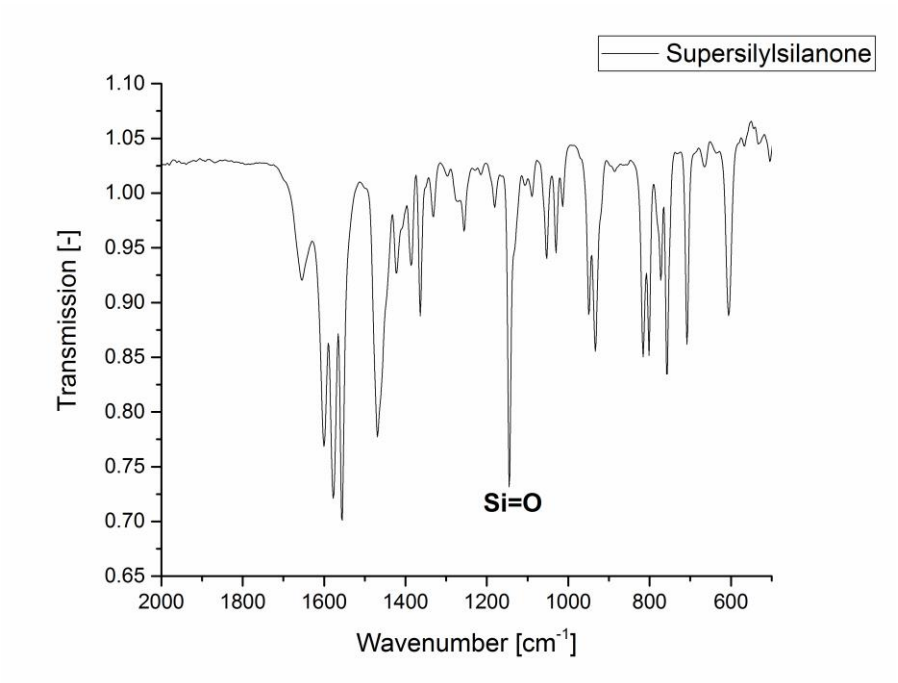


Figure S18: IR spectrum of silanone **2b** (cm$^{-1}$): 1649 (w), 1599 (m), 1577 (m), 1550 (s), 1463 (m), 1359 (w), 1144 (s, Si=O), 1051 (w), 1029 (w), 945 (w), 936 (m), 808 (m), 755 (m), 705 (m), 606 (m).

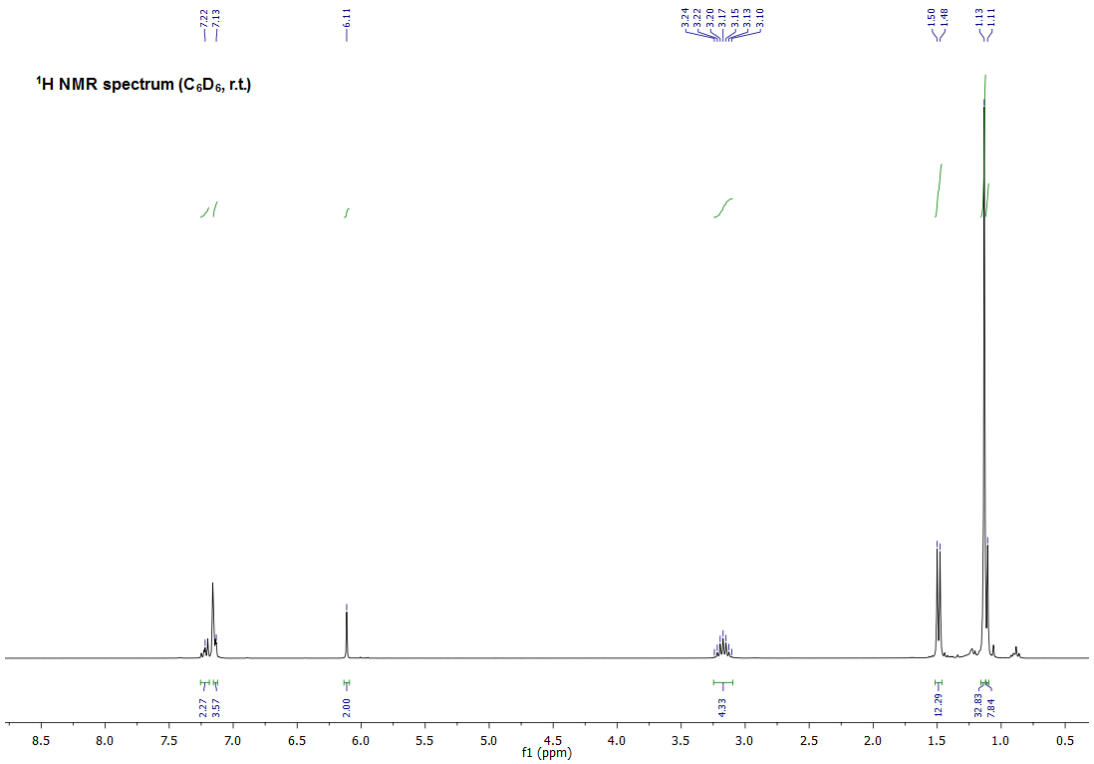


Figure S19: $^{1}$H NMR spectrum of silanone **2b** ($C_6D_6$, r.t.).

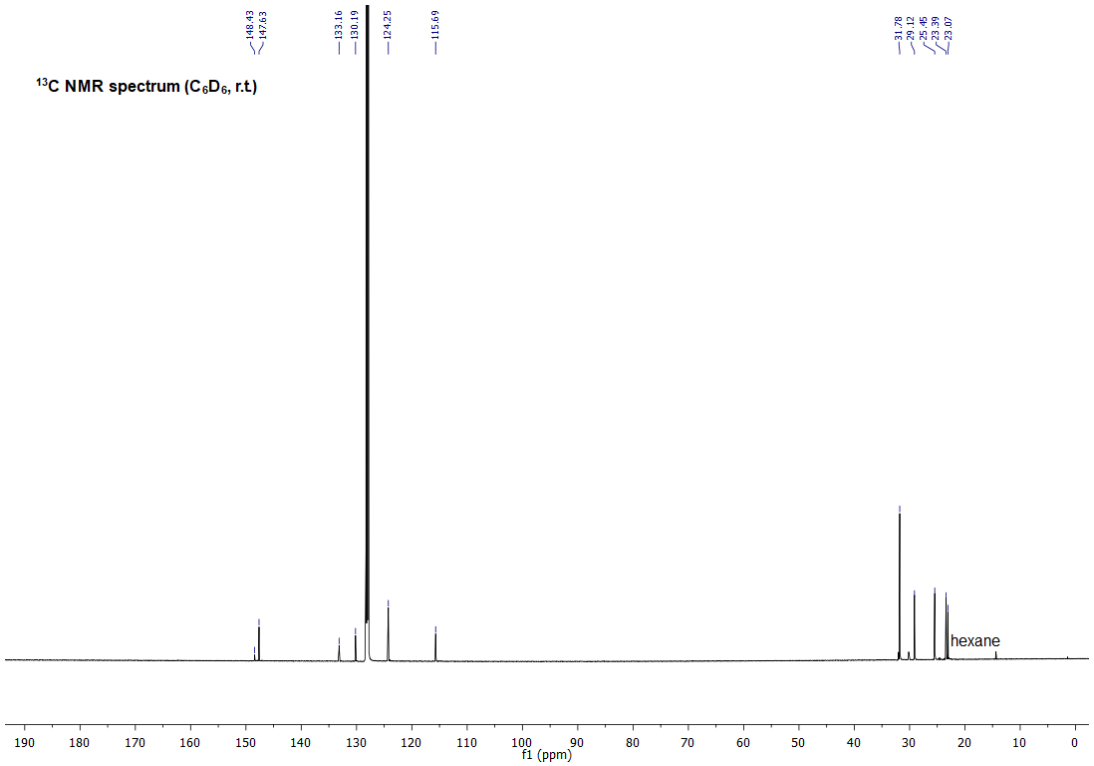


Figure S20: $^{13}$C NMR spectrum of silanone **2b** ($C_6D_6$, r.t.).

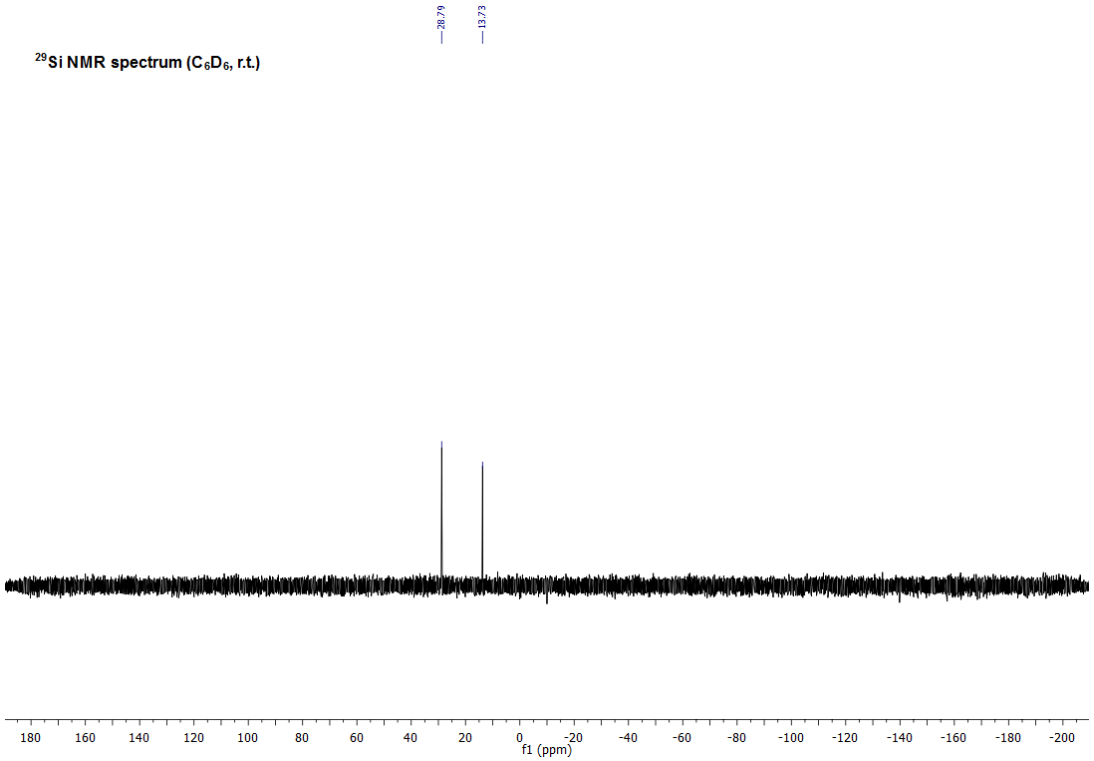


Figure S21: $^{29}$Si NMR spectrum of silanone **2b** ($C_6D_6$, r.t.).

**Synthesis of IPrNSi($O_2C$=O)$SiR_3$ (R = TMS 3a, R = *t*-Bu 3b)**

Similarly to the reaction of silepin **1a** with $CO_2$[S1], both silanones **2** can be directly converted with $CO_2$ to the respective silicon carbonate complexes **3**. Generally, a solution of **2** in $C_6D_6$ (0.5 mL) was exposed to $CO_2$ gas (1 bar) at room temperature in a J. Young PTFE tube. Monitoring the reaction *via* NMR spectroscopy showed the direct and quantitative formation of silicon carbonate complexes **3**.

**Compound 3a:**

The NMR shifts of this reaction product are identical to the published data.[S1]

$^1$H NMR (500 MHz, $C_6D_6$, r.t.): δ = 7.30 – 7.26 (m, 2H, *p*-C*H*-Ar), 7.19 – 7.16 (m, 4H, *m*-C*H*-Ar), 5.93 (s, 2H, C*H*-N), 2.95 (hept, *J* = 6.9 Hz, 4H, C*H*), 1.47 (d, *J* = 6.9 Hz, 12H, C$H_3$), 1.08 (d, *J* = 6.9 Hz, 12H, C$H_3$), 0.18 (s, 27H, Si*TMS*$_3$).

$^{13}$C NMR (126 MHz, $C_6D_6$, r.t.): δ = 150.4 ($O_2C$=O), 146.7 (*C*-Ar), 145.6 (N-*C*-N), 133.2 (*C*-Ar), 130.7 (*C*H-Ar), 124.8 (*C*H-Ar), 116.0 (*C*H-N), 29.2 (*C*H), 25.2 (*C*$H_3$), 23.2 (*C*$H_3$), 2.5 (Si*TMS*$_3$).

$^{29}$Si NMR (99 MHz, $C_6D_6$, r.t.): δ = -9.8 (*TMS*$_3$), -35.0 (*central Si*), -134.3 (*Si*TMS$_3$).

**Compound 3b:**

$^1$H NMR (500 MHz, $C_6D_6$, r.t.): δ = 7.33 – 7.26 (m, 2H, *p*-C*H*-Ar), 7.22 – 7.16 (m, 4H, *m*-C*H*-Ar), 5.97 (s, 2H, C*H*-N), 2.96 (hept, *J* = 6.9 Hz, 4H, C*H*), 1.45 (d, *J* = 6.9 Hz, 12H, C$H_3$), 1.08 (d, *J* = 6.9 Hz, 12H, C$H_3$), 1.05 (s, 27H, Si*t-Bu*$_3$).

$^{13}$C NMR (126 MHz, $C_6D_6$, r.t.): δ = 150.7 ($O_2C$=O), 146.8 (*C*-Ar), 145.5 (N-*C*-N), 133.3 (*C*-Ar), 130.6 (*C*H-Ar), 124.7 (*C*H-Ar), 116.2 (*C*H-N), 31.4 (C(*C*$H_3$)$_3$), 29.2 (*C*H), 25.4 (*C*$H_3$), 22.7 (*C*(C$H_3$)$_3$), 22.6 (*C*$H_3$).

$^{29}$Si NMR (99 MHz, $C_6D_6$, r.t.): δ = 5.5 (Si*t*-Bu$_3$), -43.0 (*central Si*).

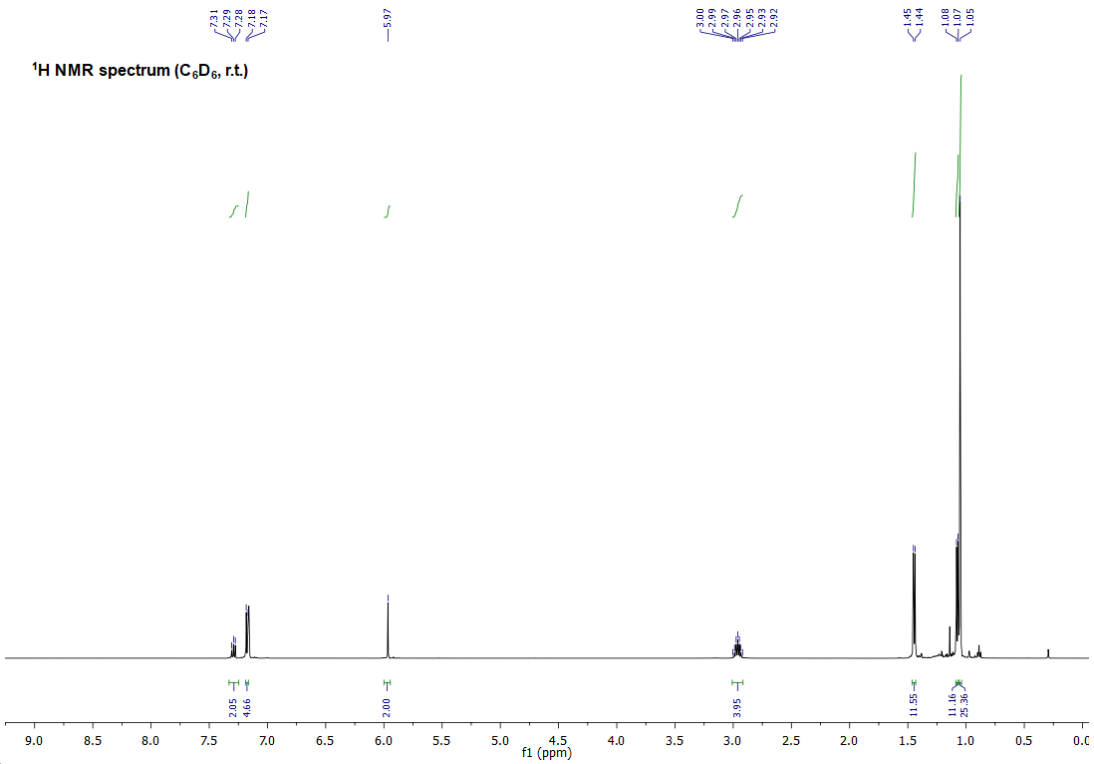


Figure S22: $^{1}$H NMR spectrum of silicon carbonate complex **3b** ($C_6D_6$, r.t.).

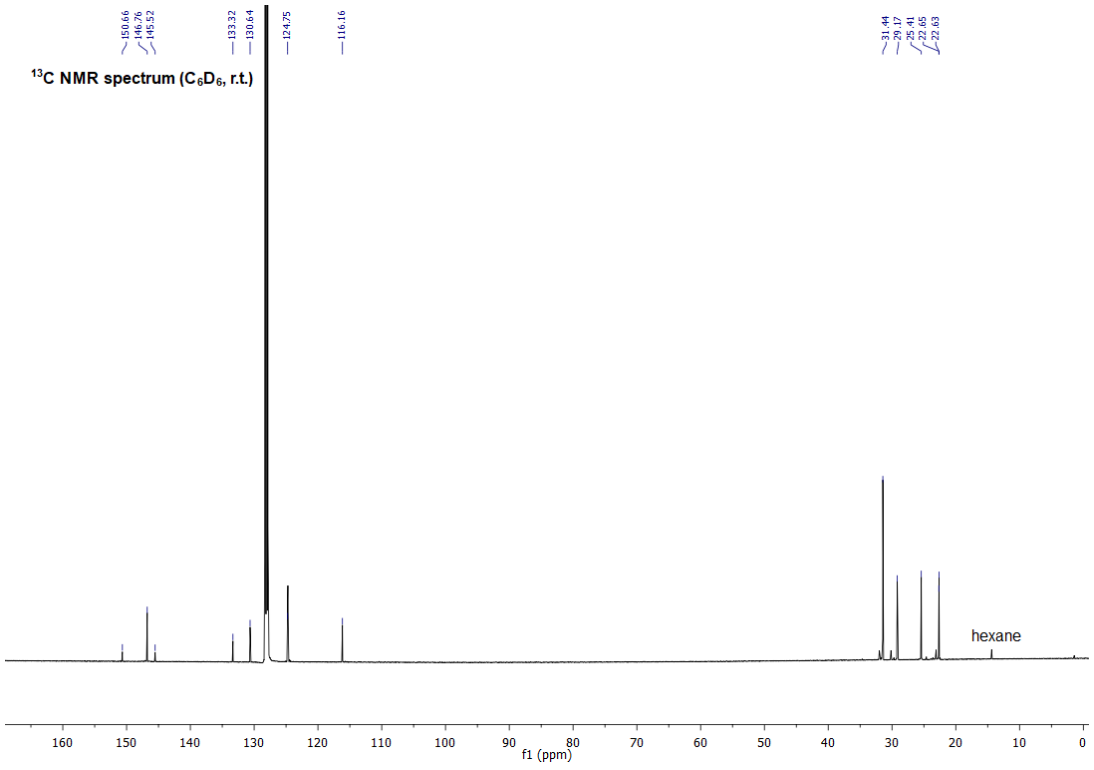


Figure S23: $^{13}$C NMR spectrum of silicon carbonate complex **3b** ($C_6D_6$, r.t.).

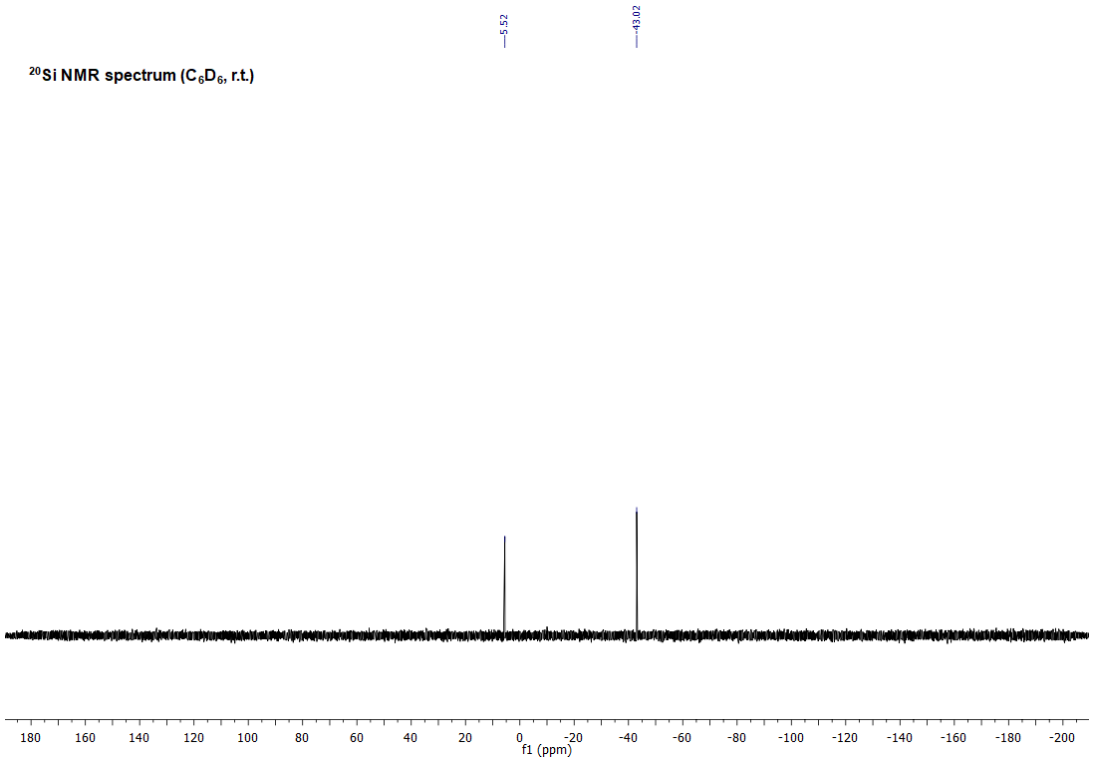


Figure S24: $^{29}$Si NMR spectrum of silicon carbonate complex **3b** ($C_6D_6$, r.t.).

**Synthesis of IPrNSi(OMe)(OH)SiR$_3$ (R = TMS 4a, R = *t*-Bu 4b)**

To a yellowish solution of **2a** (35 mg, 50.4 μmol, 1.00 eq) in toluene (2 mL) were added a few drops of methanol (dried and degassed). The solution immediately turned colorless and was stirred for additional 20 min. Removal of all volatiles and crystallization in toluene/*n*-hexane at -35 °C for 2 days gave compound **4a** (26 mg, 35.7 μmol, 71%) as colorless crystals suitable for single crystal X-ray analysis. The analogue procedure was repeated for the preparation of compound **4b** (69%). For the synthesis of **4a**, also acetonitrile solutions of tetra-coordinate silanone **2a** × $CD_3CN$ were used successfully.

**Compound 4a:**

$^1$H NMR (500 MHz, $C_6D_6$, r.t.): δ = 7.15 – 7.09 (m, 6H, C*H*-Ar), 5.94 (s, 2H, C*H*-N), 3.41 (s, 3H, OMe), 3.17 (overlapping hept, *J* = 6.9 Hz, 4H, C*H*), 1.45 (d, *J* = 6.9 Hz, 6H, C$H_3$), 1.42 (d, *J* = 6.9 Hz, 6H, C$H_3$) 1.13 (d, *J* = 6.9 Hz, 6H, C$H_3$), 1.11 (d, *J* = 6.9 Hz, 6H, C$H_3$), 0.28 (s, 27H, Si*TMS*$_3$).

$^{13}$C NMR (126 MHz, $C_6D_6$, r.t.): δ = 148.1 (*C*-Ar), 148.1 (*C*-Ar), 143.7 (N-*C*-N), 134.8 (*C*-Ar), 129.9 (*C*H-Ar), 124.4 (*C*H-Ar), 124.1 (*C*H-Ar), 114.9 (*C*H-N), 49.6 (O*C*H$_3$), 29.2 (*C*H), 28.9 (*C*H), 25.5 (*C*H$_3$), 25.2 (*C*H$_3$), 23.1 (*C*H$_3$), 23.0 (*C*H$_3$), 3.1 (Si*TMS*$_3$).

$^{29}$Si NMR (99 MHz, $C_6D_6$, r.t.): δ = -10.6 (*TMS*$_3$), -38.6 (*central Si*), -137.6 (*Si*TMS$_3$).

EA experimental (calculated): C 60.07 (61.18), H 9.21 (9.30), N 5.64 (5.78) %.

**Compound 4b:**

$^1$H NMR (500 MHz, $C_6D_6$, r.t.): δ = 7.18 – 7.14 (m, 2H, *m*-C*H*-Ar), 7.12 – 7.07 (m, 4H, *p*-C*H*-Ar) 5.96 (s, 2H, C*H*-N), 3.45 (s, 3H, OMe), 3.22 (hept, *J* = 6.9 Hz, 2H, C*H*), 3.11 (hept, *J* = 6.9 Hz, 2H, C*H*) 1.38 (d, *J* = 6.9 Hz, 12H, C$H_3$), 1.23 (s, 27H, Si*t-Bu*$_3$). 1.11 (d, *J* = 6.9 Hz, 6H, C$H_3$) 1.10 (d, *J* = 6.9 Hz, 6H, C$H_3$).

$^{13}$C NMR (126 MHz, $C_6D_6$, r.t.): δ = 148.0 (*C*-Ar), 147.9 (*C*-Ar), 143.2 (N-*C*-N), 134.9 (*C*-Ar), 129.9 (*C*H-Ar), 124.3 (*C*H-Ar), 124.1 (*C*H-Ar), 115.0 (*C*H-N), 49.7 (O*C*H$_3$), 31.9 (C(*C*H$_3$)$_3$), 28.9 (*C*H), 28.8 (*C*H), 25.7 (*C*H$_3$), 25.5 (*C*H$_3$), 22.7 (*C*H$_3$), 22.5 (*C*(CH$_3$)$_3$), 22.4 (*C*H$_3$).

$^{29}$Si NMR (99 MHz, $C_6D_6$, r.t.): δ = 1.2 (Si*t*-Bu$_3$), -46.6 (*central Si*).

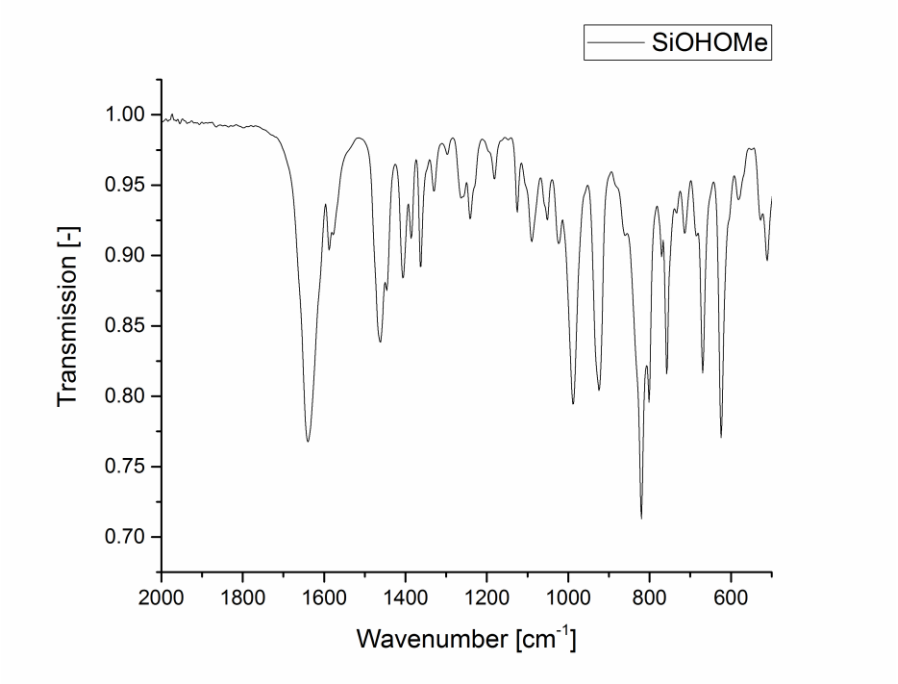


Figure S25: IR spectrum of compound **4a** ($cm^{-1}$): 1635 (s), 1584 (w), 1463 (m), 1403 (w), 1361 (w), 1237 (w), 1093 (w), 985 (s), 925 (s), 824 (s), 757 (m), 666 (m), 624 (s).

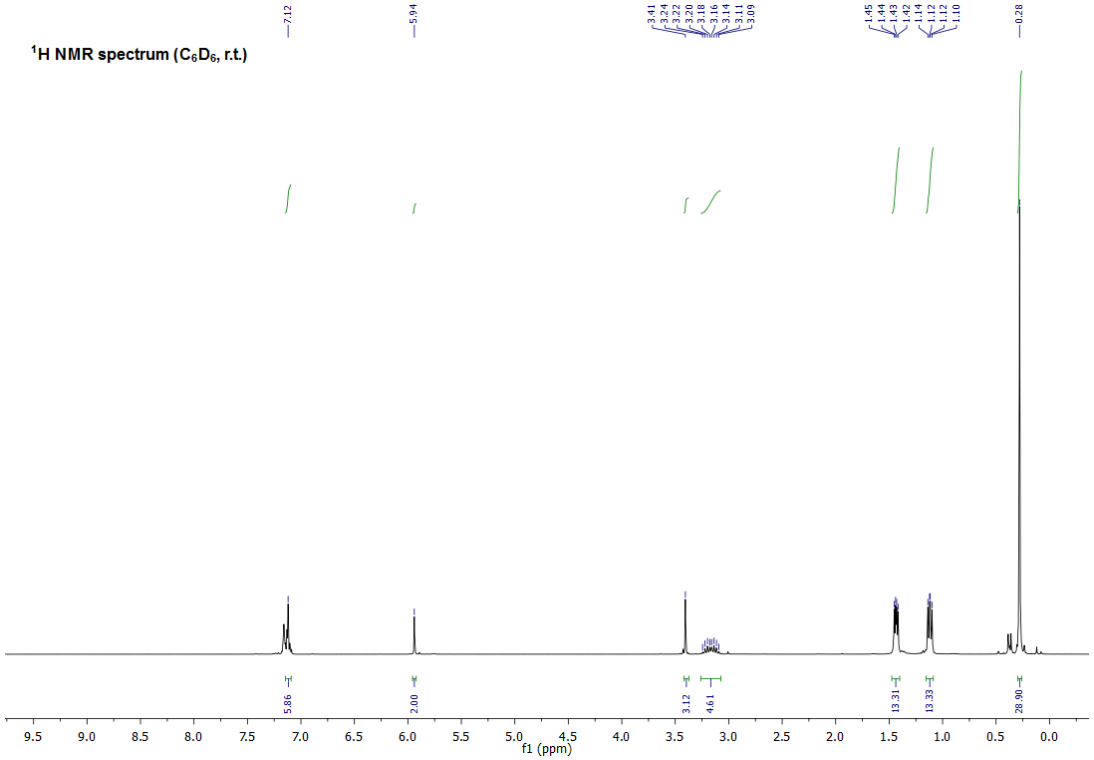


Figure S26: $^{1}H$ NMR spectrum of compound **4a** ($C_6D_6$, r.t.).

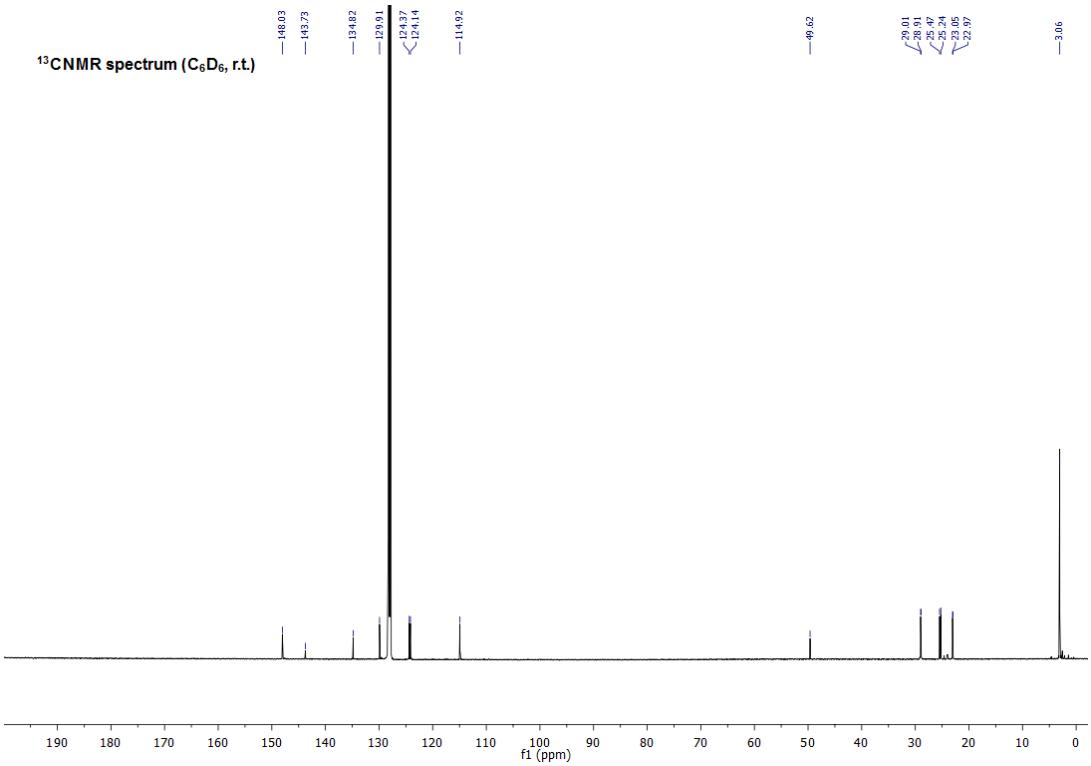


Figure S27: $^{13}C$ NMR spectrum of compound **4a** ($C_6D_6$, r.t.).

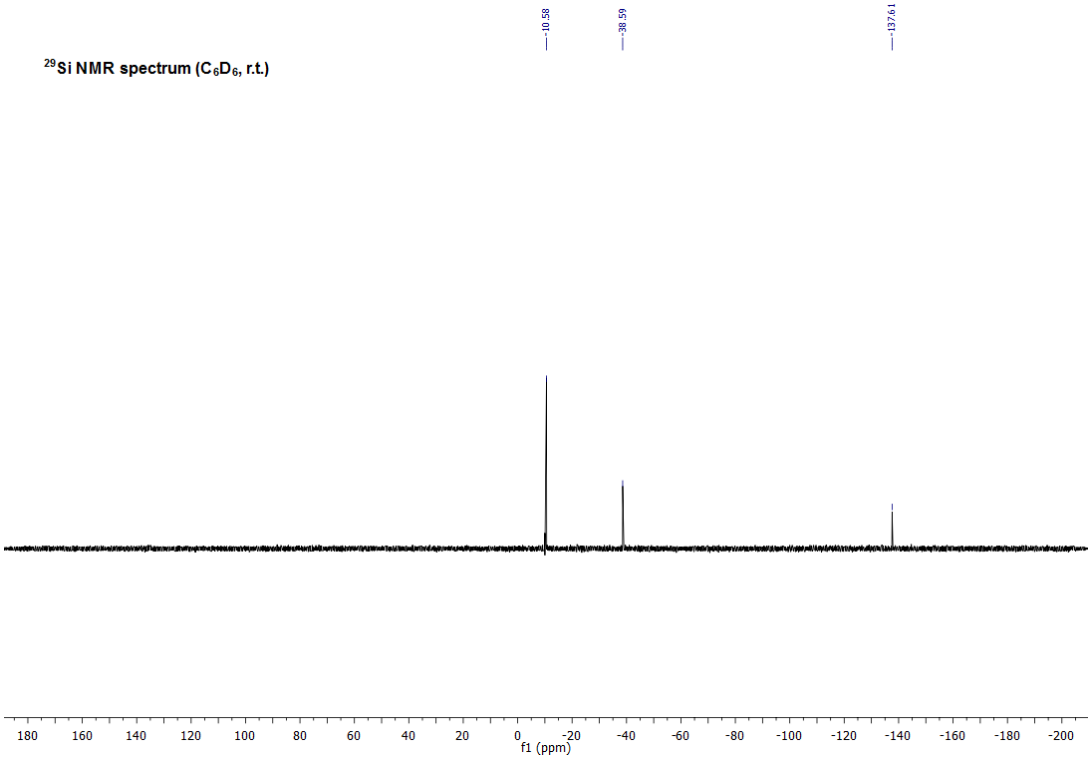


Figure S28: $^{29}Si$ NMR spectrum of compound **4a** ($C_6D_6$, r.t.).

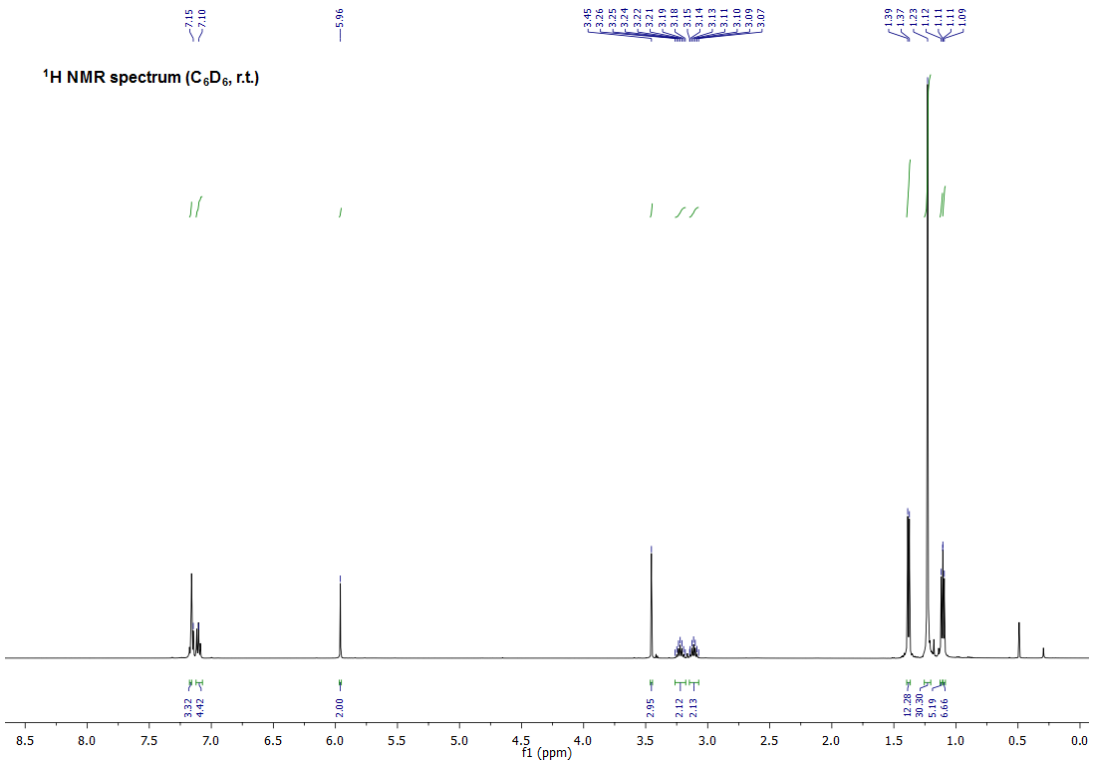


Figure S29: $^{1}$H NMR spectrum of compound **4b** ($C_6D_6$, r.t.).

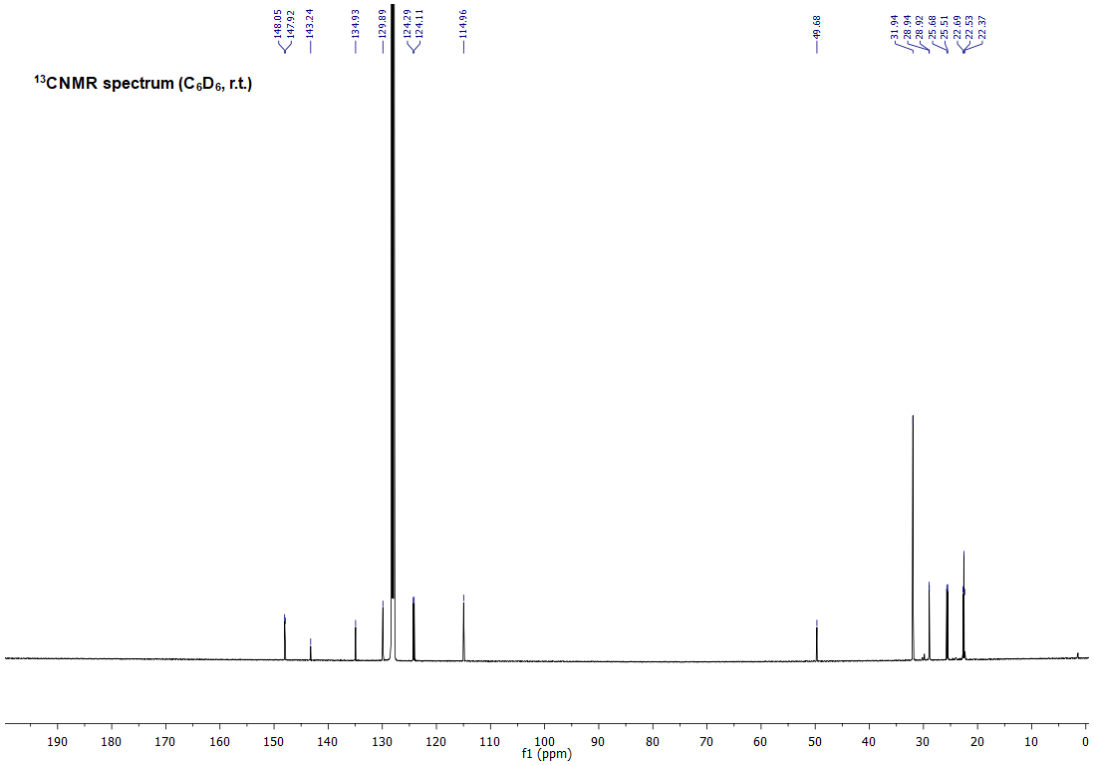


Figure S30: $^{13}$C NMR spectrum of compound **4b** ($C_6D_6$, r.t.).

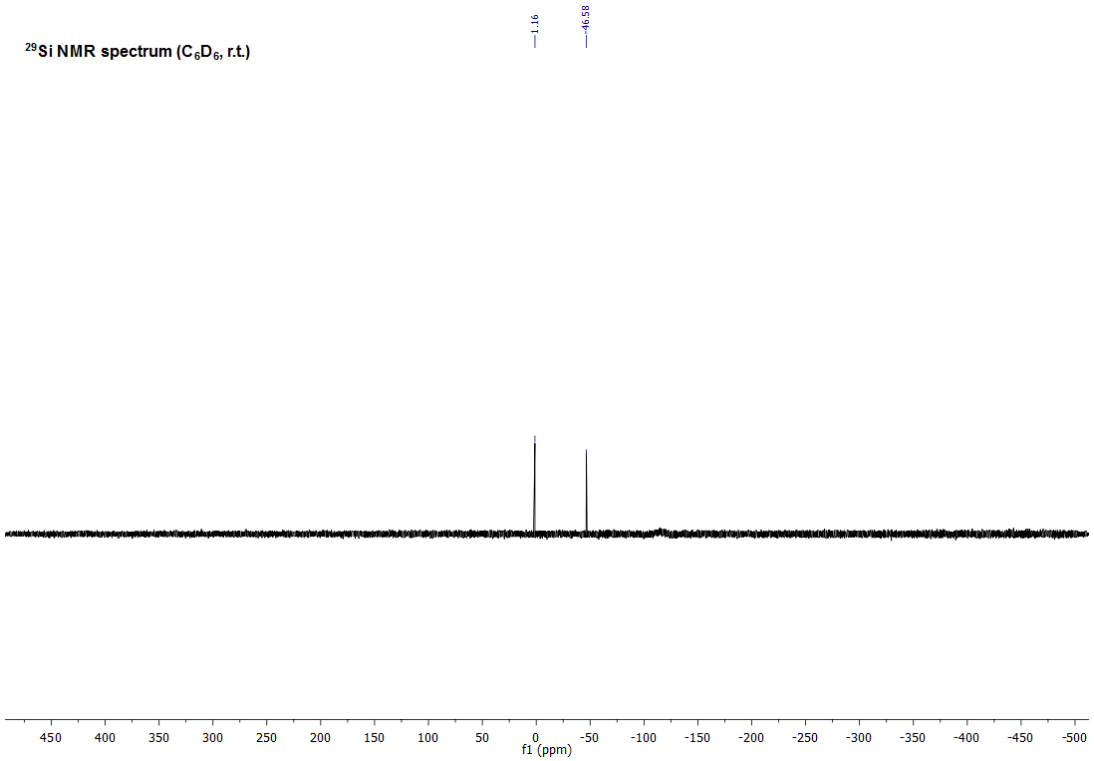


Figure S31: $^{29}$Si NMR spectrum of compound **4b** ($C_6D_6$, r.t.).

**Trapping Experiments of Transient Disilene INT with Ethylene and $IMe_4$**

**Synthesis of $IPrNTMSOSi(CH_2CH_2)SiTMS_2$ (5)**

A J. Young PTFE tube was loaded with solid silanone **2a** (14 mg, 20.2 µmol, 1.00 eq), addition of THF-$d_8$ (0.5 mL) instantly formed a strongly yellow colored solution of transient disilene **INT** (NMR data see above). Subsequently, the solution was exposed to ethylene gas (1 bar) and monitored *via* NMR spectroscopy. After 10 min the yellow color faded completely and full conversion to 1,2-disilacyclobutane **5** was detected (structure verified *via* 2D NMR experiments and matching theoretical NMR shifts). In a second experiment, the slow decomposition of **2a** in $C_6D_6$ was repeated in ethylene atmosphere, here as well the formation of 1,2-disiletane **5** was observed.

$^1$H NMR (500 MHz, THF-$d_8$, r.t.): δ = 7.35 – 7.30 (m, 2H, *m*-C*H*-Ar), 7.27 – 7.23 (m, 4H, *m*-C*H*-Ar), 6.55 (s, 2H, C*H*-N), 3.20 (hept, *J* = 6.9 Hz, 2H, C*H*), 3.12 (hept, *J* = 6.9 Hz, 2H, C*H*), 1.32 (d, *J* = 6.9 Hz, 12H, C$H_3$), 1.30 (d, *J* = 6.9 Hz, 6H, C$H_3$) 1.21 (d, *J* = 6.9 Hz, 6H, C$H_3$), 1.15 (d, *J* = 6.9 Hz, 6H, C$H_3$), 0.99 – 0.94 (m, 2H, Si(C$H_2$CH$_2$)Si), 0.50 – 0.41 (m, 2H, Si(CH$_2$C$H_2$)Si), 0.39 – 0.36 (m, 1H, Si(C$H_2$CH$_2$)Si), 0.06 (s, 9H, Si*TMS*$_2$), -0.07 (s, 9H, Si*TMS*$_2$) -0.11 (s, 9H, O*TMS*).

$^{13}$C NMR (126 MHz, THF-$d_8$, r.t.): δ = 148.3 (*C*-Ar), 148.1 (*C*-Ar), 143.1 (N-*C*-N), 135.7 (*C*-Ar), 130.0 (*C*H-Ar), 125.0 (*C*H-Ar), 124.9 (*C*H-Ar), 116.1 (*C*H-N), 31.1 (Si(*C*H$_2$CH$_2$)Si), 29.5 (*C*H), 24.5 (*C*H$_3$), 24.0 (*C*H$_3$), 3.2 (O*TMS*), 1.6 (Si*TMS*$_2$), 1.5 (Si*TMS*$_2$),-0.3 (Si(CH$_2$*C*H$_2$)Si).

$^{29}$Si NMR (99 MHz, THF-$d_8$, r.t.): δ = 4.3 (O*TMS*), -14.6 (Si*TMS*$_2$), -14.8 (Si*TMS*$_2$), -35.7 (*Si*OTMS), -39.8 (*Si*TMS$_2$).

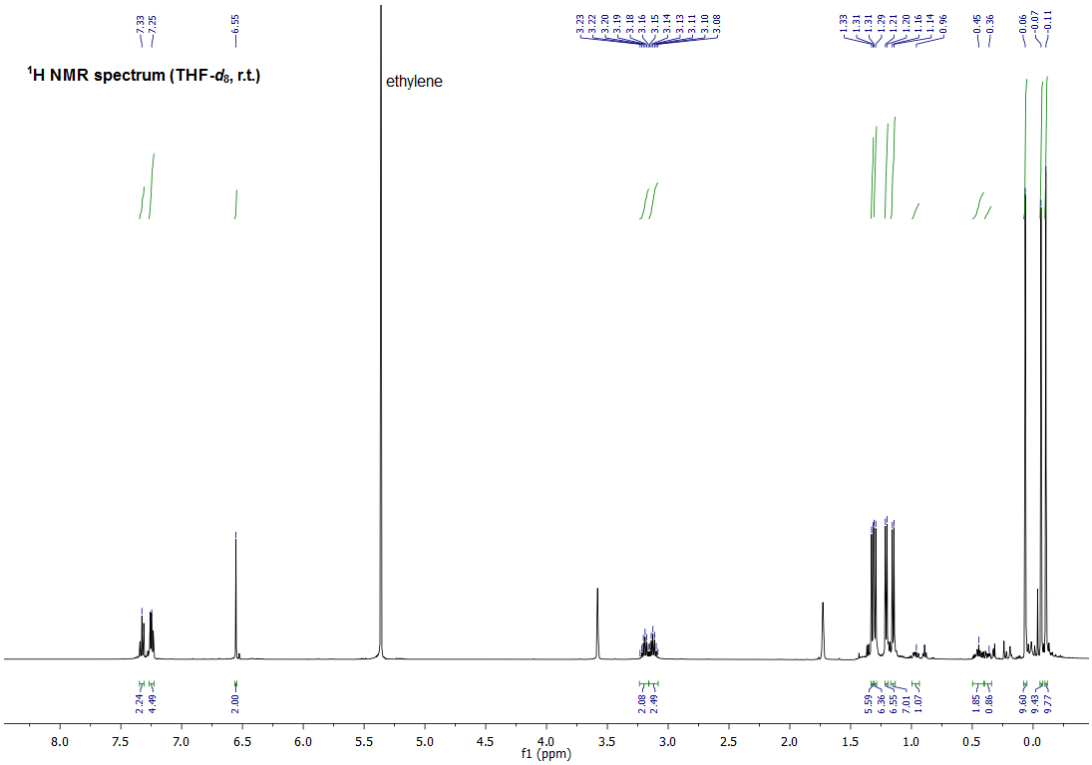


Figure S32: $^{1}$H NMR spectrum of 1,2-disiletane **5** (THF-$d_8$, r.t.).

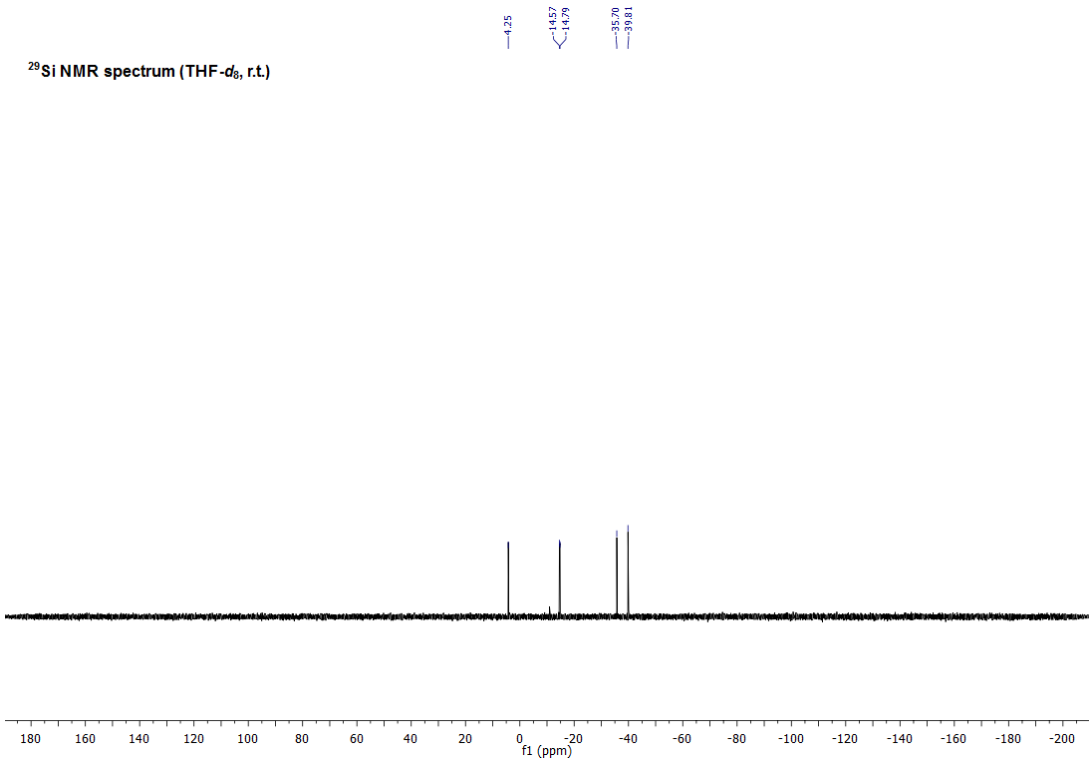


Figure S33: $^{29}$Si NMR spectrum of 1,2-disiletane **5** (THF-$d_8$, r.t.)

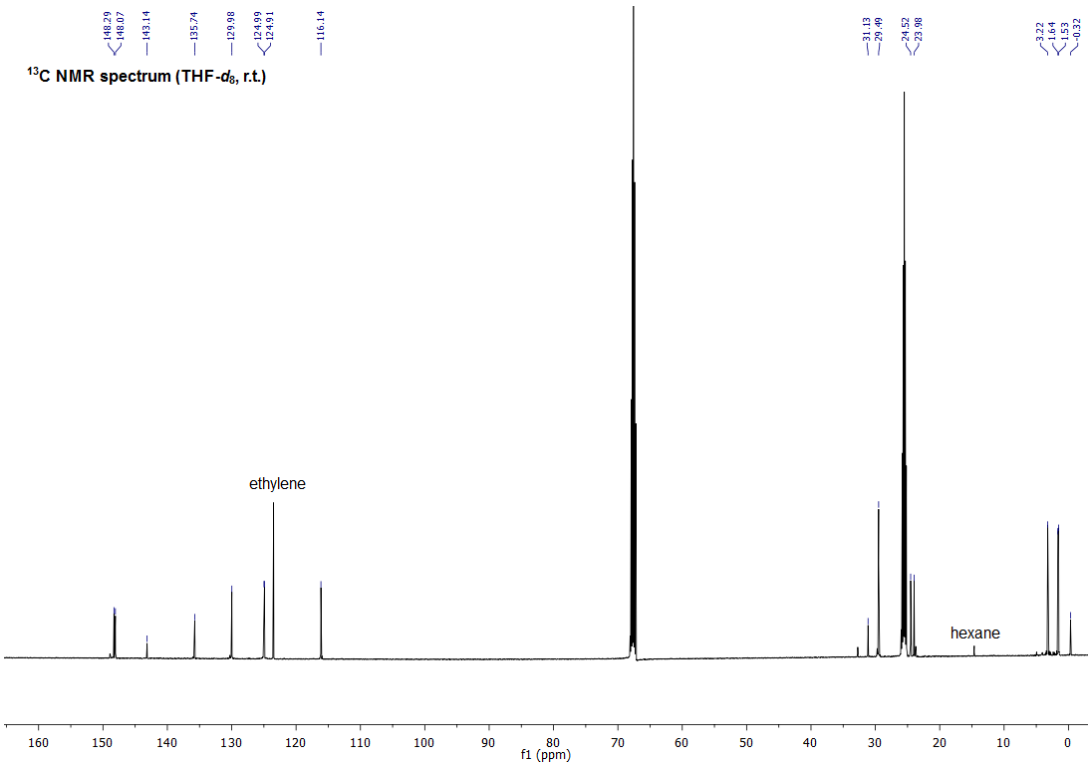


Figure S34: $^{13}$C NMR spectrum of 1,2-disiletane **5** (THF-$d_8$, r.t.)

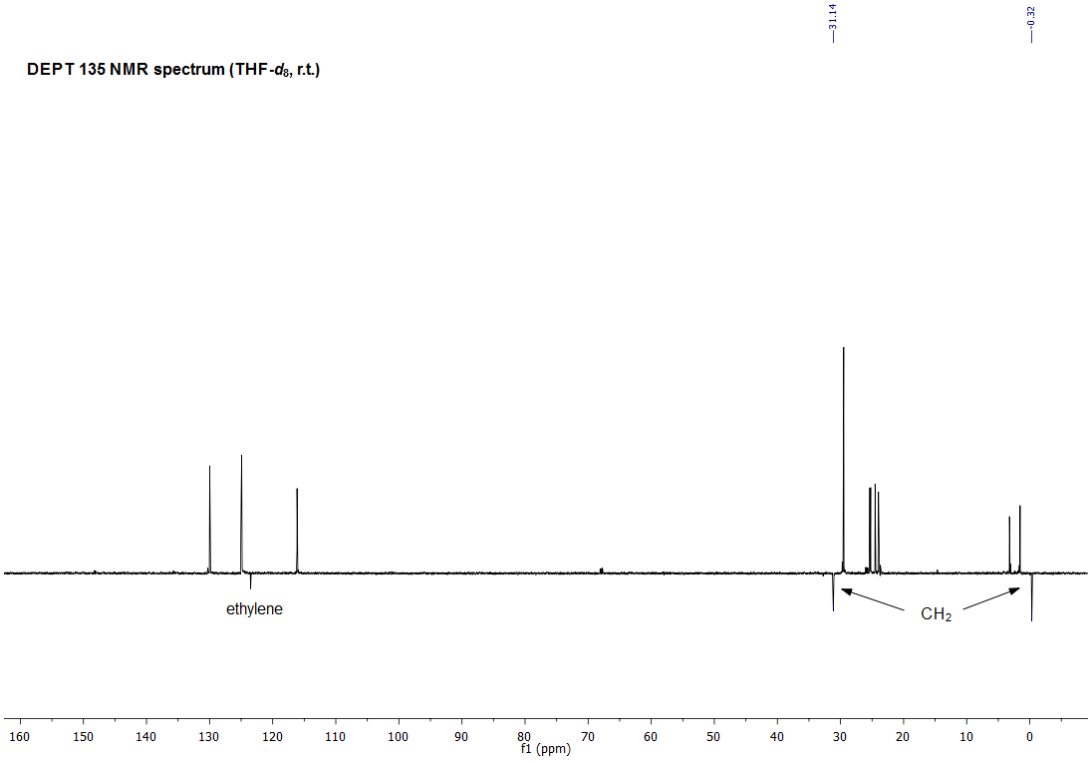


Figure S35: DEPT 135 NMR spectrum of 1,2-disiletane **5** (THF-$d_8$, r.t.)

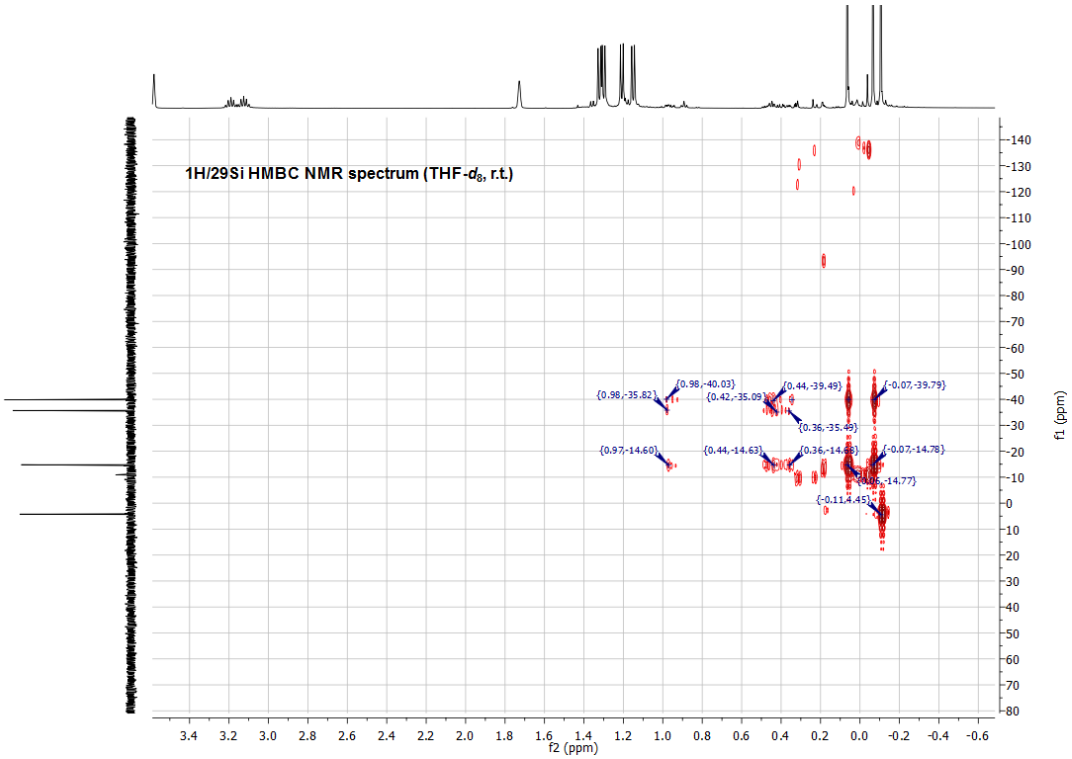


Figure S36: $^{1}H/^{29}Si$ HMBC NMR spectrum of 1,2-disiletane **5** (THF-$d_8$, r.t.)

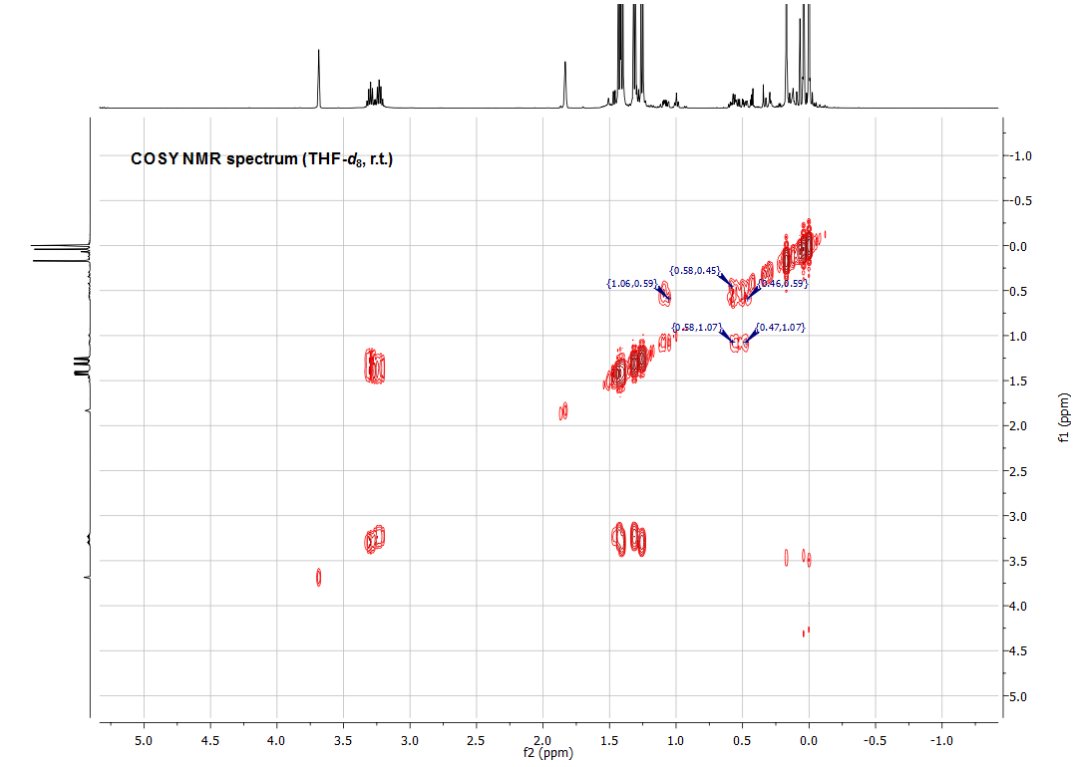


Figure S37: COSY NMR spectrum of 1,2-disiletane **5** (THF-$d_8$, r.t.)

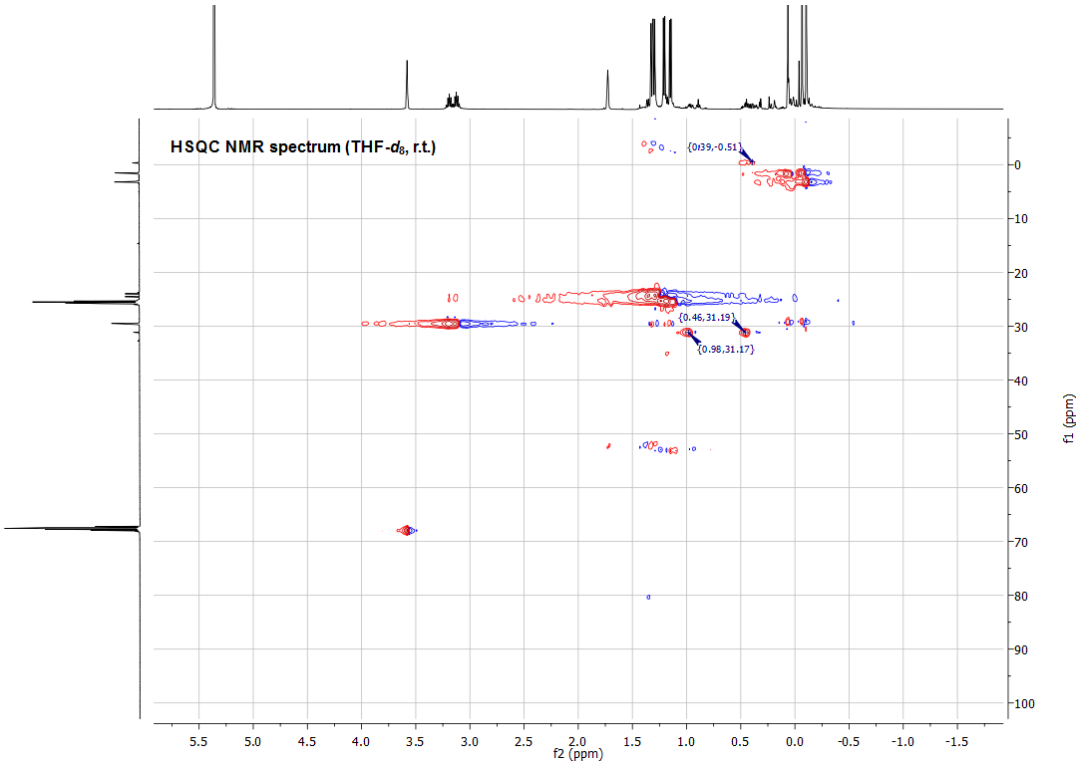


Figure S38: HSQC NMR spectrum of 1,2-disiletane **5** (THF-$d_8$, r.t.)

**Synthesis of $IMe_4$ Stabilized Zwitterionic Disilene (6)**

To a yellowish toluene (2 mL) solution of **2a** (29 mg, 41.9 μmol, 1.00 eq) was added $IMe_4$ (5.2 mg, 41.9 μmol, 1.00 eq) in toluene (1 mL). The solution immediately turned orange-red and was stirred additional 20 min. Removal of all volatiles and crystallization from *n*-hexane at -35 °C for 1 day gave $IMe_4$ stabilized zwitterionic disilene **6** (20 mg, 24.4 μmol, 58%) as orange-red crystals suitable for single crystal X-ray analysis. Compound **6** is permanently stable as a solid and in $C_6D_6$ solution at room temperature. Alternatively, intermediary disilene **INT** can also be trapped, by first inducing the 1,3-silyl migration of silanone **2a** with THF, followed by the addition of $IMe_4$.

$^1$H NMR (500 MHz, $C_6D_6$, r.t.): δ = 7.22 – 7.13 (m, 4H, *m*-C*H*-Ar), 6.98 – 6.93 (m, 2H, *p*-C*H*-Ar), 5.91 (s, 2H, C*H*-N), 3.44 (hept, *J* = 6.9 Hz, 2H, C*H*), 3.13 (s, 6H, $IMe_4$-NC$H_3$), 3.09 (hept, *J* = 6.9 Hz, 2H, C*H*), 1.40 (d, *J* = 6.9 Hz, 12H, C$H_3$), 1.34 (s, 6H, $IMe_4$-C$H_3$), 1.12 (d, *J* = 6.9 Hz, 6H, C$H_3$), 1.08 (d, *J* = 6.9 Hz, 6H, C$H_3$), 0.42 (s, 18H, Si*TMS*$_2$), 0.28 (s, 9H, O*TMS*).

$^{13}$C NMR (126 MHz, $C_6D_6$, r.t.): δ = 156.3 ($IMe_4$-N-*C*-N), 148.3 (*C*-Ar), 148.2 (*C*-Ar), 140.2 (N-*C*-N), 135.9 (*C*-Ar), 129.2 (*C*H-Ar), 124.8 (*C*H-Ar), 124.3 (*C*H-Ar), 124.2 ($IMe_4$-*C*=*C*), 115.3 (*C*H-N), 33.2 ($IMe_4$-NC$H_3$), 28.7 (*C*H), 28.4 (*C*H), 25.7 (*C*$H_3$), 24.5 (*C*$H_3$), 22.0 (*C*$H_3$), 7.9 ($IMe_4$-C*C*$H_3$), 7.2 (Si*TMS*$_2$), 4.8 (O*TMS*).

$^{29}$Si NMR (99 MHz, $C_6D_6$, r.t.): δ = 6.1 (O*TMS*), -7.1 (Si*TMS*$_2$), -35.2 (*Si*OTMS), -174.6 (*Si*TMS$_2$).

EA experimental (calculated): C 62.37 (63.10), H 9.16 (9.24), N 8.06 (8.56) %.

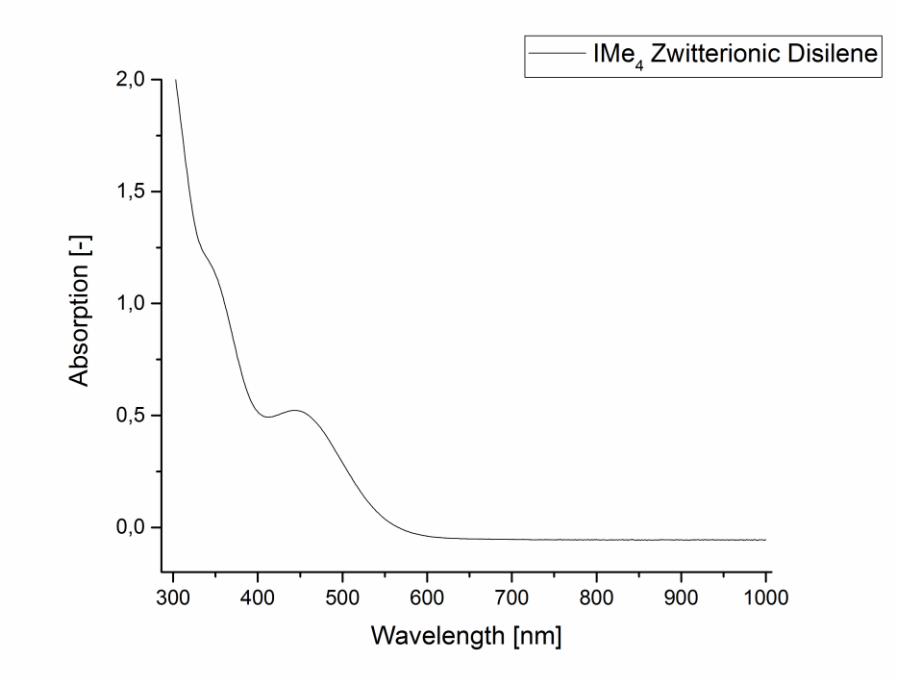


Figure S39. UV-Vis spectrum of $IMe_4$ stabilized zwitterionic disilene **6** $\lambda_{max}$ (r.t., toluene, $4.0\times10^{-4}$ M) = 342, 449 nm.

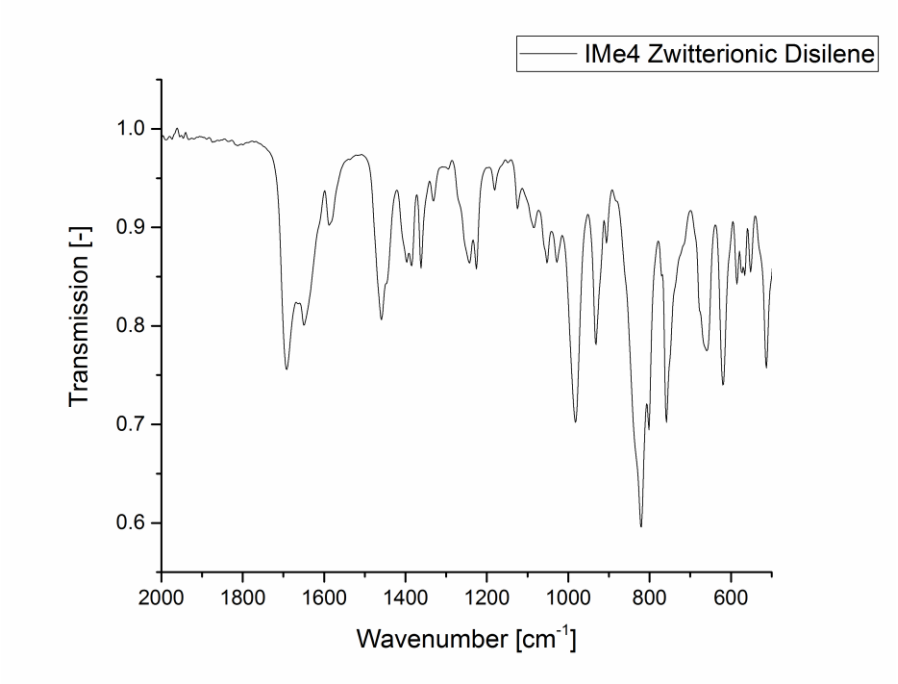


Figure S40: IR spectrum of $IMe_4$ stabilized zwitterionic disilene **6** ($cm^{-1}$): 1690 (m), 1641 (m), 1586 (s), 1454 (m), 1401 (s), 1229 (s), 978 (m), 929 (m), 832 (s), 751 (m), 662 (m), 615 (m).

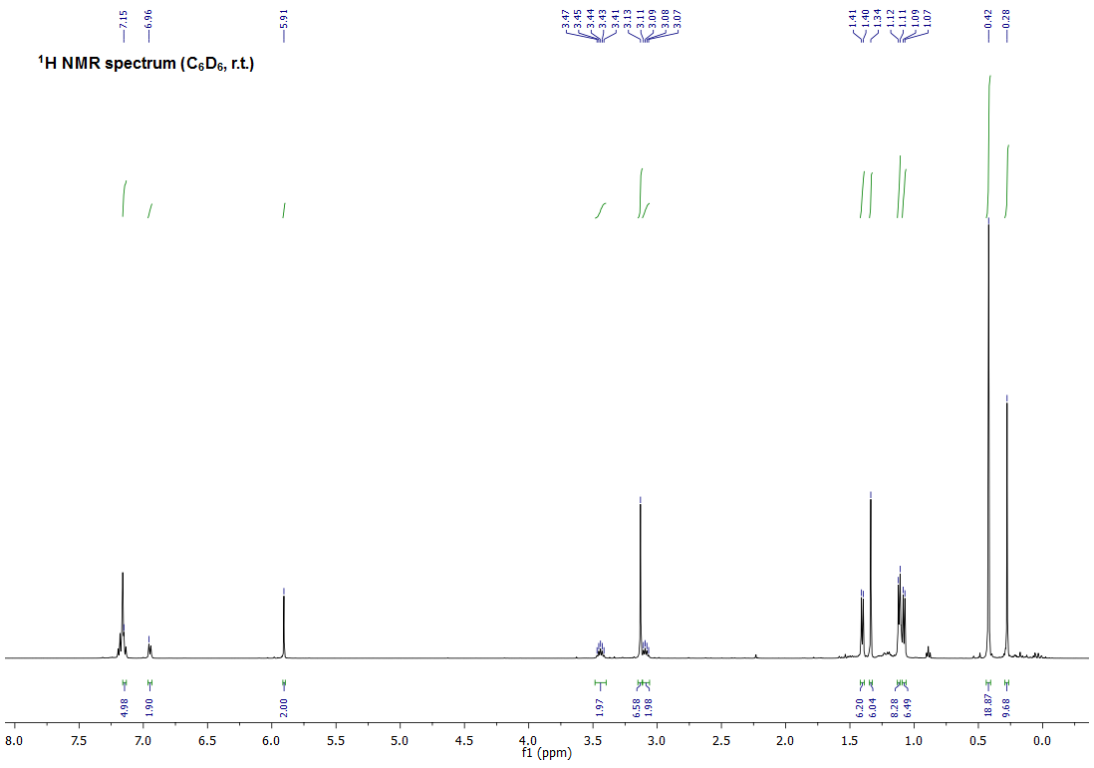


Figure S41: $^1H$ NMR spectrum of $IMe_4$ stabilized zwitterionic disilene **6** ($C_6D_6$, r.t.).

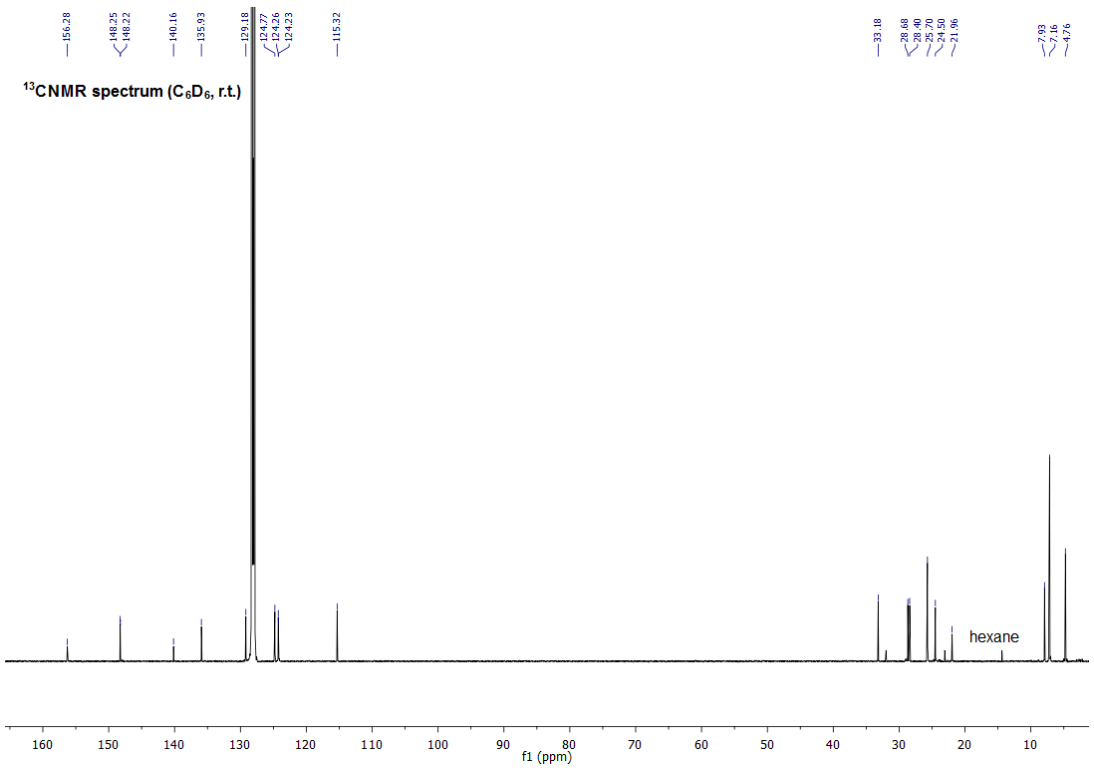


Figure S42: $^{13}C$ NMR spectrum of $IMe_4$ stabilized zwitterionic disilene **6** ($C_6D_6$, r.t.).

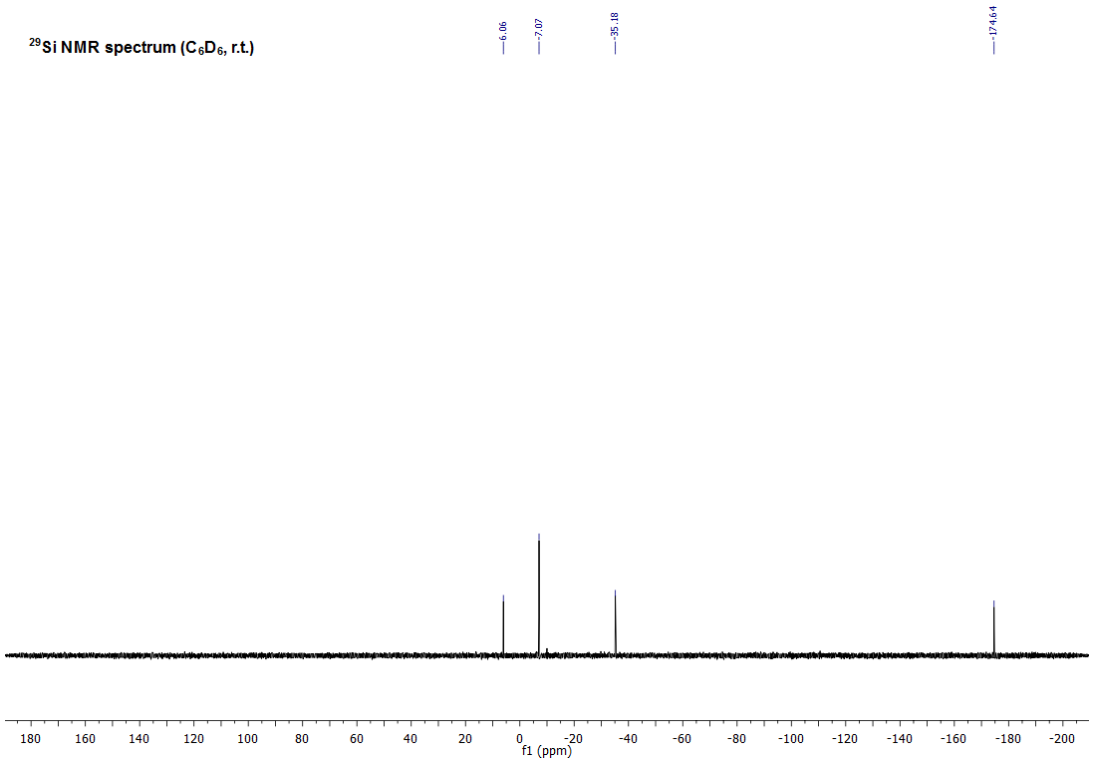


Figure S43: $^{29}Si$ NMR spectrum of $IMe_4$ stabilized zwitterionic disilene **6** ($C_6D_6$, r.t.).

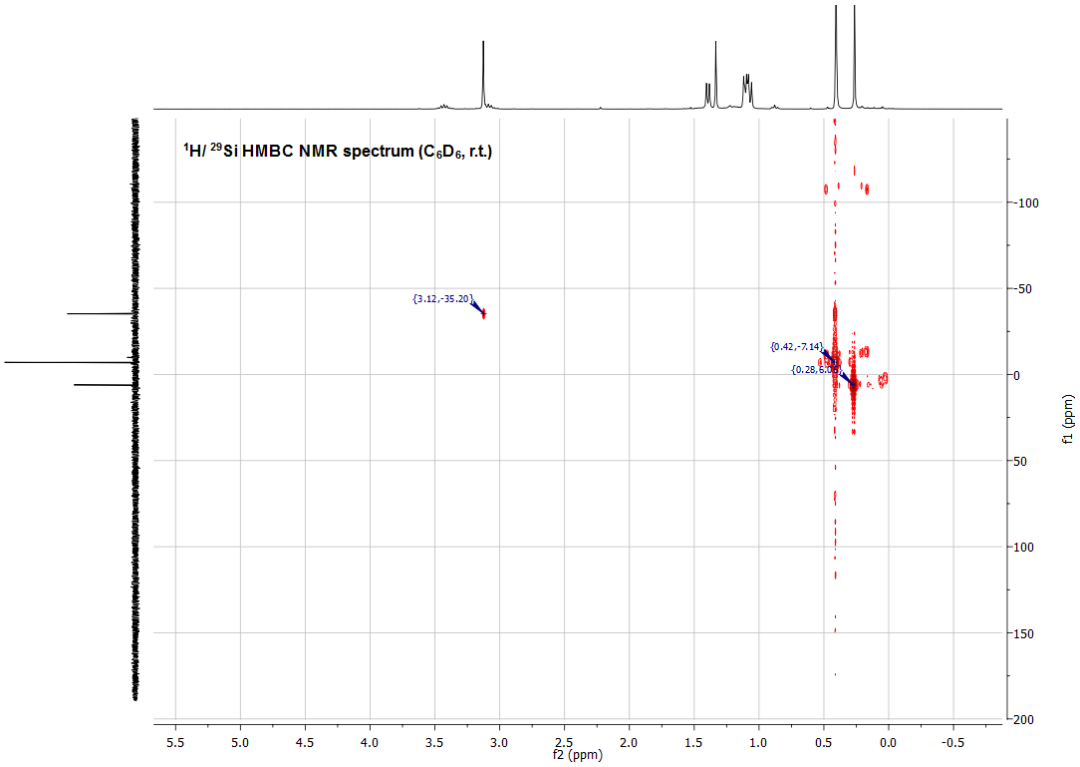


Figure S44: $^{1}H/^{29}Si$ HMBC NMR spectrum of $IMe_4$ stabilized zwitterionic disilene **6** ($C_6D_6$, r.t.).

**Synthesis of IPrNSi(II)OSi*t*-Bu$_3$ (7)**

As already stated, silanone **2b** quantitatively forms *N*,*O*-silylene **7** in $C_6D_6$ or THF-$d_8$ at room temperature within 48 h ($t_{1/2}$ = 24 h). By heating the solution to 60 °C, this transformation can be accelerated and full conversion was detected by NMR spectroscopy in less than 1 h. Hence, a solution of **2b** (100 mg, 155 µmol, 1.00 eq) in toluene (5 mL) was heated to 60 °C for 1 h. Removal of all volatiles gave *N*,*O*-silylene **7** as colorless solid (100 mg, 155 µmol, quantitative yield). Crystals suitable for single crystal X-ray analysis were obtained by cooling a concentrated *n*-hexane solution of **7** at -35 °C for several days. *N*,*O*-Silylene **7** is completely stable as a solid and in solution at room temperature.

$^1$H NMR (500 MHz, $C_6D_6$, r.t.): δ = 7.24 – 7.17 (m, 2H, *p*-C*H*-Ar), 7.15 – 7.09 (m, 4H, *m*-C*H*-Ar), 5.99 (s, 2H, C*H*-N), 3.10 (hept, *J* = 6.8 Hz, 4H, C*H*), 1.46 (d, *J* = 6.8 Hz, 12H, C$H_3$), 1.17 (d, *J* = 6.8 Hz, 12H, C$H_3$), 1.07 (s, 27H, Si*t*-*Bu*$_3$).

$^{13}$C NMR (126 MHz, $C_6D_6$, r.t.): δ =, 147.7 (*C*-Ar), 146.6 (N-*C*-N) 133.5 (*C*-Ar), 129.9 (*C*H-Ar), 124.0 (*C*H-Ar), 114.9 (*C*H-N), 30.3 (C(*C*H$_3$)$_3$), 29.1 (*C*H), 24.6 (*C*H$_3$), 23.8 (*C*H$_3$), 22.8 (*C*(CH$_3$)$_3$).

$^{29}$Si NMR (99 MHz, $C_6D_6$, r.t.): δ = 58.9 (*central Si*), 4.4 (Si*t*-Bu$_3$).

EA experimental (calculated): C 71.92 (72.50), H 10.02 (9.83), N 6.31 (6.50) %.

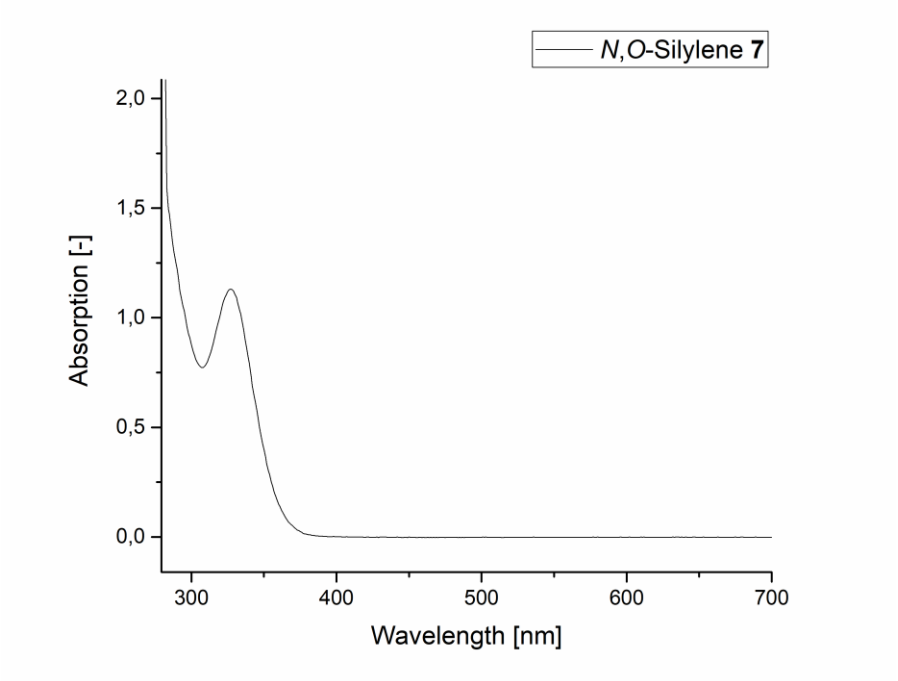


Figure S45. UV-Vis spectrum of *N*,*O*-silylene **7** $\lambda_{max}$ (r.t., toluene, $8.0\times10^{-4}$ M) = 328 nm.

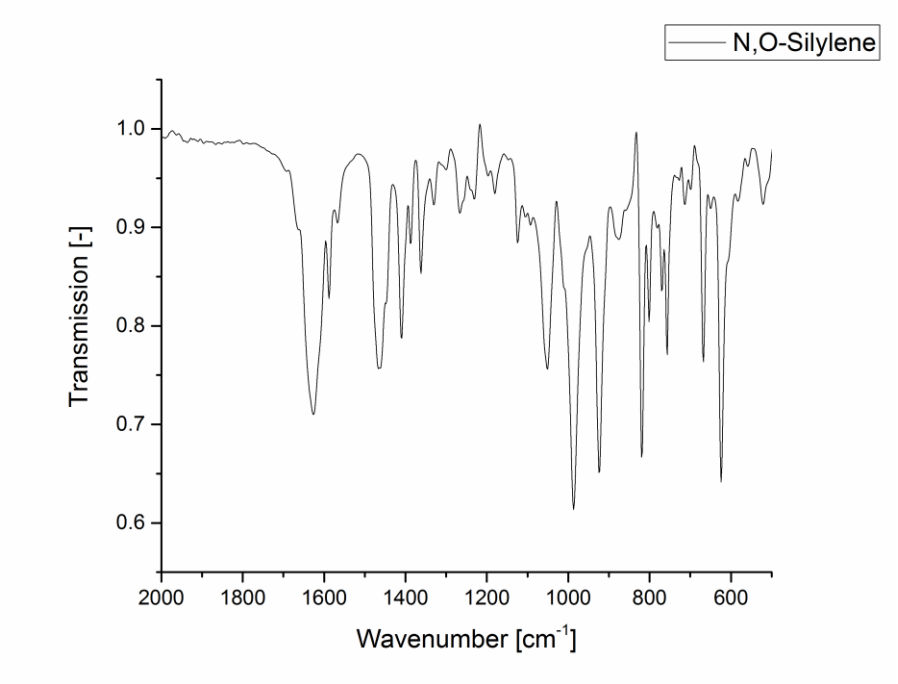


Figure S46: IR spectrum of *N*,*O*-silylene **7** ($cm^{-1}$): 1624 (s), 1459 (m), 1405 (m), 1365 (s), 1049 (m), 980 (s), 917 (s), 819 (s), 758 (m), 666 (m), 621 (s).

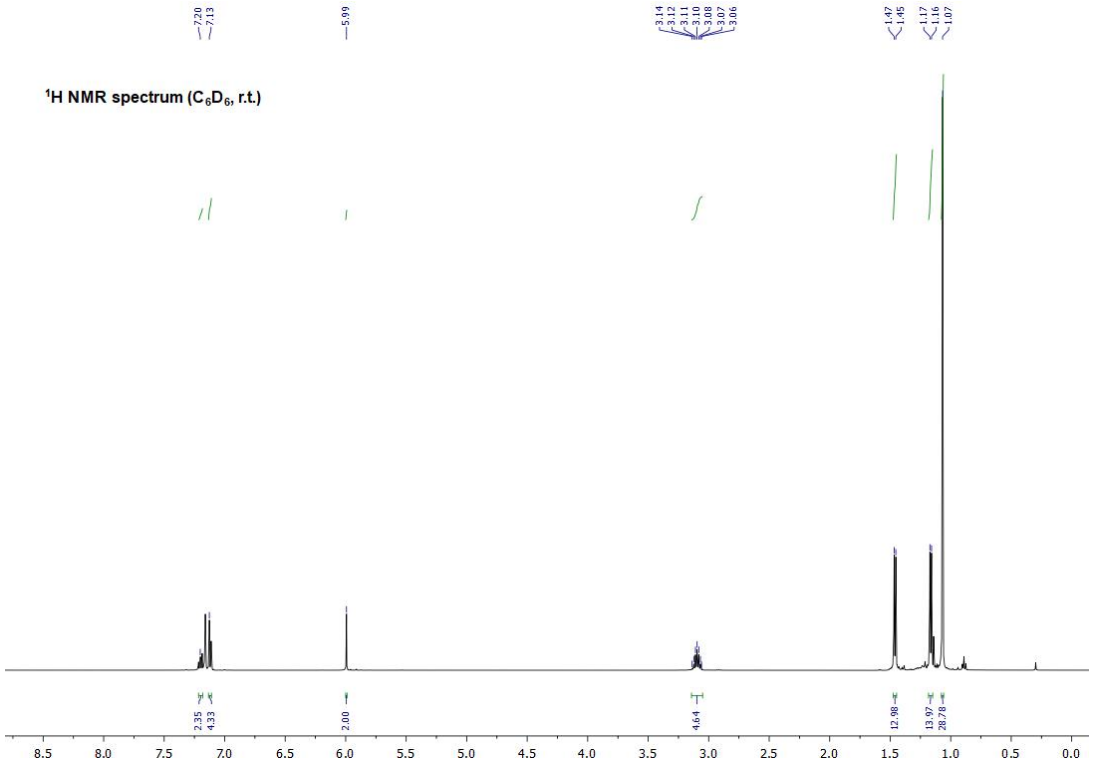


Figure S47: $^{1}H$ NMR spectrum of *N*,*O*-silylene **7** ($C_6D_6$, r.t.).

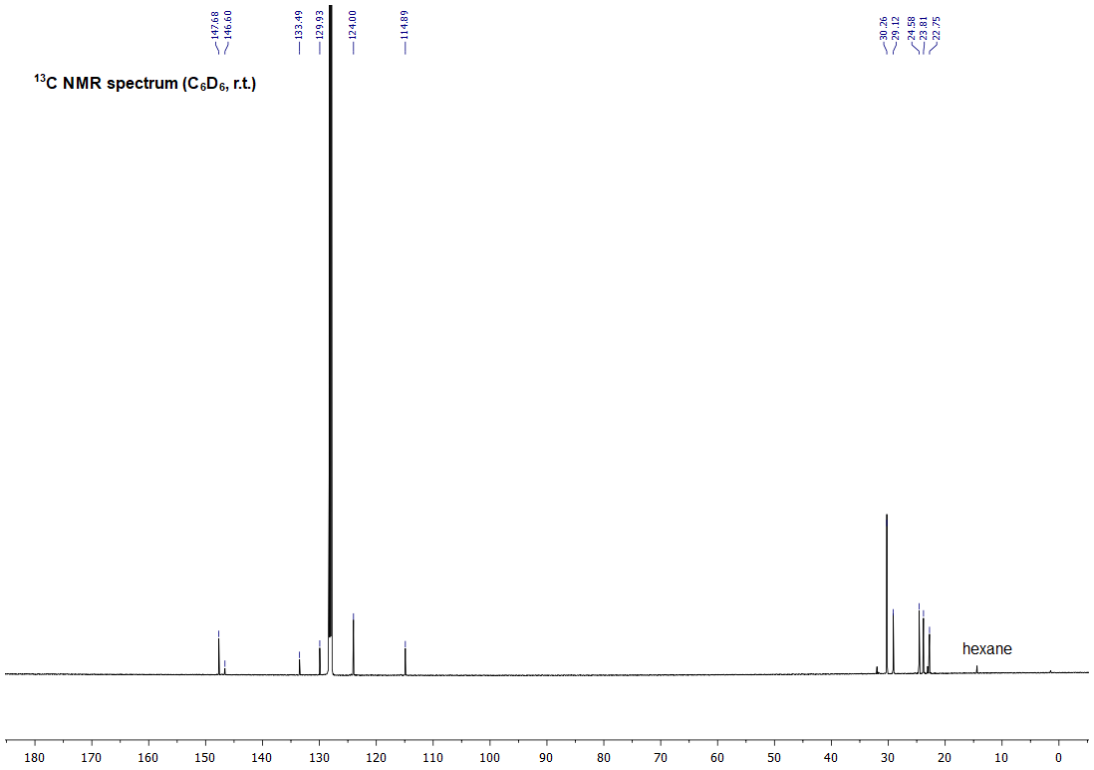


Figure S48: $^{13}$C NMR spectrum of *N*,*O*-silylene **7** ($C_6D_6$, r.t.).

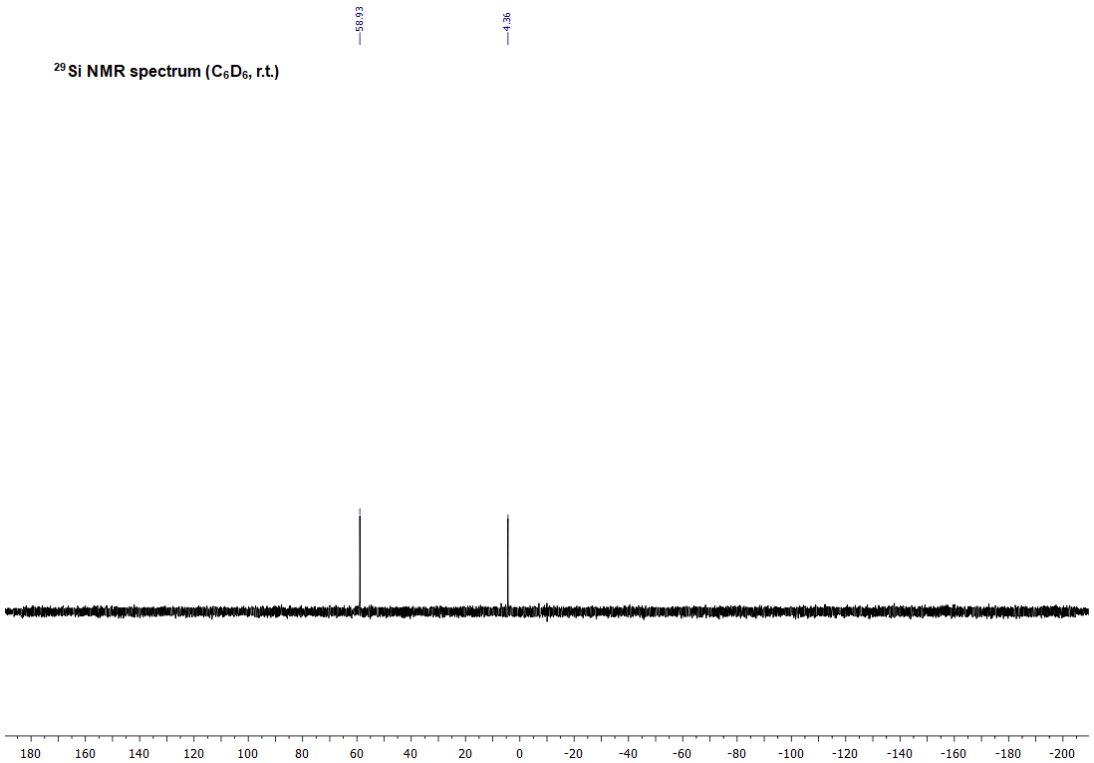


Figure S49: $^{29}$Si NMR spectrum of *N*,*O*-silylene **7** ($C_6D_6$, r.t.).

**NMR Studies on the Reactivity of *N,O*-Silylene 7 towards Ethylene and Hydrogen**

**Synthesis of IPrNSi($CH_2CH_2$)OSi*t*-$Bu_3$ (8)**

A $C_6D_6$ (0.5 mL) solution of *N,O*-silylene **7** (15 mg, 23.2 µmol, 1.00 eq) in a J. Young PTFE tube was exposed to ethylene or hydrogen gas (1 bar), respectively. With ethylene, monitoring the reaction at room temperature showed silirane **8** as sole product after 20 min reaction time. Removal of all volatiles gave compound **8** as a colorless sticky solid (15.7 mg, 23.2 µmol, quantitative yield). Compound **8** is completely stable as a solid and in solution at room temperature. For hydrogen, no activation was observed even after heating the reaction solution to 60 °C for several days.

$^1$H NMR (500 MHz, $C_6D_6$, r.t.): δ = 7.26 – 7.21 (m, 2H, *p*-C*H*-Ar), 7.14 – 7.11 (m, 4H, *m*-C*H*-Ar), 5.94 (s, 2H, C*H*-N), 3.15 (hept, *J* = 6.8 Hz, 4H, C*H*), 1.40 (d, *J* = 6.8 Hz, 12H, C$H_3$), 1.15 (d, *J* = 6.8 Hz, 12H, C$H_3$), 1.07 (s, 27H, Si*t*-*Bu*$_3$), 0.91 – 0.85 (m, 2H, Si(C$H_2$-C$H_2$), 0.03 – -0.03 (m, 2H, Si(C$H_2$-C$H_2$).

$^{13}$C NMR (126 MHz, $C_6D_6$, r.t.): δ = 147.5 (*C*-Ar), 142.7 (N-*C*-N), 134.5 (*C*-Ar), 129.8 (*C*H-Ar), 123.0 (*C*H-Ar), 114.6 (*C*H-N), 30.2 (C(*C*$H_3$)$_3$), 29.0 (*C*H), 24.7 (*C*$H_3$), 23.4 (*C*$H_3$), 23.1 (*C*(CH$_3$)$_3$), 4.8 (*C*$H_2$*C*$H_2$).

$^{29}$Si NMR (99 MHz, $C_6D_6$, r.t.): δ = 3.4 (Si*t*-Bu$_3$), -75.0 (*central Si*).

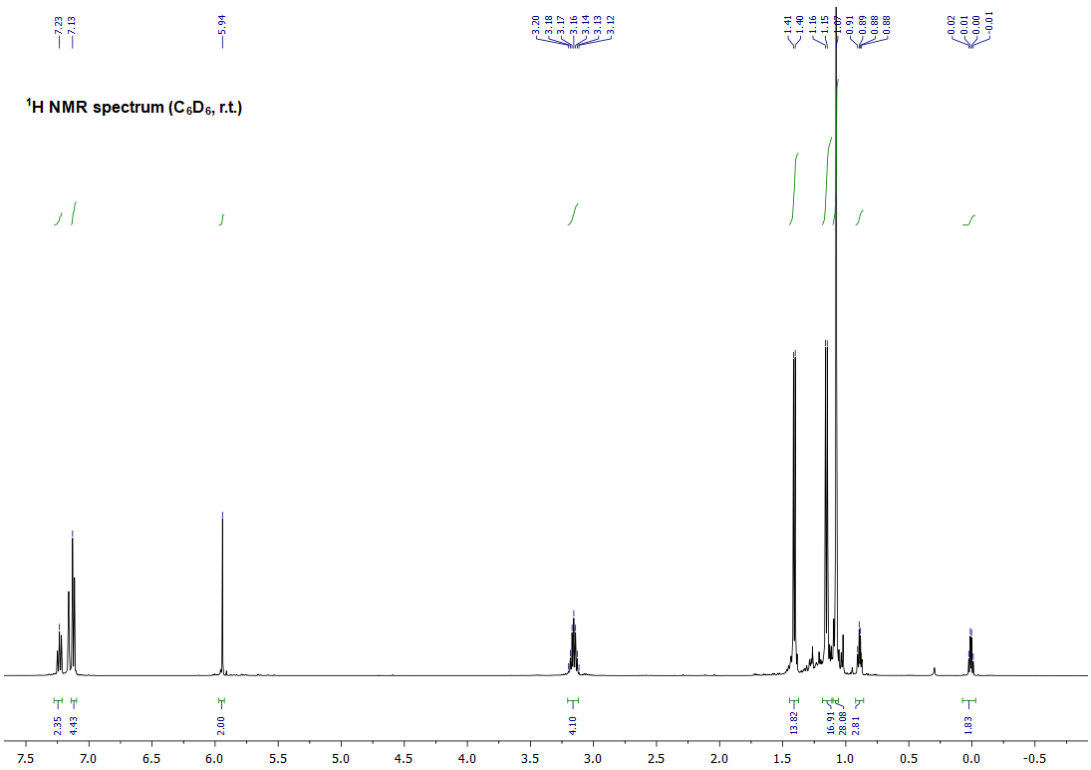


Figure S50: $^1$H NMR spectrum of silirane **8** ($C_6D_6$, r.t.).

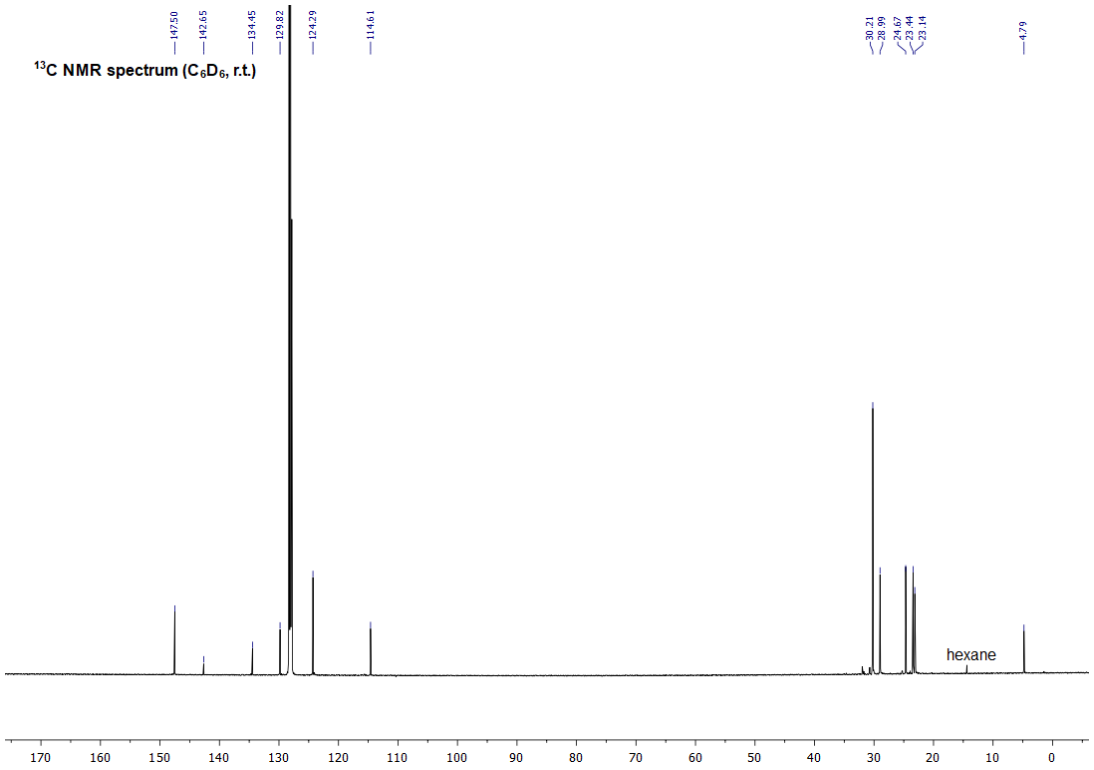


Figure S51: $^{13}C$ NMR spectrum of silirane **8** ($C_6D_6$, r.t.).

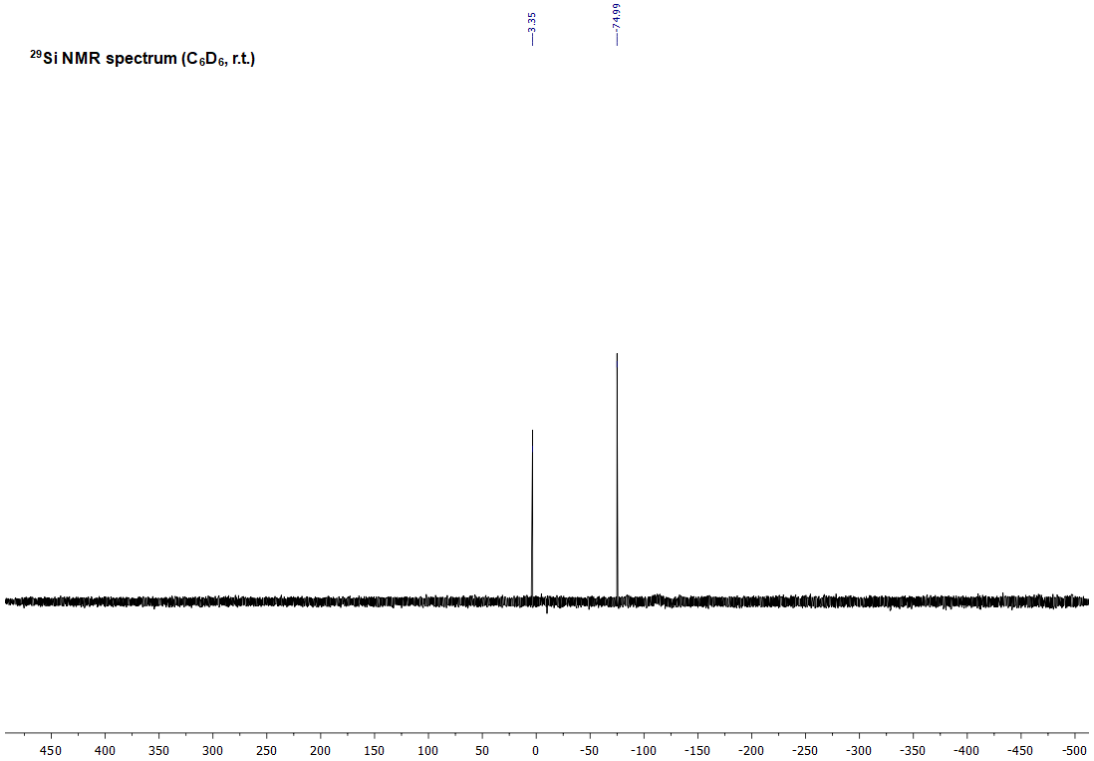


Figure S52: $^{29}Si$ NMR spectrum of silirane **8** ($C_6D_6$, r.t.).

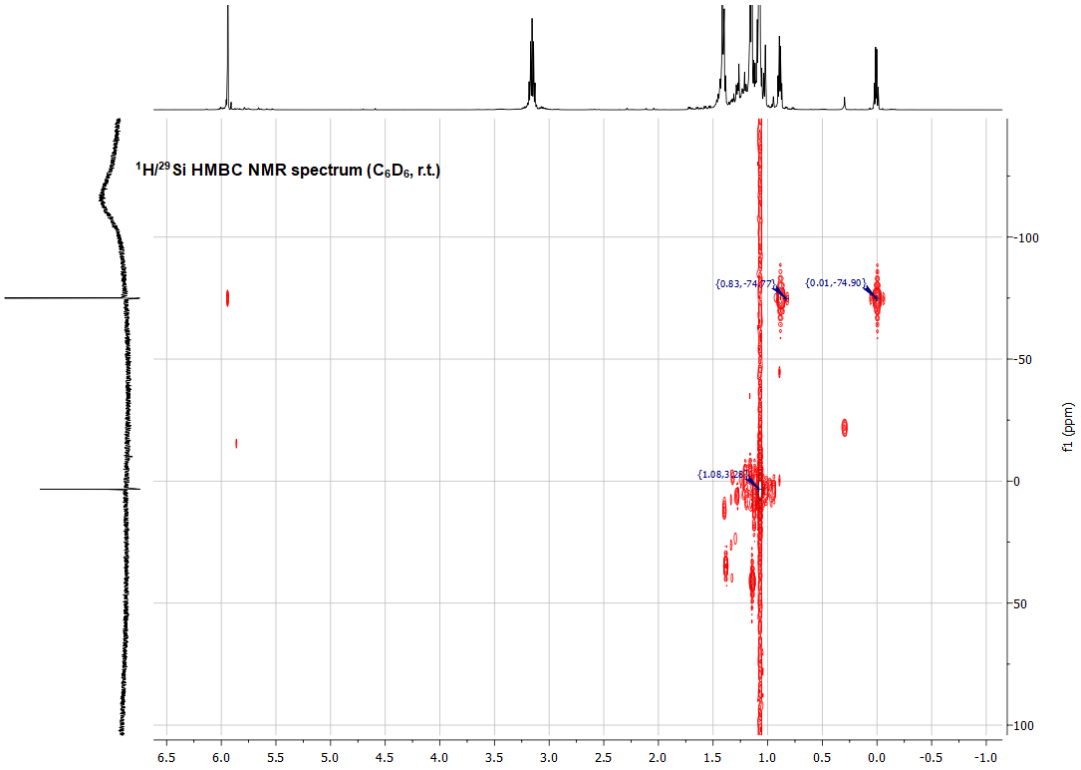


Figure S53: $^{1}H/^{29}Si$ HMBC NMR spectrum of silirane **8** ($C_6D_6$, r.t.).

# 2. X-ray Crystallographic Data

## A) General information

The X-ray intensity data of **2a** × **$CD_3CN$**, **4a**, **6** and **7** were collected on an X-ray single crystal diffractometer equipped with a CMOS detector (Bruker Photon-100), an IMS microsource with MoKα radiation (λ = 0.71073 Å) and a Helios mirror optic by using the APEX III software package.[S6] The X-ray intensity data of **2b** were collected on an X-ray single crystal diffractometer equipped with a CMOS detector (Bruker Photon-100), a rotating anode (Bruker TXS) with MoKα radiation (λ = 0.71073 Å) and a Helios mirror optic by using the APEX III software package.[S6] The measurements were performed on single crystals coated with perfluorinated ether. The crystals were fixed on the top of a microsampler, transferred to the diffractometer and frozen under a stream of cold nitrogen. A matrix scan was used to determine the initial lattice parameters. Reflections were merged and corrected for Lorenz and polarization effects, scan speed, and background using SAINT.[S7] Absorption corrections, including odd and even ordered spherical harmonics were performed using SADABS.[S7] Space group assignments were based upon systematic absences, E statistics, and successful refinement of the structures. Structures were solved by direct methods with the aid of successive difference Fourier maps, and were refined against all data using the APEX III software in conjunction with SHELXL-2014[S8] and SHELXLE[S9]. H atoms bound to aluminium atoms were allowed to refine freely. Other H atoms were placed in calculated positions and refined using a riding model, with methylene and aromatic C–H distances of 0.99 and 0.95 Å, respectively, and $U_{iso}(H) = 1.2 \cdot U_{eq}(C)$. Full-matrix least-squares refinements were carried out by minimizing $\Delta w(F_o^2 - F_c^2)^2$ with SHELXL-97[S10] weighting scheme. Neutral atom scattering factors for all atoms and anomalous dispersion corrections for the non-hydrogen atoms were taken from International Tables for Crystallography.[S11] The image of the crystal structure was generated by Mercury.[S12] CCDC 1577580-1577584 contain the supplementary data for the structures. These data can be obtained free of charge from the Cambridge Crystallographic Data Centre.

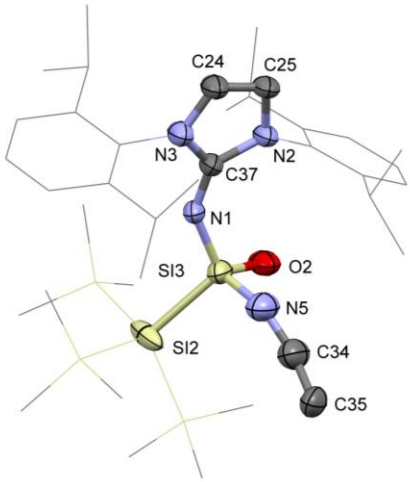


Figure S54: Molecular structure of silanone **2a** × **$CD_3CN$** in the solid state with ellipsoids set at the 50% probability level. For clarity, hydrogen atoms and co-crystallized solvent molecules are omitted and TMS as well as Dipp groups are simplified as wireframes. Selected bond lengths (Å) and angles (deg): Si3–O2 1.632(6), Si3–N5 1.749(7), Si3–N1 1.670(5), N1–C37 1.277(7), C37–N2 1.390(8), C37–N3 1.397(9), N1–Si3–Si2 114.1(4), C37–N1–Si3 142.1(9).

Table S1: Sample and crystal data for **2a** × **$CD_3CN$**.

| | | |
|---|---|---|
| **Identification code** | WenDa48 | |
| **Chemical formula** | $C_{38}H_{66}N_4OSi_5$ | |
| **Formula weight** | 735.39 | |
| **Temperature** | 100(2) K | |
| **Wavelength** | 0.71073 Å | |
| **Crystal size** | 0.133 mm x 0.276 mm x 0.278 mm | |
| **Crystal habit** | clear colorless fragment | |
| **Crystal system** | monoclinic | |
| **Space group** | $P\ 1\ 2_1/n\ 1$ | |
| **Unit cell dimensions** | a = 10.3704(11) Å | α = 90° |
| | b = 33.835(3) Å | β = 97.371(3)° |
| | c = 12.9525(12) Å | γ = 90° |
| **Volume** | 4507.2(8) $Å^3$ | |
| **Z** | 4 | |
| **Density (calculated)** | 1.084 $g/cm^3$ | |
| **Absorption coefficient** | 0.190 $mm^{-1}$ | |
| **F(000)** | 1600 | |

Table S2: Data collection and structure refinement for **2a** × **$CD_3CN$**.

| | | |
|---|---|---|
| **Diffractometer** | Bruker D8 Venture, CMOS detector (Bruker Photon-100) | |
| **Radiation source** | IMS microsource, Mo | |
| **Theta range for data collection** | 2.32 to 25.03° | |
| **Index ranges** | -12<=h<=12, -40<=k<=40, -15<=l<=15 | |
| **Reflections collected** | 48889 | |
| **Independent reflections** | 7974 [R(int) = 0.0423] | |
| **Coverage of independent reflections** | 99.9% | |
| **Absorption correction** | multi-scan | |
| **Min. and max. transmission** | 0.6905 and 0.7453 | |
| **Refinement method** | Full-matrix least-squares on $F^2$ | |
| **Refinement program** | SHELXL-2014/7 (Sheldrick, 2014) | |
| **Function minimized** | $\Sigma\, w(F_o^2 - F_c^2)^2$ | |
| **Data / restraints / parameters** | 7974 / 682 / 902 | |
| **Goodness-of-fit on $F^2$** | 1.217 | |
| **$\Delta/\sigma_{max}$** | 0.011 | |
| **Final R indices** | 5222 data; I>2σ(I) | R1 = 0.0941, wR2 = 0.2488 |
| | all data | R1 = 0.1366, wR2 = 0.2777 |
| **Weighting scheme** | $w=1/[\sigma^2(F_o^2)+(0.1137P)^2+6.2488P]$ where $P=(F_o^2+2F_c^2)/3$ | |
| **Largest diff. peak and hole** | 1.312 and -0.629 eÅ$^{-3}$ | |
| **R.M.S. deviation from mean** | 0.073 eÅ$^{-3}$ | |

Table S3: Sample and crystal data for **2b**.

| | | |
|---|---|---|
| **Identification code** | ReiDo8 | |
| **Chemical formula** | $C_{30}H_{63}N_3OSi_3$ | |
| **Formula weight** | 646.10 | |
| **Temperature** | 100(2) K | |
| **Wavelength** | 0.71073 Å | |
| **Crystal size** | 0.138 mm x 0.144 mm x 0.517 mm | |
| **Crystal habit** | clear colorless fragment | |
| **Crystal system** | monoclinic | |
| **Space group** | *P* 1 $2_1/c$ 1 | |
| **Unit cell dimensions** | a = 13.987(10) Å | α = 90° |
| | b = 21.397(15) Å | β = 92.58(2)° |
| | c = 27.532(12) Å | γ = 90° |
| **Volume** | 8231(10) $Å^3$ | |
| **Z** | 8 | |
| **Density (calculated)** | 1.043 $g/cm^3$ | |
| **Absorption coefficient** | 0.117 $mm^{-1}$ | |
| **F(000)** | 2832 | |

Table S4: Data collection and structure refinement for **2b**.

| | | |
|---|---|---|
| **Diffractometer** | Bruker D8 Venture, CMOS detector (Bruker Photon-100) | |
| **Radiation source** | TXS rotating anode, Mo | |
| **Theta range for data collection** | 1.92 to 25.03° | |
| **Index ranges** | -16<=h<=16, -25<=k<=25, -32<=l<=32 | |
| **Reflections collected** | 193064 | |
| **Independent reflections** | 14326 [R(int) = 0.0786] | |
| **Coverage of independent reflections** | 98.4% | |
| **Absorption correction** | multi-scan | |
| **Min. and max. transmission** | 0.6460 and 0.7453 | |
| **Refinement method** | Full-matrix least-squares on $F^2$ | |
| **Refinement program** | SHELXL-2014/7 (Sheldrick, 2014) | |
| **Function minimized** | $\Sigma\, w(F_o^2 - F_c^2)^2$ | |
| **Data / restraints / parameters** | 14326 / 557 / 1300 | |
| **Goodness-of-fit on $F^2$** | 1.108 | |
| **$\Delta/\sigma_{max}$** | 0.001 | |
| **Final R indices** | 11065 data; I>2σ(I) | R1 = 0.0788, wR2 = 0.1647 |
| | all data | R1 = 0.1059, wR2 = 0.1786 |
| **Weighting scheme** | $w=1/[\sigma^2(F_o^2)+(0.0344P)^2+20.6132P]$ where $P=(F_o^2+2F_c^2)/3$ | |
| **Largest diff. peak and hole** | 0.533 and -0.469 $eÅ^{-3}$ | |
| **R.M.S. deviation from mean** | 0.062 $eÅ^{-3}$ | |

Table S5: Sample and crystal data for **4a**.

| | | |
|---|---|---|
| **Identification code** | WenDa39 | |
| **Chemical formula** | $C_{37}H_{67}N_3O_2Si_5$ | |
| **Formula weight** | 726.38 | |
| **Temperature** | 100(2) K | |
| **Wavelength** | 0.71073 Å | |
| **Crystal size** | 0.134 mm x 0.180 mm x 0.509 mm | |
| **Crystal habit** | clear colorless fragment | |
| **Crystal system** | monoclinic | |
| **Space group** | *P* 1 $2_1$/*n* 1 | |
| **Unit cell dimensions** | a = 13.2302(14) Å | α = 90° |
| | b = 11.9923(13) Å | β = 96.613(3)° |
| | c = 28.620(3) Å | γ = 90° |
| **Volume** | 4510.7(8) $Å^3$ | |
| **Z** | 4 | |
| **Density (calculated)** | 1.070 $g/cm^3$ | |
| **Absorption coefficient** | 0.190 $mm^{-1}$ | |
| **F(000)** | 1584 | |

Table S6: Data collection and structure refinement for **4a**.

| | | |
|---|---|---|
| **Diffractometer** | Bruker D8 Venture, CMOS detector (Bruker Photon-100) | |
| **Radiation source** | IMS microsource, Mo | |
| **Theta range for data collection** | 2.22 to 25.03° | |
| **Index ranges** | -15<=h<=15, -11<=k<=11, -34<=l<=34 | |
| **Reflections collected** | 39229 | |
| **Independent reflections** | 7963 [R(int) = 0.0595] | |
| **Coverage of independent reflections** | 99.9% | |
| **Absorption correction** | multi-scan | |
| **Min. and max. transmission** | 0.5815 and 0.7453 | |
| **Refinement method** | Full-matrix least-squares on $F^2$ | |
| **Refinement program** | SHELXL-2014/7 (Sheldrick, 2014) | |
| **Function minimized** | $\Sigma\, w(F_o^2 - F_c^2)^2$ | |
| **Data / restraints / parameters** | 7963 / 0 / 446 | |
| **Goodness-of-fit on $F^2$** | 1.082 | |
| **$\Delta/\sigma_{max}$** | 0.001 | |
| **Final R indices** | 5981 data; I>2σ(I) | R1 = 0.0563, wR2 = 0.1234 |
| | all data | R1 = 0.0832, wR2 = 0.1342 |
| **Weighting scheme** | $w=1/[\sigma^2(F_o^2)+(0.0351P)^2+9.0134P]$ where $P=(F_o^2+2F_c^2)/3$ | |
| **Largest diff. peak and hole** | 0.483 and -0.402 eÅ$^{-3}$ | |
| **R.M.S. deviation from mean** | 0.065 eÅ$^{-3}$ | |

Table S7: Sample and crystal data for **6**.

| | | |
|---|---|---|
| **Identification code** | WenDa40 | |
| **Chemical formula** | $C_{43}H_{75}N_5OSi_5$ | |
| **Formula weight** | 818.53 | |
| **Temperature** | 100(2) K | |
| **Wavelength** | 0.71073 Å | |
| **Crystal size** | 0.133 mm x 0.148 mm x 0.167 mm | |
| **Crystal habit** | clear orange fragment | |
| **Crystal system** | triclinic | |
| **Space group** | *P* -1 | |
| **Unit cell dimensions** | a = 12.4388(5) Å | α = 103.4770(10)° |
| | b = 20.3429(7) Å | β = 99.6220(10)° |
| | c = 20.7659(8) Å | γ = 94.4910(10)° |
| **Volume** | 5000.2(3) $Å^3$ | |
| **Z** | 2 | |
| **Density (calculated)** | 1.087 $g/cm^3$ | |
| **Absorption coefficient** | 0.178 $mm^{-1}$ | |
| **F(000)** | 1784 | |

Table S8: Data collection and structure refinement for **6**.

| | | |
|---|---|---|
| **Diffractometer** | Bruker D8 Venture, CMOS detector (Bruker Photon-100) | |
| **Radiation source** | IMS microsource, Mo | |
| **Theta range for data collection** | 1.39 to 25.03° | |
| **Index ranges** | -14<=h<=14, -24<=k<=24, -24<=l<=24 | |
| **Reflections collected** | 93632 | |
| **Independent reflections** | 17649 [R(int) = 0.0682] | |
| **Coverage of independent reflections** | 99.9% | |
| **Absorption correction** | multi-scan | |
| **Min. and max. transmission** | 0.7185 and 0.7453 | |
| **Refinement method** | Full-matrix least-squares on $F^2$ | |
| **Refinement program** | SHELXL-2014/7 (Sheldrick, 2014) | |
| **Function minimized** | $\Sigma\, w(F_o^2 - F_c^2)^2$ | |
| **Data / restraints / parameters** | 17649 / 84 / 1095 | |
| **Goodness-of-fit on $F^2$** | 1.025 | |
| **$\Delta/\sigma_{max}$** | 0.001 | |
| **Final R indices** | 13203 data; I>2σ(I) | R1 = 0.0476, wR2 = 0.0957 |
| | all data | R1 = 0.0748, wR2 = 0.1063 |
| **Weighting scheme** | $w=1/[\sigma^2(F_o^2)+(0.0327P)^2+5.0730P]$ where $P=(F_o^2+2F_c^2)/3$ | |
| **Largest diff. peak and hole** | 0.469 and -0.419 $eÅ^{-3}$ | |
| **R.M.S. deviation from mean** | 0.051 $eÅ^{-3}$ | |

Table S9: Sample and crystal data for **7**.

| | | |
|---|---|---|
| **Identification code** | WenDa47 | |
| **Chemical formula** | $C_{39}H_{63}N_3OSi_3$ | |
| **Formula weight** | 646.10 | |
| **Temperature** | 100(2) K | |
| **Wavelength** | 0.71073 Å | |
| **Crystal size** | 0.176 mm x 0.179 mm x 0.217 mm | |
| **Crystal habit** | clear colorless fragment | |
| **Crystal system** | monoclinic | |
| **Space group** | *P* 1 $2_1/c$ 1 | |
| **Unit cell dimensions** | a = 34.475(3) Å | α = 90° |
| | b = 10.6878(9) Å | β = 107.847(3)° |
| | c = 22.1910(19) Å | γ = 90° |
| **Volume** | 7783.1(12) $Å^3$ | |
| **Z** | 4 | |
| **Density (calculated)** | 1.103 $g/cm^3$ | |
| **Absorption coefficient** | 0.123 $mm^{-1}$ | |
| **F(000)** | 2832 | |

Table S10: Data collection and structure refinement for **7**.

| | | |
|---|---|---|
| **Diffractometer** | Bruker D8 Venture, CMOS detector (Bruker Photon-100) | |
| **Radiation source** | IMS microsource, Mo | |
| **Theta range for data collection** | 2.20 to 25.03° | |
| **Index ranges** | -41<=h<=41, -12<=k<=12, -26<=l<=26 | |
| **Reflections collected** | 152111 | |
| **Independent reflections** | 13754 [R(int) = 0.0652] | |
| **Coverage of independent reflections** | 99.9% | |
| **Absorption correction** | multi-scan | |
| **Min. and max. transmission** | 0.7188 and 0.7452 | |
| **Refinement method** | Full-matrix least-squares on $F^2$ | |
| **Refinement program** | SHELXL-2014/7 (Sheldrick, 2014) | |
| **Function minimized** | $\Sigma\, w(F_o^2 - F_c^2)^2$ | |
| **Data / restraints / parameters** | 13754 / 54 / 905 | |
| **Goodness-of-fit on $F^2$** | 1.081 | |
| **$\Delta/\sigma_{max}$** | 0.001 | |
| **Final R indices** | 10907 data; I>2σ(I) | R1 = 0.0491, wR2 = 0.1006 |
| | all data | R1 = 0.0704, wR2 = 0.1084 |
| **Weighting scheme** | $w=1/[\sigma^2(F_o^2)+(0.0377P)^2+6.6255P]$ where $P=(F_o^2+2F_c^2)/3$ | |
| **Largest diff. peak and hole** | 0.378 and -0.326 $eÅ^{-3}$ | |
| **R.M.S. deviation from mean** | 0.049 $eÅ^{-3}$ | |

# 3. Computational Calculations

## A) General

All calculations were performed at the B3LYP[S13-S15]/6-311+G(d) level of theory using Gaussian 09[S16]. The geometry of compounds **2b**, **6** and **7** were optimized starting from the solid state structures. The nature of stationary points found was assessed by frequency calculations, excluding **6**, where due to the size of the system, frequency calculations where only performed on the reduced system (Dipp groups replaced by 2,6-dimethyl-phenyl groups). Natural bond orbital (NBO)[S17] analyses were performed using the NBO 3.1 program implemented in Gaussian.

## B) Theoretical Investigations

**Influences on Si=O bonds and Related Structures**

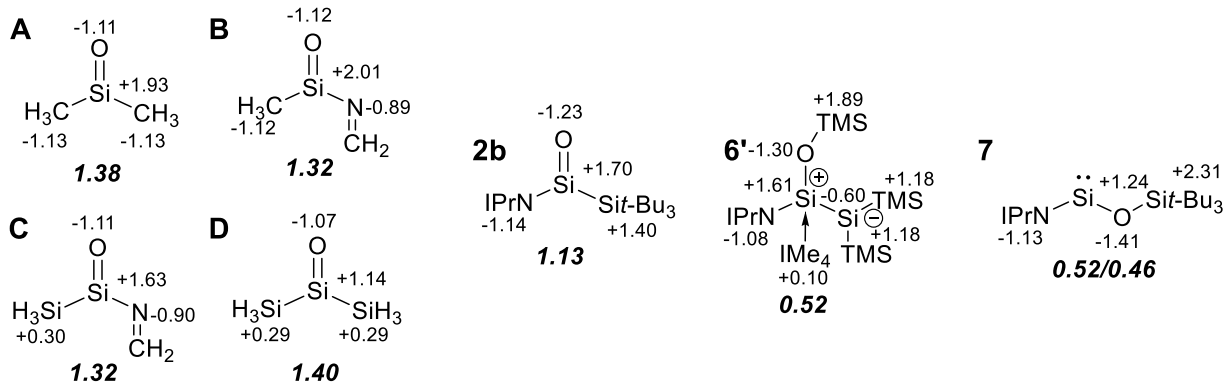


Figure S55: NPA charges and WBIs (bold & italic) of the corresponding Si-O bond of **2b**, **6**, **7** and comparable smaller silanones **A**-**D**.

By comparing smaller silanones **A**, **B**, **C** and **D**, the influence of silyl and imino groups on the Si=O moiety were investigated. As expected implementation of a π-donating imino function increases the polarization of the Si=O bond (see NPA charges O/Si of **A**: -1.11/+1.93 and **B**: -1.12/+2.01). However, addition of silyl moieties effectively reduces the positive charge at the silicon center (**B** (+2.01) and **C** (+1.63) or **A** (+1.93) and **D** (+1.14)). Most likely this is a result of inductive σ-donation of the silyl group to the electron deficient silicon center. Further, hyperconjugation of Si-C σ-orbitals with the π*-orbital of the Si=O moiety may also have a similar effect.

For compound **6** the obtained crystallographic and theoretical data point to resonance form **6'** with a zwitterionic Si1-Si2 bond (WBI 1.04) and a dative Si-NHC bond (WBI 0.60) as most fitting representation (Table S11). Still, we would like to note, that several more, but less likely, canonical forms (e.g. delocalization of the positive charge inside the NHI or NHC moiety) are generally imaginable.

Table S11: Selected WBI and NPA charges of **6**.

| Bond | WBI | NPA charges |
|---|---|---|
| Si1Si2 | 1.04 | 1.61/-0.60 |
| Si2Si3 | 0.99 | -0.60/1.18 |
| Si2Si4 | 0.98 | -0.60/1.18 |
| Si1O | 0.52 | 1.61/-1.30 |
| $Si1C^{IMe4}$ | 0.60 | 1.61/0.10 |
| Si1N | 0.73 | 1.61/-1.08 |
| $NC^{Imin}$ | 1.60 | -1.08/0.67 |

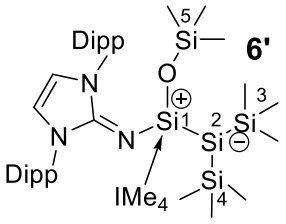


## Calculated IR Stretching Frequencies of 2b, 6 and 7

Table S12: Experimental and calculated IR frequencies B3LYP/6-311+G(2d,2p)).

| Compound | Mode | Exp. ν [$cm^{-1}$] | Calc. ν [$cm^{-1}$] |
|---|---|---|---|
| **2b** | stretch. Si=O | 1144 | 1155 |
| | stretch. C=N | 1649 | 1647 |
| **6** | asym. stretch. Si-O-Si | 978 | 967 |
| | stretch. C=N | 1690 | 1751 |
| **7** | asym. stretch. Si-O-Si | 980 | 992 |
| | stretch. C=N | 1624 | 1684 |

asym. stretch.: asymmetric stretching

## Calculated NMR Values

NMR chemical shifts were calculated at the SMD-B3LYP/6-311+G(2d,2p) level of theory based on the optimized geometries and referenced to tetramethylsilane. In the case of **5** and **6** the NMR shifts on this level where not satisfying (only the *Si*$TMS_2$ moiety showed a huge variance compared to experiment, indicating an incorrect representation of this moiety), inclusion of Grimme's dispersion[S18] improved the results in these cases, whereas only negligible effects occurred for **2b** and **7**.

Table S13: Experimental and calculated NMR chemical shifts(δ(TMS) = 0; SMD-B3LYP/6-311+G(2d,2p)).

| Compound | Si | Exp. δ($^{29}$Si) [ppm] | Calc. δ($^{29}$Si) [ppm] | Δ [ppm] |
|---|---|---|---|---|
| **2b** | *central Si* | 28.8 | 33.3[a] | -4.5 |
| | *Sit*-$Bu_3$ | 13.7 | 18.6[a] | -4.9 |
| **5** | O*TMS* | 4.3 | 2.0[b,c] | 2.3 |
| | Si*TMS*$_2$ | -14.6 | -19.8[b,c] | 5.2 |
| | Si*TMS*$_2$ | -14.8 | -20.1[b,c] | 5.3 |
| | *Si*OTMS | -35.7 | -37.6[b,c] | 1.9 |
| | *Si*$TMS_2$ | -39.8 | -41.4[b,c] | 1.6 |

| | | | | |
|---|---|---|---|---|
| **6** | O*TMS* | 6.1 | 11.7 [a,c] | -5.6 |
| | Si*TMS*$_2$ | -7.1 | -3.4 [a,c] | -3.7 |
| | *Si*OTMS | -35.2 | -32.8 [a,c] | -2.4 |
| | *Si*TMS$_2$ | -174.6 | -170.5 [a,c] | -4.1 |
| **7** | *central Si* | 58.9 | 54.4 [a] | 4.5 |
| | *Sit*-Bu$_3$ | 4.4 | 5.5 [a] | -1.1 |
| **INT** | O*TMS* | 4.3 | 17.1 [b,c] | -12.8 |
| | Si*TMS*$_2$ | -7.2 | -3.0 [b,c] | -4.2 |
| | *Si*OTMS | -8.0 | 59.5 [b,c] | -67.5 |
| | *Si*TMS$_2$ | -196.6 | -198.2 [b,c] | 1.6 |

[a] solvent benzene, [b] solvent tetrahydrofuran, [c] calculated including Grimme's dispersion[S18]

## Calculated UV-VIS Values

Table S14: Excerpt of the TD-DFT calculation of **2b**.

| Wavelength [nm] | MO contributions | f | Contributions |
|---|---|---|---|
| **285.07** | HOMO→LUMO | 0.0019 | 92.97% |
| | HOMO→LUMO+4 | | 3.83% |
| **283.97** | HOMO-1→LUMO+4 | 0.0035 | 6.10% |
| | HOMO→LUMO | | 5.23% |
| | HOMO→LUMO+1 | | 30.30% |
| | HOMO→LUMO+4 | | 53.32% |
| **273.99** | HOMO→LUMO+1 | 0.0046 | 45.36% |
| | HOMO→LUMO+2 | | 7.75% |
| | HOMO→LUMO+3 | | 17.04% |
| | HOMO→LUMO+4 | | 25.10% |
| **272.50** | HOMO→LUMO+1 | 0.0030 | 21.56% |
| | HOMO→LUMO+2 | | 45.32% |
| | HOMO→LUMO+3 | | 28.56% |
| | HOMO→LUMO+4 | | 3.05% |
| **269.98** | HOMO→LUMO+2 | 0.0004 | 44.09% |
| | HOMO→LUMO+3 | | 52.74% |
| **273.99** | HOMO-1→LUMO+1 | 0.0046 | 15.04% |
| | HOMO-1→LUMO+4 | | 70.11% |
| | HOMO→LUMO+4 | | 10.86% |

Table S15: Excerpt of the TD-DFT calculation of **7**

| Wavelength [nm] | MO contributions | f | Contributions |
|---|---|---|---|
| **340.57** | HOMO→LUMO | 0.0262 | 94.98% |
| | HOMO→LUMO+3 | | 2.16% |
| **335.05** | HOMO→LUMO+1 | 0.0001 | 98.87% |
| **320.66** | HOMO→LUMO+2 | 0.0007 | 6.52% |
| | HOMO→LUMO+3 | | 81.48% |
| | HOMO→LUMO+4 | | 9.88% |
| **319.73** | HOMO→LUMO+2 | 0.0006 | 92.63% |
| | HOMO→LUMO+3 | | 4.90% |
| **318.47** | HOMO→LUMO | 0.0010 | 2.14% |
| | HOMO→LUMO+3 | | 10.14% |
| | HOMO→LUMO+4 | | 85.79% |
| **291.46** | HOMO→LUMO+5 | 0.0026 | 93.82% |
| | HOMO→LUMO+6 | | 2.69% |

## Energy Difference between 2b and 7

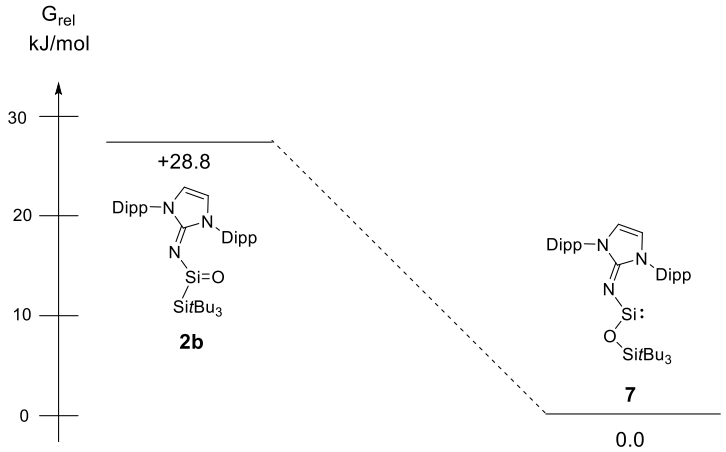


Figure S56: Energy difference between **2b** and **7**.

## Orbitals of Calculated Species

### Silanone 2b and Comparable Smaller Silanones

To illustrate the electronic influences of NHI and silyl ligands on the Si=O orbitals, the energy and shape of π and π* orbitals of silanone **2b** and analogue orbitals of smaller silanones **A**, **B**, **C** and **D** were compared. In general, both orbitals of **2b** look similar to structure **C**, but are significantly higher in energy than those of $Me_2Si=O$ **A**. Furthermore, the π/π*-energy splitting is increased (ΔE in **2b** 7.37 eV vs. **A** 6.92 eV), illustrating its total stabilization, which can mainly be attributed to the NHI ligand by general decreasing the energy of the π-orbital and increasing the energy of the π*-orbital (see orbitals of **A** and **B**

for comparison) by mixing with the corresponding orbital of the imino group. By comparing the orbitals of structure **A** and **D** as well as **B** and **C**, it becomes evident that silyl groups not only decrease π/π*-orbitals in energy, but also lower the energy difference between these Si=O orbitals. On the first sight this observation may be considered as counteracting stabilization effect. However, we believe that hyperconjugation of the Si-C σ-orbitals of the silyl group with the π*-orbital of the Si=O moiety (see LUMO of **D**) is far more relevant to preserve the Si=O double bond nature and to effectively reduce the positive charge at the silicon center (already seen at the WBI and NPA charges of **A** and **D**).

Table S16: Representation of the most important orbitals of **2b**.

**2b**

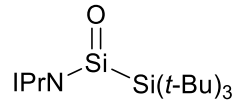


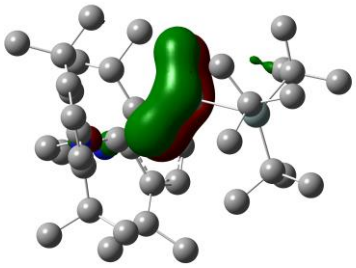

**π (Si=O)**
**HOMO-10 (-7.78 eV)**

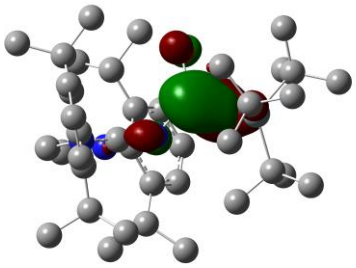

**π* (Si=O)**
**LUMO+4 (-0.41 eV)**

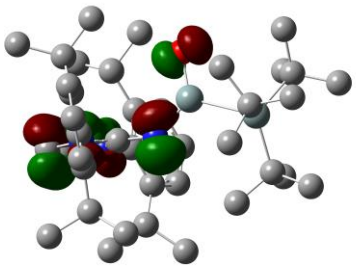

**HOMO (-5.82 eV)**

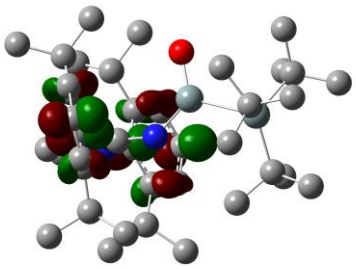

**LUMO (-0.73 eV)**

Table S17: Representation of π and π* orbitals of **A**, **B**, **C** and **D**.

| | | |
|---|---|---|
| **A** 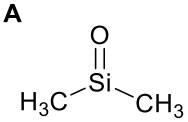 | 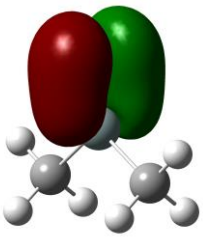 **π (Si=O)** **HOMO-1 (-8.18 eV)** | 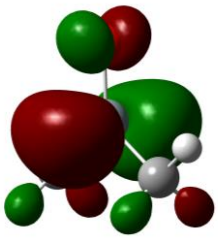 **π* (Si=O)** **LUMO (-1.26 eV)** |
| **B** 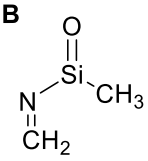 | 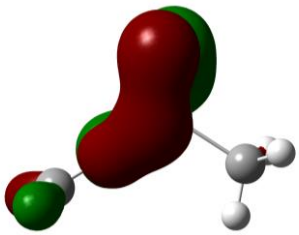 **π (Si=O)** **HOMO-2 (-8.44 eV)** | 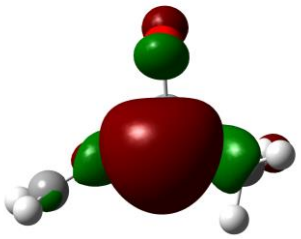 **π* (Si=O)** **LUMO+1 (-1.00 eV)** |
| **C** 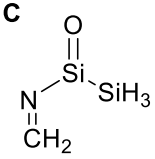 | 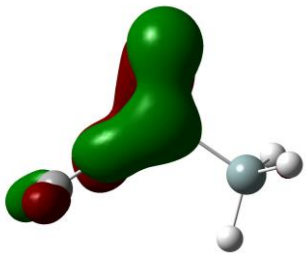 **π (Si=O)** **HOMO-2 (-8.61 eV)** | 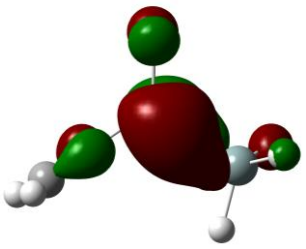 **π* (Si=O)** **LUMO+1 (-1.53 eV)** |
| **D** 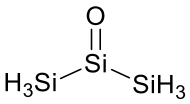 | 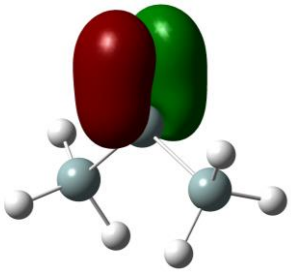 **π (Si=O)** **HOMO-1 (-8.65 eV)** | 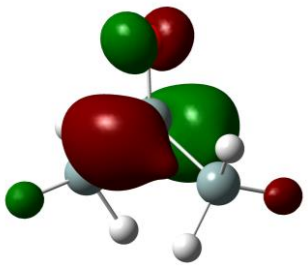 **π* (Si=O)** **LUMO (-2.76 eV)** |

## IMe$_4$ Zwitterionic Disilene 6

Table S18: Representation of the most important orbitals of **6**.

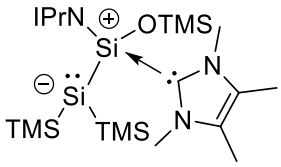


**6'**

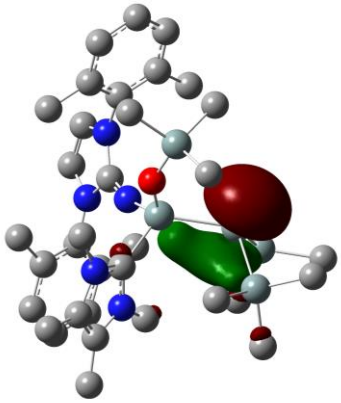

**mainly lone pair of Si(2)**

**HOMO (-3.54 eV)**

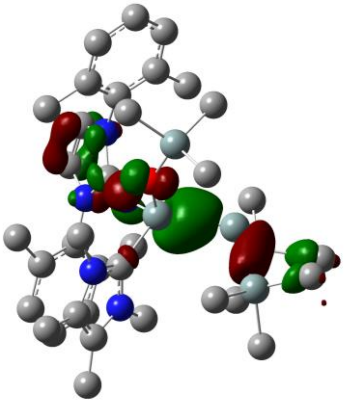

**σ-bond (Si1Si2)**

**HOMO-3 (-6.11 eV)**

### *N,O*-Silylene 7

The HOMO of *N,O*-silylene **7** exhibits mainly lone pair character ($Si_n$), the LUMO resembles the empty $Si_{3p}$ orbital with a HOMO-LUMO gap of 4.33 eV. Both orbitals show only minor contributions from donating N or O atoms. For orbitals lower in energy some interactions of silicon with nitrogen, and even lower, minor interactions with oxygen can be found. HOMO-6 represents the lone pair on nitrogen atom $N_n$ with obvious mixing with the empty $Si_{3p}$ orbital, illustrating partial Si-N double bond character (similarly to HOMO-10 of silanone **2b**). For oxygen, the related lone pair orbital $O_n$ (seen in HOMO-2, HOMO-15 and even HOMO-21) shows almost no extent towards the silicon center. Similar low-lying orbital interactions (Si-S) have been found for related dithiolato silylene by Power *et al.*.[S19]

Table S19: Representation of the most important orbitals of **7**.

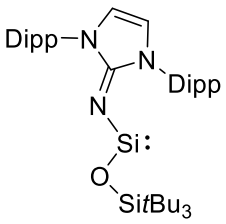


**7**

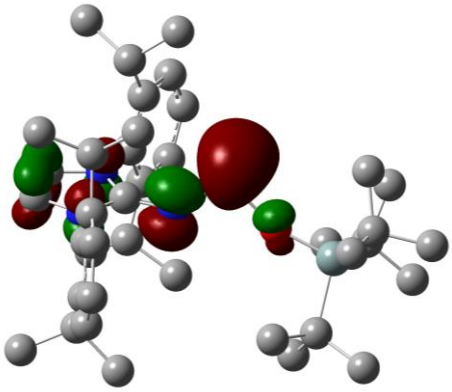

**lone pair $Si_n$**

**HOMO (-5.04 eV)**

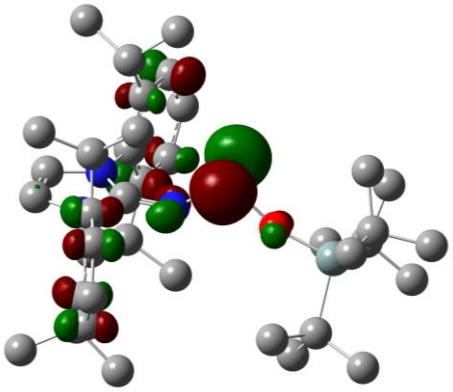

**empty $Si_{3p}$**

**LUMO (-0.71 eV)**

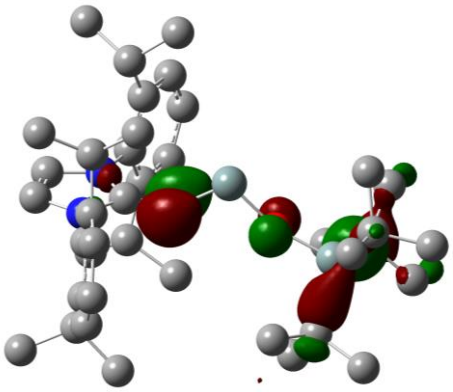

**HOMO-2 (-6.56 eV)**

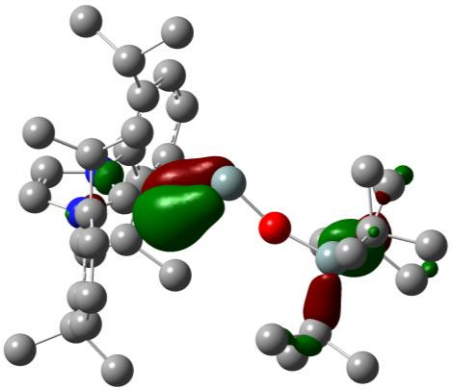

**Mixing of $N_n$ and $Si_{3p}$ orbital**

**HOMO-6 (-6.96 eV)**

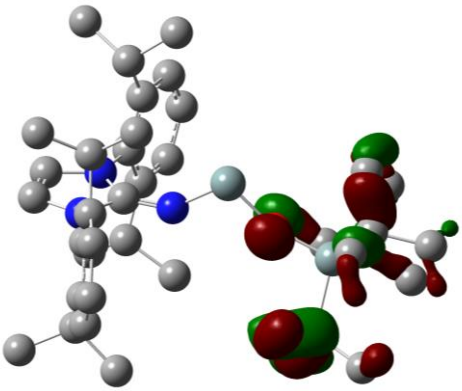

**HOMO-15 (-8.82 eV)**

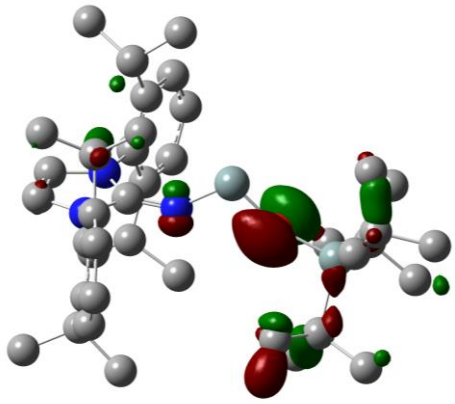

**HOMO-21 (-9.09 eV)**

# C) Calculated Structures

Table S20: Cartesian coordinated (x,y,z) for the optimized structure of **INT**.

| | | | |
|---|---|---|---|
| Si | -0.084421 | -0.990804 | 0.065906 |
| Si | 1.274059 | -2.268833 | 1.364051 |
| Si | 2.346298 | -0.452781 | 2.483878 |
| Si | 2.852935 | -2.657372 | -0.398189 |
| Si | -2.168470 | -3.078355 | -0.992106 |
| O | -1.166992 | -1.718455 | -0.953212 |
| N | -0.263453 | 0.641853 | 0.024790 |
| N | -0.139748 | 2.886932 | -0.742623 |
| N | -2.051480 | 2.248578 | 0.121667 |
| C | -0.780905 | 1.793941 | -0.186205 |
| C | -1.002909 | 3.982143 | -0.776884 |
| H | -0.688692 | 4.930580 | -1.178073 |
| C | -2.179025 | 3.591257 | -0.245045 |
| H | -3.100265 | 4.127509 | -0.092472 |
| C | 1.208927 | 2.871299 | -1.227811 |
| C | 1.480348 | 2.234532 | -2.446581 |
| C | 2.801123 | 2.238573 | -2.900102 |
| H | 3.043414 | 1.739947 | -3.832888 |
| C | 3.805031 | 2.862379 | -2.165892 |
| H | 4.826627 | 2.851979 | -2.531625 |
| C | 3.508859 | 3.480968 | -0.955336 |
| H | 4.301544 | 3.938381 | -0.372316 |
| C | 2.204317 | 3.486451 | -0.457133 |
| C | 0.389096 | 1.550400 | -3.228427 |
| H | 0.063743 | 0.634787 | -2.727066 |
| C | 1.884310 | 4.072300 | 0.894195 |
| H | 1.447848 | 3.313701 | 1.549876 |
| C | -3.138633 | 1.413362 | 0.542799 |
| C | -3.447469 | 1.335350 | 1.906624 |
| C | -4.541212 | 0.549429 | 2.279913 |
| H | -4.802532 | 0.466481 | 3.330022 |
| C | -5.296142 | -0.120321 | 1.321475 |
| H | -6.145130 | -0.722876 | 1.627960 |
| C | -4.964000 | -0.028502 | -0.027230 |
| H | -5.556664 | -0.557825 | -0.766246 |
| C | -3.870362 | 0.734727 | -0.442360 |
| C | -2.622306 | 2.072109 | 2.929501 |
| H | -1.598706 | 1.692532 | 2.958384 |
| C | -3.463947 | 0.809586 | -1.891178 |
| H | -3.226914 | 1.831632 | -2.195826 |
| C | 3.435590 | -1.208523 | 3.846724 |
| H | 2.842505 | -1.809854 | 4.542563 |
| H | 3.941353 | -0.427627 | 4.426467 |
| H | 4.206306 | -1.862690 | 3.427937 |
| C | 3.453141 | 0.709893 | 1.468831 |
| H | 4.318310 | 0.196191 | 1.042263 |
| H | 3.835004 | 1.523145 | 2.098274 |
| H | 2.900571 | 1.160789 | 0.643179 |
| C | 1.066601 | 0.666847 | 3.336057 |
| H | 0.493999 | 1.214844 | 2.583817 |
| H | 1.555033 | 1.398043 | 3.990616 |
| H | 0.359908 | 0.093458 | 3.943634 |
| C | 3.125448 | -1.278461 | -1.682519 |
| H | 2.247870 | -1.166487 | -2.329016 |
| H | 3.977513 | -1.516426 | -2.331688 |
| H | 3.315486 | -0.306469 | -1.224535 |
| C | 4.523665 | -2.985296 | 0.450595 |
| H | 4.448977 | -3.809985 | 1.165834 |
| H | 4.897983 | -2.113377 | 0.992831 |
| H | 5.278553 | -3.259923 | -0.295415 |
| C | 2.460658 | -4.214723 | -1.409873 |
| H | 2.247421 | -5.077876 | -0.773247 |
| H | 3.317419 | -4.471147 | -2.044349 |
| H | 1.600352 | -4.068479 | -2.066946 |
| C | -3.012333 | -3.213442 | 0.677693 |
| H | -3.550458 | -2.296435 | 0.930900 |
| H | -2.273465 | -3.396930 | 1.463764 |
| H | -3.731045 | -4.039505 | 0.699073 |

| | | | |
|---|---|---|---|
| C | -1.162753 | -4.619466 | -1.338523 |
| H | -1.803986 | -5.507320 | -1.308780 |
| H | -0.374968 | -4.754809 | -0.593501 |
| H | -0.689858 | -4.591169 | -2.323952 |
| C | -3.405903 | -2.800585 | -2.376771 |
| H | -4.005720 | -3.701488 | -2.543612 |
| H | -2.901995 | -2.563333 | -3.318657 |
| H | -4.093895 | -1.983452 | -2.152158 |
| H | -4.255404 | 0.437730 | -2.543150 |
| H | -2.572464 | 0.199122 | -2.061582 |
| H | 0.732999 | 1.281318 | -4.228250 |
| H | -3.047058 | 1.963795 | 3.928694 |
| H | -0.494089 | 2.186417 | -3.332283 |
| H | 1.163838 | 4.892546 | 0.830438 |
| H | 2.785017 | 4.453130 | 1.377379 |
| H | -2.558499 | 3.140184 | 2.703796 |

Table S21: Cartesian coordinated (x,y,z) for the optimized structure of **2b**.

| | | | |
|---|---|---|---|
| Si | 0.952533 | 0.098959 | 0.874213 |
| Si | 3.200795 | 0.116559 | 0.065987 |
| O | 0.790816 | 0.138393 | 2.419141 |
| N | -0.313454 | 0.012973 | -0.206669 |
| N | -2.503725 | 1.010456 | -0.213832 |
| N | -2.401561 | -1.182610 | -0.187088 |
| C | -1.608304 | -0.046705 | -0.173750 |
| C | -3.811539 | 0.524225 | -0.251152 |
| H | -4.658236 | 1.188338 | -0.279000 |
| C | -3.748748 | -0.821903 | -0.236314 |
| H | -4.529184 | -1.563221 | -0.254807 |
| C | -2.141899 | 2.402534 | -0.124265 |
| C | -2.152438 | 3.023883 | 1.138595 |
| C | -1.814815 | 4.381243 | 1.189912 |
| H | -1.810966 | 4.893610 | 2.145682 |
| C | -1.484361 | 5.084145 | 0.039672 |
| H | -1.221985 | 6.135659 | 0.104526 |
| C | -1.489008 | 4.447037 | -1.197166 |
| H | -1.231787 | 5.013831 | -2.084550 |
| C | -1.818201 | 3.094381 | -1.308820 |
| C | -2.565306 | 2.300859 | 2.417425 |
| H | -2.664943 | 1.237268 | 2.190156 |
| C | -1.516689 | 2.417214 | 3.536813 |
| H | -1.876010 | 1.901235 | 4.432537 |
| H | -1.330059 | 3.458386 | 3.817164 |
| H | -0.574698 | 1.947274 | 3.248574 |
| C | -3.943992 | 2.799921 | 2.893718 |
| H | -4.270225 | 2.236113 | 3.772581 |
| H | -4.709046 | 2.688117 | 2.119790 |
| H | -3.910848 | 3.857424 | 3.172629 |
| C | -1.877939 | 2.416977 | -2.674274 |
| H | -1.722684 | 1.346566 | -2.518976 |
| C | -3.268982 | 2.599756 | -3.313936 |
| H | -3.319862 | 2.085215 | -4.278447 |
| H | -3.483449 | 3.658584 | -3.488301 |
| H | -4.064828 | 2.199564 | -2.681461 |
| C | -0.782587 | 2.891639 | -3.640839 |
| H | -0.788465 | 2.273208 | -4.542877 |
| H | 0.210243 | 2.819578 | -3.193269 |
| H | -0.935112 | 3.925617 | -3.963352 |
| C | -1.912201 | -2.534618 | -0.101200 |
| C | -1.581006 | -3.208833 | -1.292360 |
| C | -1.123877 | -4.524838 | -1.185911 |
| H | -0.861961 | -5.076225 | -2.082401 |
| C | -1.001479 | -5.142860 | 0.053474 |
| H | -0.640672 | -6.164980 | 0.114839 |
| C | -1.345259 | -4.459110 | 1.212607 |
| H | -1.253686 | -4.958309 | 2.170945 |
| C | -1.812463 | -3.141152 | 1.166018 |
| C | -1.760300 | -2.569163 | -2.664437 |
| H | -1.917774 | -1.498530 | -2.516975 |
| C | -0.521346 | -2.719917 | -3.561301 |
| H | -0.664984 | -2.171411 | -4.496841 |
| H | -0.327239 | -3.763095 | -3.826291 |

| | | | |
|---|---|---|---|
| H | 0.371346 | -2.323314 | -3.074683 |
| C | -3.014099 | -3.126988 | -3.365666 |
| H | -3.914015 | -2.977068 | -2.763202 |
| H | -3.169948 | -2.632192 | -4.329224 |
| H | -2.918476 | -4.200569 | -3.554250 |
| C | -2.251442 | -2.447908 | 2.452486 |
| H | -2.452016 | -1.399606 | 2.221100 |
| C | -3.567546 | -3.063860 | 2.968715 |
| H | -3.918375 | -2.524561 | 3.853445 |
| H | -3.433502 | -4.112306 | 3.251748 |
| H | -4.360146 | -3.025015 | 2.215809 |
| C | -1.169748 | -2.461859 | 3.545563 |
| H | -1.551660 | -1.973119 | 4.446932 |
| H | -0.281023 | -1.910546 | 3.234311 |
| H | -0.883589 | -3.479916 | 3.826567 |
| C | 4.118689 | 1.248458 | 1.396235 |
| C | 3.308436 | 2.536321 | 1.682002 |
| H | 3.857797 | 3.152402 | 2.405860 |
| H | 2.339214 | 2.308224 | 2.130236 |
| H | 3.143251 | 3.154687 | 0.799713 |
| C | 4.246096 | 0.521262 | 2.754350 |
| H | 4.690531 | 1.208470 | 3.486376 |
| H | 4.898016 | -0.353121 | 2.709709 |
| H | 3.271077 | 0.216988 | 3.140579 |
| C | 5.533595 | 1.660753 | 0.932631 |
| H | 6.023439 | 2.239162 | 1.726647 |
| H | 5.517968 | 2.296085 | 0.044181 |
| H | 6.177690 | 0.804504 | 0.718103 |
| C | 3.297078 | 0.859296 | -1.754243 |
| C | 4.674205 | 0.621429 | -2.412073 |
| H | 4.690973 | 1.081570 | -3.408844 |
| H | 4.893047 | -0.439529 | -2.549355 |
| H | 5.497338 | 1.058441 | -1.843052 |
| C | 2.215773 | 0.236567 | -2.666361 |
| H | 2.246179 | 0.724742 | -3.649665 |
| H | 1.209538 | 0.363014 | -2.262364 |
| H | 2.371448 | -0.827915 | -2.837385 |
| C | 3.036427 | 2.380157 | -1.733377 |
| H | 3.004982 | 2.759178 | -2.763158 |
| H | 3.819315 | 2.935212 | -1.215221 |
| H | 2.079472 | 2.633145 | -1.267964 |
| C | 3.782392 | -1.768690 | 0.147942 |
| C | 3.287861 | -2.572870 | -1.073695 |
| H | 3.545384 | -3.631200 | -0.937418 |
| H | 3.750932 | -2.253055 | -2.008816 |
| H | 2.202703 | -2.522454 | -1.195926 |
| C | 5.321759 | -1.894627 | 0.198144 |
| H | 5.603743 | -2.955728 | 0.196058 |
| H | 5.750000 | -1.455188 | 1.100201 |
| H | 5.812194 | -1.432419 | -0.662045 |
| C | 3.196173 | -2.470250 | 1.394732 |
| H | 3.585010 | -3.495665 | 1.450074 |
| H | 2.106181 | -2.547986 | 1.348785 |
| H | 3.443046 | -1.974741 | 2.332102 |

Table S22: Cartesian coordinated (x,y,z) for the optimized structure of **5**.

| | | | |
|---|---|---|---|
| Si | 0.487020 | -0.382597 | -0.994271 |
| Si | 2.243979 | -0.869050 | 0.495466 |
| Si | 2.126946 | -0.264207 | 2.766412 |
| Si | 4.347904 | -0.401921 | -0.451662 |
| Si | 0.922848 | 2.295854 | -2.516061 |
| O | 0.788461 | 0.653571 | -2.259057 |
| N | -1.008265 | 0.046967 | -0.333072 |
| N | -2.879017 | 0.667591 | 0.983225 |
| N | -2.765781 | -1.458687 | 0.415542 |
| C | 0.886913 | -2.197802 | -1.435233 |
| H | 0.073288 | -2.870592 | -1.711539 |
| H | 1.598119 | -2.188391 | -2.269097 |
| C | 1.617779 | -2.613724 | -0.112049 |
| H | 0.899227 | -3.029162 | 0.600911 |
| H | 2.387354 | -3.376340 | -0.266577 |
| C | -2.079312 | -0.243852 | 0.282344 |

| | | | |
|---|---|---|---|
| C | -4.003360 | 0.029375 | 1.506776 |
| H | -4.740202 | 0.566693 | 2.079802 |
| C | -3.936035 | -1.271445 | 1.160996 |
| H | -4.604390 | -2.089826 | 1.368929 |
| C | -2.632898 | 2.077270 | 0.992774 |
| C | -2.969580 | 2.821272 | -0.147625 |
| C | -2.701681 | 4.191385 | -0.140922 |
| H | -2.943771 | 4.784994 | -1.016950 |
| C | -2.123733 | 4.796835 | 0.971508 |
| H | -1.912936 | 5.861410 | 0.959522 |
| C | -1.810590 | 4.041083 | 2.096909 |
| H | -1.357059 | 4.517492 | 2.960418 |
| C | -2.061153 | 2.666263 | 2.127539 |
| C | -3.593081 | 2.146599 | -1.340185 |
| H | -2.895634 | 1.435465 | -1.787407 |
| C | -1.733143 | 1.837763 | 3.341284 |
| H | -1.150126 | 0.957632 | 3.073264 |
| C | -2.459541 | -2.655254 | -0.307658 |
| C | -1.942995 | -3.756701 | 0.389669 |
| C | -1.670878 | -4.922809 | -0.329479 |
| H | -1.258271 | -5.782396 | 0.189256 |
| C | -1.908926 | -4.986900 | -1.698725 |
| H | -1.685156 | -5.897388 | -2.245257 |
| C | -2.426257 | -3.883440 | -2.370234 |
| H | -2.606795 | -3.936454 | -3.439340 |
| C | -2.711771 | -2.698311 | -1.688447 |
| C | -1.686713 | -3.683189 | 1.872259 |
| H | -1.143590 | -2.776825 | 2.138842 |
| C | -3.243900 | -1.496586 | -2.422968 |
| H | -4.046931 | -1.004908 | -1.869072 |
| C | 3.696542 | -0.681445 | 3.747055 |
| H | 3.925730 | -1.750775 | 3.712575 |
| H | 3.587904 | -0.399992 | 4.800639 |
| H | 4.567380 | -0.147787 | 3.354332 |
| C | 1.872840 | 1.615245 | 2.826730 |
| H | 2.750601 | 2.143459 | 2.441171 |
| H | 1.706981 | 1.960119 | 3.853434 |
| H | 1.016479 | 1.927510 | 2.223873 |
| C | 0.660924 | -1.127347 | 3.603643 |
| H | -0.258876 | -0.991337 | 3.029961 |
| H | 0.486575 | -0.733564 | 4.610848 |
| H | 0.835522 | -2.203471 | 3.694836 |
| C | 4.799391 | 1.417951 | -0.155283 |
| H | 4.024855 | 2.096320 | -0.522400 |
| H | 5.733879 | 1.678271 | -0.664484 |
| H | 4.939018 | 1.628151 | 0.909831 |
| C | 5.708425 | -1.480005 | 0.315774 |
| H | 5.498034 | -2.545385 | 0.179593 |
| H | 5.811718 | -1.301636 | 1.390060 |
| H | 6.679530 | -1.275221 | -0.149288 |
| C | 4.307379 | -0.743996 | -2.315037 |
| H | 4.179323 | -1.812490 | -2.514651 |
| H | 5.243829 | -0.432099 | -2.791114 |
| H | 3.486473 | -0.217834 | -2.807339 |
| C | 0.912243 | 3.195283 | -0.864719 |
| H | 1.733918 | 2.866802 | -0.221453 |
| H | -0.019950 | 3.010315 | -0.325248 |
| H | 1.010543 | 4.278170 | -0.994824 |
| C | -0.516232 | 2.866540 | -3.582486 |
| H | -0.404311 | 3.917472 | -3.870486 |
| H | -1.467122 | 2.769378 | -3.054110 |
| H | -0.584123 | 2.277746 | -4.502556 |
| C | 2.534522 | 2.600800 | -3.435018 |
| H | 2.655323 | 3.661219 | -3.681406 |
| H | 2.566072 | 2.039297 | -4.374016 |
| H | 3.403865 | 2.299249 | -2.845064 |
| H | -4.486214 | 1.582300 | -1.057283 |
| H | -3.627225 | -1.775356 | -3.406055 |
| H | -2.454284 | -0.753192 | -2.566061 |
| H | -1.104487 | -4.541077 | 2.213025 |
| H | -2.620704 | -3.667719 | 2.443015 |
| H | -1.159481 | 2.413316 | 4.069138 |
| H | -2.640010 | 1.477256 | 3.837146 |

| | | | |
|---|---|---|---|
| H | -3.878970 | 2.873273 | -2.102269 |

Table S23: Cartesian coordinated (x,y,z) for the optimized structure of **6**

| | | | |
|---|---|---|---|
| Si | 0.086278 | -0.710726 | -0.233549 |
| Si | 0.857753 | -1.816848 | 1.685182 |
| Si | 1.292703 | -0.415120 | 3.544640 |
| Si | 2.971021 | -2.790628 | 1.156254 |
| Si | -1.513532 | -3.342955 | -1.142879 |
| O | -0.753305 | -1.848222 | -1.151440 |
| N | -0.775799 | 0.743805 | -0.116799 |
| N | -1.361508 | 3.039605 | 0.220431 |
| N | -3.022876 | 1.585108 | 0.290070 |
| N | 1.575395 | -0.501708 | -2.915418 |
| N | 2.533302 | 0.576306 | -1.318040 |
| C | -1.625136 | 1.653600 | 0.107563 |
| C | -2.541006 | 3.748040 | 0.458870 |
| H | -2.543449 | 4.819465 | 0.569492 |
| C | -3.550904 | 2.863072 | 0.499510 |
| H | -4.606690 | 3.011967 | 0.653059 |
| C | -0.104546 | 3.687885 | 0.007272 |
| C | 0.380273 | 3.828724 | -1.305303 |
| C | 1.571306 | 4.533853 | -1.498003 |
| H | 1.953978 | 4.660455 | -2.506520 |
| C | 2.254569 | 5.092307 | -0.421036 |
| H | 3.173646 | 5.645557 | -0.587762 |
| C | 1.755438 | 4.947719 | 0.869055 |
| H | 2.290689 | 5.381774 | 1.707854 |
| C | 0.568628 | 4.246223 | 1.107614 |
| C | -0.373548 | 3.258857 | -2.478852 |
| H | -0.400191 | 2.167184 | -2.436331 |
| C | 0.029179 | 4.116965 | 2.509779 |
| H | -0.317549 | 3.104787 | 2.720616 |
| C | -3.894705 | 0.454623 | 0.134331 |
| C | -4.431964 | -0.150469 | 1.281796 |
| C | -5.409943 | -1.134786 | 1.108854 |
| H | -5.836344 | -1.615575 | 1.983656 |
| C | -5.834737 | -1.506290 | -0.161987 |
| H | -6.597091 | -2.270254 | -0.277207 |
| C | -5.277429 | -0.905170 | -1.285994 |
| H | -5.612355 | -1.196380 | -2.276816 |
| C | -4.301293 | 0.086492 | -1.158856 |
| C | -3.973284 | 0.239908 | 2.662916 |
| H | -2.909346 | 0.034837 | 2.797908 |
| C | -3.718365 | 0.754839 | -2.377511 |
| H | -3.852209 | 1.840064 | -2.345712 |
| C | 1.438406 | -0.174066 | -1.601841 |
| C | 2.751649 | 0.028429 | -3.442805 |
| C | 3.353663 | 0.715786 | -2.431954 |
| C | 0.628742 | -1.256738 | -3.731625 |
| H | -0.254034 | -1.459644 | -3.138504 |
| H | 1.074931 | -2.201626 | -4.048767 |
| H | 0.361509 | -0.674854 | -4.615714 |
| C | 3.169134 | -0.191777 | -4.857443 |
| H | 3.284268 | -1.255450 | -5.086880 |
| H | 4.128933 | 0.287858 | -5.050213 |
| H | 2.448150 | 0.219794 | -5.571013 |
| C | 4.628744 | 1.489005 | -2.407627 |
| H | 5.067731 | 1.528668 | -3.404811 |
| H | 5.370860 | 1.037216 | -1.742167 |
| H | 4.470374 | 2.518360 | -2.073204 |
| C | 2.811797 | 1.189953 | -0.022840 |
| H | 2.380669 | 2.188010 | 0.026777 |
| H | 3.888400 | 1.249057 | 0.124892 |
| H | 2.382000 | 0.564503 | 0.757165 |
| C | 1.975556 | -1.546926 | 4.920829 |
| H | 1.305372 | -2.391313 | 5.107520 |
| H | 2.082360 | -0.993785 | 5.861667 |
| H | 2.958039 | -1.961509 | 4.675408 |
| C | 2.497583 | 1.073769 | 3.485044 |
| H | 3.498529 | 0.780305 | 3.155520 |
| H | 2.600369 | 1.510308 | 4.486473 |

| | | | |
|---|---|---|---|
| H | 2.148550 | 1.869836 | 2.820653 |
| C | -0.334970 | 0.297753 | 4.238192 |
| H | -0.835295 | 0.959110 | 3.524501 |
| H | -0.154286 | 0.875697 | 5.152565 |
| H | -1.036073 | -0.504501 | 4.486612 |
| C | 4.552528 | -1.866518 | 1.714328 |
| H | 4.695410 | -0.925764 | 1.173879 |
| H | 5.439703 | -2.485917 | 1.532212 |
| H | 4.537690 | -1.628023 | 2.781274 |
| C | 3.060508 | -4.481290 | 2.032696 |
| H | 2.276007 | -5.155724 | 1.675975 |
| H | 2.922355 | -4.378241 | 3.113599 |
| H | 4.027017 | -4.972453 | 1.866217 |
| C | 3.268306 | -3.146066 | -0.698241 |
| H | 2.447889 | -3.705061 | -1.153904 |
| H | 4.179326 | -3.744190 | -0.821911 |
| H | 3.403794 | -2.224548 | -1.272819 |
| C | -2.561612 | -3.613909 | 0.386964 |
| H | -3.313508 | -2.832566 | 0.514262 |
| H | -1.935482 | -3.625641 | 1.282273 |
| H | -3.088248 | -4.573553 | 0.324602 |
| C | -0.256178 | -4.738034 | -1.291056 |
| H | -0.772181 | -5.700139 | -1.387959 |
| H | 0.383281 | -4.798563 | -0.407407 |
| H | 0.389993 | -4.629838 | -2.167907 |
| C | -2.594635 | -3.375714 | -2.692748 |
| H | -3.168752 | -4.307212 | -2.746506 |
| H | -2.002217 | -3.313801 | -3.611942 |
| H | -3.311660 | -2.550739 | -2.701501 |
| H | -4.519629 | -0.319028 | 3.424520 |
| H | -4.119451 | 1.305599 | 2.860128 |
| H | -2.644614 | 0.564773 | -2.452939 |
| H | -4.193793 | 0.385366 | -3.288042 |
| H | 0.794112 | 4.373007 | 3.244448 |
| H | -0.822493 | 4.784804 | 2.675909 |
| H | -1.411895 | 3.601544 | -2.490702 |
| H | 0.090119 | 3.557532 | -3.421063 |

Table S24: Cartesian coordinated (x,y,z) for the optimized structure of **7**.

| | | | |
|---|---|---|---|
| Si | 0.569249 | -0.060922 | -1.326705 |
| Si | 3.658416 | -0.017648 | -0.193874 |
| O | 2.014103 | -0.071847 | -0.482027 |
| N | -0.627171 | -0.019280 | -0.128190 |
| N | -2.752876 | -1.095913 | 0.214470 |
| N | -2.731785 | 1.107181 | 0.186488 |
| C | -1.896951 | -0.004575 | 0.052983 |
| C | -4.055726 | -0.652522 | 0.454880 |
| H | -4.864905 | -1.344555 | 0.615600 |
| C | -4.042954 | 0.694296 | 0.436847 |
| H | -4.839839 | 1.404970 | 0.576050 |
| C | -2.349662 | -2.474814 | 0.176248 |
| C | -1.893300 | -3.080636 | 1.362633 |
| C | -1.521098 | -4.426602 | 1.304179 |
| H | -1.160015 | -4.921323 | 2.199817 |
| C | -1.607029 | -5.144462 | 0.117448 |
| H | -1.313179 | -6.189342 | 0.093777 |
| C | -2.068869 | -4.527508 | -1.038891 |
| H | -2.133688 | -5.101086 | -1.957440 |
| C | -2.446254 | -3.181193 | -1.038199 |
| C | -1.797196 | -2.324423 | 2.682365 |
| H | -2.176501 | -1.313777 | 2.518297 |
| C | -0.337560 | -2.190790 | 3.148751 |
| H | 0.269631 | -1.692232 | 2.391362 |
| H | 0.110941 | -3.167500 | 3.353596 |
| H | -0.283383 | -1.603664 | 4.070768 |
| C | -2.676112 | -2.964740 | 3.771821 |
| H | -2.644529 | -2.365597 | 4.686864 |
| H | -2.337037 | -3.972322 | 4.029402 |
| H | -3.720151 | -3.038267 | 3.454773 |
| C | -2.968727 | -2.539286 | -2.318629 |
| H | -3.087384 | -1.469620 | -2.131945 |
| C | -1.985472 | -2.687746 | -3.492068 |

| | | | |
|---|---|---|---|
| H | -2.367691 | -2.164042 | -4.373484 |
| H | -1.839861 | -3.734488 | -3.774096 |
| H | -1.008710 | -2.262915 | -3.249922 |
| C | -4.356969 | -3.094943 | -2.689574 |
| H | -5.077784 | -2.954482 | -1.879402 |
| H | -4.313111 | -4.165834 | -2.909980 |
| H | -4.748486 | -2.589914 | -3.577834 |
| C | -2.303947 | 2.477435 | 0.110674 |
| C | -2.304772 | 3.125491 | -1.139841 |
| C | -1.914573 | 4.467565 | -1.176138 |
| H | -1.904984 | 4.997397 | -2.122430 |
| C | -1.538972 | 5.137999 | -0.018396 |
| H | -1.237421 | 6.179715 | -0.069462 |
| C | -1.549272 | 4.478398 | 1.204582 |
| H | -1.256171 | 5.016017 | 2.100099 |
| C | -1.930298 | 3.136726 | 1.297798 |
| C | -2.760484 | 2.429989 | -2.417943 |
| H | -2.829221 | 1.360128 | -2.208586 |
| C | -4.166610 | 2.909511 | -2.827675 |
| H | -4.896991 | 2.747633 | -2.030415 |
| H | -4.513474 | 2.370978 | -3.714808 |
| H | -4.168021 | 3.977687 | -3.065233 |
| C | -1.765941 | 2.599192 | -3.578079 |
| H | -1.674420 | 3.642413 | -3.893556 |
| H | -2.103187 | 2.027286 | -4.447585 |
| H | -0.772017 | 2.236015 | -3.308237 |
| C | -1.969251 | 2.449825 | 2.658388 |
| H | -2.138163 | 1.384086 | 2.491142 |
| C | -0.641957 | 2.579564 | 3.423063 |
| H | -0.420831 | 3.617201 | 3.689271 |
| H | 0.194990 | 2.197971 | 2.835868 |
| H | -0.686991 | 2.009537 | 4.355936 |
| C | -3.144056 | 2.974280 | 3.506039 |
| H | -3.033487 | 4.040882 | 3.723815 |
| H | -3.196017 | 2.443904 | 4.461773 |
| H | -4.101735 | 2.839473 | 2.996137 |
| C | 4.524188 | 0.710879 | -1.794988 |
| C | 4.291957 | 2.233036 | -1.925476 |
| H | 3.230299 | 2.494285 | -1.925221 |
| H | 4.708550 | 2.584247 | -2.878547 |
| H | 4.780891 | 2.806283 | -1.136008 |
| C | 3.928914 | 0.077337 | -3.074505 |
| H | 4.076000 | -1.000710 | -3.131834 |
| H | 4.414158 | 0.515975 | -3.956562 |
| H | 2.857360 | 0.268611 | -3.167278 |
| C | 6.049708 | 0.468107 | -1.797992 |
| H | 6.550302 | 0.902604 | -0.929048 |
| H | 6.497468 | 0.928451 | -2.688439 |
| H | 6.305904 | -0.592910 | -1.828841 |
| C | 4.186878 | -1.867677 | 0.167592 |
| C | 4.270418 | -2.702958 | -1.129503 |
| H | 4.465639 | -3.752289 | -0.873043 |
| H | 5.076606 | -2.384381 | -1.792392 |
| H | 3.336198 | -2.681282 | -1.697572 |
| C | 5.552128 | -1.967210 | 0.883254 |
| H | 5.546877 | -1.490047 | 1.865629 |
| H | 6.366411 | -1.522160 | 0.305438 |
| H | 5.812784 | -3.021765 | 1.043383 |
| C | 3.119787 | -2.558280 | 1.048905 |
| H | 3.010298 | -2.101207 | 2.031811 |
| H | 3.404233 | -3.606462 | 1.210891 |
| H | 2.137418 | -2.555594 | 0.572757 |
| C | 3.849482 | 1.155924 | 1.359912 |
| C | 2.943815 | 2.396640 | 1.180909 |
| H | 1.902902 | 2.113783 | 1.012234 |
| H | 3.250061 | 3.037795 | 0.354759 |
| H | 2.977785 | 3.009261 | 2.091515 |
| C | 5.298673 | 1.630421 | 1.598322 |
| H | 5.342753 | 2.255905 | 2.499715 |
| H | 5.685799 | 2.235799 | 0.775690 |
| H | 5.993613 | 0.800598 | 1.752720 |
| C | 3.363372 | 0.453357 | 2.647077 |
| H | 3.377183 | 1.168290 | 3.480247 |

| | | | |
|---|---|---|---|
| H | 3.998572 | -0.384681 | 2.940021 |
| H | 2.338592 | 0.086461 | 2.552354 |

Table S25: Cartesian coordinated (x,y,z) for the optimized structure of **A**.

| | | | |
|---|---|---|---|
| C | 1.555676 | -0.860994 | -0.000244 |
| Si | -0.000008 | 0.176612 | 0.000224 |
| O | -0.000102 | 1.711546 | -0.000060 |
| H | 1.603002 | -1.501429 | 0.886858 |
| H | 1.587871 | -1.526051 | -0.869628 |
| H | 2.441798 | -0.225061 | -0.015973 |
| C | -1.555565 | -0.861185 | 0.000294 |
| H | -2.441770 | -0.225360 | 0.015680 |
| H | -1.602558 | -1.501749 | -0.886735 |
| H | -1.587925 | -1.526126 | 0.869759 |

Table S26: Cartesian coordinated (x,y,z) for the optimized structure of **B**.

| | | | |
|---|---|---|---|
| Si | -0.029949 | 0.021074 | -0.182146 |
| O | 0.155622 | 1.508267 | 0.139147 |
| N | 1.234258 | -1.031106 | -0.553655 |
| C | 2.122670 | -1.533476 | -1.280612 |
| H | 2.216039 | -1.316564 | -2.353530 |
| H | 2.861648 | -2.230743 | -0.867536 |
| C | -1.609286 | -0.953318 | -0.044707 |
| H | -1.606945 | -1.836226 | -0.687240 |
| H | -1.753132 | -1.290187 | 0.986170 |
| H | -2.461251 | -0.321388 | -0.302827 |

Table S27: Cartesian coordinated (x,y,z) for the optimized structure of **C**.

| | | | |
|---|---|---|---|
| Si | 0.008395 | 0.021673 | -0.107122 |
| O | 0.173786 | 1.466324 | 0.388174 |
| N | 1.255903 | -0.958284 | -0.659438 |
| Si | -1.993293 | -1.205993 | -0.038167 |
| H | -1.814195 | -2.517085 | -0.711124 |
| H | -2.373633 | -1.417512 | 1.379627 |
| H | -3.048688 | -0.425728 | -0.727415 |
| C | 2.143621 | -1.511541 | -1.347026 |
| H | 2.269016 | -1.315517 | -2.420120 |
| H | 2.844360 | -2.228951 | -0.902551 |

Table S28: Cartesian coordinated (x,y,z) for the optimized structure of **D.**

| | | | |
|---|---|---|---|
| Si | -0.000758 | 0.115697 | -0.018421 |
| O | 0.000000 | 1.658096 | -0.049417 |
| Si | -2.047135 | -1.094679 | 0.094921 |
| H | -1.930788 | -2.337928 | -0.712299 |
| H | -2.291555 | -1.472906 | 1.511728 |
| H | -3.159314 | -0.255816 | -0.409784 |
| Si | 2.046507 | -1.096834 | -0.084908 |
| H | 1.912266 | -2.340907 | 0.718178 |
| H | 2.324183 | -1.472213 | -1.496205 |
| H | 3.146587 | -0.258449 | 0.446705 |

# 4. References


(S1) Wendel, D.; Porzelt, A.; Herz, F. A. D.; Sarkar, D.; Jandl, C.; Inoue, S.; Rieger, B., *J. Am. Chem. Soc.* **2017**, *139*, 8134-8137.

(S2) Lui, M. W.; Merten, C.; Ferguson, M. J.; McDonald, R.; Xu, Y.; Rivard, E., *Inorg. Chem.* **2015**, *54*, 2040-2049.

(S3) Kuhn, N.; Kratz, T., *Synthesis* **1993**, *1993*, 561-562.

(S4) Wiberg, N.; Amelunxen, K.; Lerner, H. W.; Schuster, H.; Nöth, H.; Krossing, I.; Schmidt-Amelunxen, M.; Seifert, T., *J. Organomet. Chem.* **1997**, *542*, 1-18.

(S5) Ishida, S.; Abe, T.; Hirakawa, F.; Kosai, T.; Sato, K.; Kira, M.; Iwamoto, T., *Chem. Eur. J.* **2015**, *21*, 15100-15103.

(S6) *APEX suite of crystallographic software*, APEX 3 version 2015.5-2; Bruker AXS Inc.: Madison, Wisconsin, USA, **2015**.

(S7) *SAINT*, Version 7.56a and SADABS Version 2008/1; Bruker AXS Inc.: Madison, Wisconsin, USA, **2008**.

(S8) Sheldrick, G. M., *SHELXL-2014*, University of Göttingen, Göttingen, Germany, **2014**.

(S9) Huebschle, C. B.; Sheldrick, G. M.; Dittrich, B., *J. Appl. Cryst.* **2011**, 44, 1281.

(S10) Sheldrick, G. M., *SHELXL-97*, University of Göttingen, Göttingen, Germany, **1998**.

(S11) Wilson, A. J. C. *International Tables for Crystallography*, Vol. C, Tables 6.1.1.4 (pp. 500-502), 4.2.6.8 (pp. 219-222), and 4.2.4.2 (pp. 193-199); Kluwer Academic Publishers: Dordrecht, The Netherlands, **1992**.

(S12) Macrae, C. F., Bruno, I. J., Chisholm, J. A., Edgington, P. R., McCabe, P., Pidcock, E., Rodriguez-Monge, L., Taylor, R., van de Streek, J. & Wood, P. A., *J. Appl. Cryst.* **2008**, *41*, 466–470.

(S13) Becke, A. D., *J. Chem. Phys*. **1993**, *98*, 5648-5652.

(S14) Vosko, S. H.; Wilk, L., Nusair, M., *Can. J. Phys*. **1980**, *58*, 1200-1211.

(S15) Lee, C.; Yang, W.; Parr, R. G., *Phys. Rev. B* **1988**, *37*, 785-789.

(S16) Frisch, M. J.; Trucks, G. W.; Schlegel, H. B.; Scuseria, G. E.; Robb, M. A.; Cheeseman, J. R;.Scalmani, G.; Barone, V.; Petersson, G. A.; Nakatusji, H.; Li, X.; Caricato, M.; Marenich, A.; Bloino, J.; Janesko, B. G.; Gomperts, R.; Mennucci, B.; Hratchian, H. P.; Ortiz, J. V.; Izmaylov, A. F.; Sonnenberg, J. L.; Williams-Young, D.; Ding, F.; Lipparini, F.; Egidi, F.; Goings, J.; Peng, B.; Petrone, A.; Henderson, T.; Ranashinghe, D.; Zakrzewski, V. G.; Gao, J.; Rega, N.; Zheng, G.; Liang, W.; Hada, M.; Ehara, M.; Toyota, K.; Fukuda, R.; Hasekawa, J.; Ishida, M.; Nakajima, T.; Honda, Y; Kitao, O.; Nakao, H.; Vreven, T.; Throssell, K.; Montgomery, Jr., J. A.; Peralta, J. E.; Ogliaro, F.; Bearpark, M.; Heyd, J. J.; Brothers, E.; Kudin, K. N.; Staroverov, V. N.; Keith, T.; Kobayashi, R.; Normand, J.; Raghavachari, K; Rendell, A.; Burant, J. C.; Iyengar, S. S.; Tomasi, J.; Cossi, M.; Millam, J. M.; Klene, M.; Adamo, C.; Cammi, R.; Ochterski, J. W.; Martin, R. L.; Morokuma, K.; Farkas, O.; Forseman, J. B.; Fox, D.J., *Gaussian 09, Revision E.01*, Gaussian, Inc., Wallingford CT, **2016**.

(S17) Reed, A. E.; Curtiss, L. A.; Weinhold, F., *Chem. Rev.* **1988**, *88*, 899-926.

(S18) Grimme, S.; Antony, J.; Ehrlich, S.; Krieg, H., *J. Chem. Phys* **2010**, *132*, 154104-154119.

(S19) Rekken, B. D.; Brown, T. M.; Fettinger, J. C.; Tuononen, H. M.; Power, P. P., *J. Am. Chem. Soc.* **2012**, *134*, 6504-6507.